Cover Page

Universiteit Leiden

Author: Typas, Dimitrios
Title: DNA damage-induced ubiquitylation : emerging regulators enforce protective mechanisms
Issue Date: 2015-09-09

DNA damage-induced ubiquitylation: emerging regulators enforce protective mechanisms

Dimitrios Typas

To my mother,

who has always believed that the success

of her sons indicates hers as a parent.

DNA damage-induced ubiquitylation: emerging regulators enforce protective mechanisms

Proefschrift

ter verkrijging van de graad van Doctor aan de Universiteit Leiden,

op gezag van Rector Magnificus Prof.mr. C.J.J.M. Stolker,

volgens besluit van het College voor Promoties te verdedigen op

woensdag 9 September 2015 klokke 15:00 uur

door

Dimitrios Typas

geboren te Athene, Griekenland

in 1983

Promotiecommissie

Promotor: Prof. Dr. L. Mullenders

Co-promotor: Dr. H. van Attikum

Overige Leden: Prof. Dr. M. Tijsterman

                   Prof. Dr. T. Sixma (NKI/UvA)

                   Prof. Dr. R. Kanaar (Erasmus MC)

"The world spins. We stumble on. It is enough."

Colum McCann, Let the great world spin (2009)

TABLE OF CONTENTS

1

General introduction and aim of the thesis

1

Life across all kingdoms requires the ability to adapt to environmental changes and internally- or externally-inflicted stress. Therefore, all living creatures have evolutionarily acquired elaborate mechanisms in order to be able to adjust to the countless challenges encountered during their lifespan. Arguably, the most essential aspect of life that requires protection is genetic information, given that it is the part not only orchestrating all cellular functions but also ensuring species continuity. Genetic information, with the exception of RNA viruses, is encoded in DNA, whose integrity is thus paramount.

However, genome stability constantly encounters numerous threats, stemming from either endogenous sources, such as secondary metabolites and Reactive Oxygen Species (ROS) produced during energy production, or exogenous sources, such as UV or cosmic radiation, chemicals and other genotoxic agents. Furthermore, though endowed with highly accurate mechanisms that most often ensure precise DNA metabolism functions, cells are also challenged by erroneous DNA replication, transcription blocks, programmed induction of DNA Double Strand Breaks (DSBs) for cell differentiation, apparent during white blood cell maturation or meiosis, and volatile elements acquired during evolution, such as transposable elements. DNA damage arising due to all the aforementioned perils needs to be repaired, in order for genetic information to be maintained and cellular functions to continue normally. Alternatively, if DNA damage persists or DNA repair is inaccurate, mutations gradually emerge and the threat of chromosomal aberrations, such as amplifications, deletions and translocations, looms gravely. Though cells attempt to additionally limit genomic instability by activating other protective programs in parallel to DNA repair, such apoptosis and senescence, the eventual accumulation of certain mutations will allow few cells to escape such failsafe measures and form abnormal precursors, potentially leading to cancer, neurodegeneration, developmental abnormalities and premature ageing.

1

The DNA Damage Response (DDR)

In order to combat all those foes and ensure genomic integrity, life has evolved several protective mechanisms in response to DNA damage, collectively known as the DNA Damage Response (DDR) (Fig. 1). Like other multifaceted stress responses, DDR is spatiotemporally tightly organised, in order to ensure optimal protection in a timely fashion. Initially, cells utilise existing resources to signal and deal with DNA damage; more specifically existing proteins are modified with a vast array of Post-Translational Modifications (PTMs) [1]. PTMs constitute versatile, reversible switches that allow signal propagation and scaffolding of downstream protein factories, comprised of several repair factors [2, 3]. The most instrumental enzymes in DDR, modifying a multitude of downstream targets, are the kinases ATM and ATR [4], and the E3 ubiquitin ligases RNF8 and RNF168 [5]. Concomitantly to protein PTMs, local or global chromatin remodelling ensues to lift spatial limitations imposed by the nucleosome structure and to facilitate access of the DNA repair machinery [6]. Subsequently to the change in the PTM status of several key proteins and in the chromatin environment, miRNA-induced post-transcriptional silencing modulates the differential gene expression of existing mRNAs [7], potentially funneling it towards pro-DNA repair profiles [8, 9]. Furthermore, ribosome occupancy changes upon DNA damage, resulting in a partial translational arrest and a partial shift towards the expression of repair proteins [10, 11](Chapter 5). Finally, before DDR-related PTMs have subsided, the transcriptional response kicks in, culminating in alterations of the mRNA profile and eventually the proteome, in a manner often dependent on the originally inflicted DNA lesion [12, 13].

In the following sections I focus primarily on two key processes enabling cells to deal with all different kinds of DNA damage. Firstly, I introduce the various DNA repair mechanisms that directly reverse damage and reinstate the original genetic information, albeit not always precisely. I then elaborate on the nature of DNA Double Strand Breaks (DSBs) and DSB repair mechanisms, since most of the work presented in this thesis addresses DSB repair. Secondly, I present a brief overview of the intricate interplay between DNA damage and translational reprogramming, as a considerable part of

my work focuses on this relationship. Finally, I shortly mention how recent breakthrough in science-related technology is offering unprecedented ease in meticulously exploring the DDR.
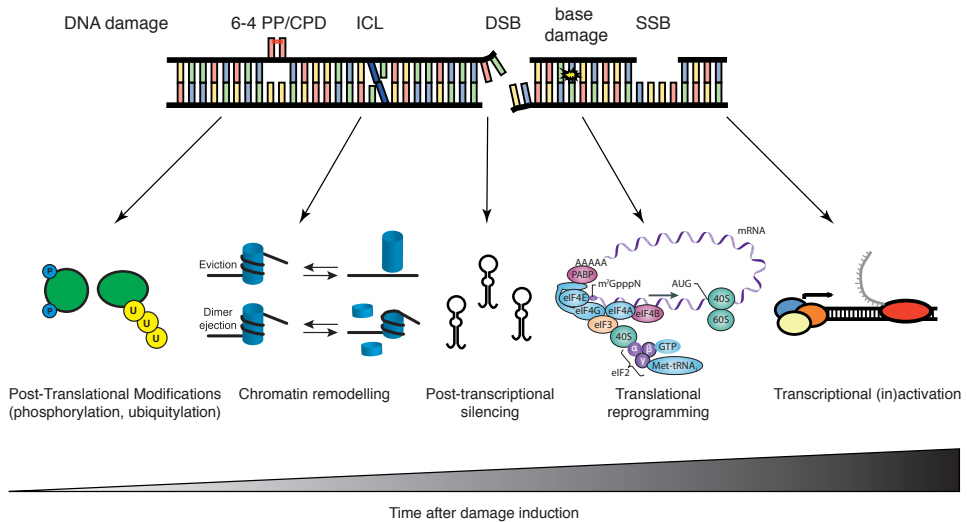

Figure 1. DNA Damage and temporal regulation of the DNA Damage Response (DDR). Most often encountered DNA damage represented graphically on double-stranded DNA. On the top part, from left to right illustrated: 6-4 PhotoProduct (6-4PP), CycloPyrimidine Dimer (CPD), Interstrand CrossLink (ICL), Double-Strand Break (DSB), base damage, Single-Strand Break (SSB). On the bottom part, major processes employed by the DDR, arranged temporally from left to right. Picture for translational reprogramming taken from Nature Reviews Cancer. 2010 Apr;10(4):254-66. Figure adapted from a slide originally made by Dr. Joris Pothof.

DNA Repair Mechanisms

Equipped with cutting-edge scientific tools, several groups have attempted to elucidate the DNA repair pathways that have evolved to counteract the diverse forms of DNA damage (Fig. 2). More precisely, it is now common knowledge that bulky lesions distorting the DNA helix structure are repaired by Nucleotide Excision Repair (NER; detailed description in Chapter 2) [14]. When such lesions arise in non-transcribed regions they are dealt with Global Genome NER (GG-NER) [15], whilst when occurring in the transcribed strand they are recognised by the elongating RNA polymerase and taken care of by Transcription Coupled NER (TC-NER) [16]. Small adducts inflicted by alterations, such as deamination, alkylation and oxidation, of single bases or small DNA stretches within the same strand are eliminated by Base Excision

1

Repair (BER) [17]. BER is also responsible for restoring DNA Single Strand Breaks (SSBs) that may appear away from the replication fork [18]. On the other hand, DSBs are primarily repaired by Non-Homologous End-Joining (NHEJ) [19] and Homologous Recombination (HR) [20]. DSBs arise in mammalian genomes as a result of programmed endogenous processes, like meiosis or V(D)J recombination, and collapsed replication forks at nicked or crosslinked DNA. Additionally, exogenous assaults by Ionising Radiation (IR), topoisomerase inhibitors or radiomimetic drugs induce DSBs [21]. Mismatch Repair (MMR) corrects the infrequent errors of replicative DNA polymerases δ and ϵ, bestowing even higher fidelity in the process of DNA replication [22]. Finally, DNA damage that blocks DNA duplication can also be bypassed by low-fidelity DNA polymerases, in a process termed Trans-Lesion Synthesis (TLS) [23]. Though beneficial in terms of dealing with the immediate danger of replication blockage, inaccurate TLS introduces genomic mutations that may accumulate over time.
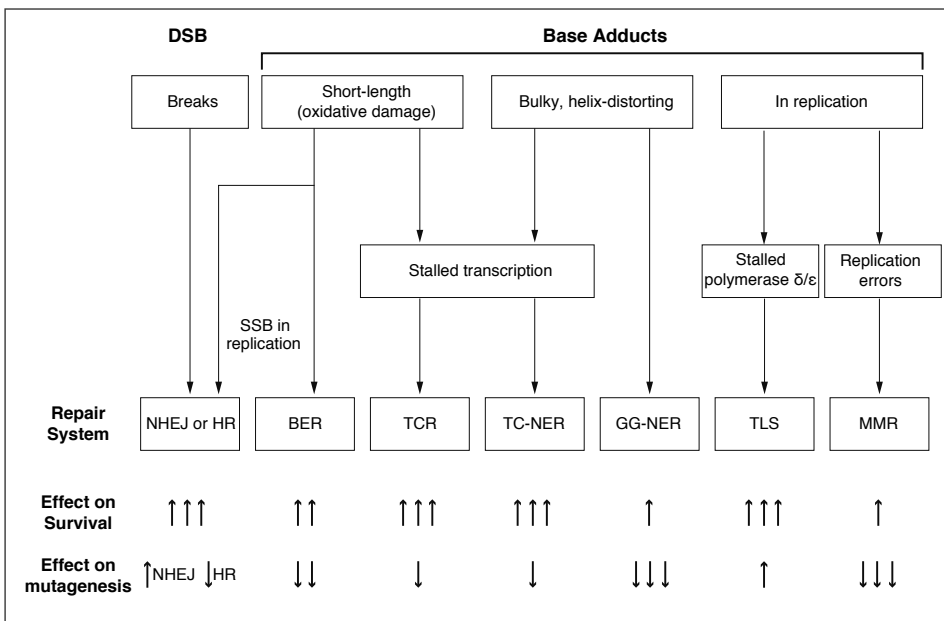
Figure 2. DNA Damage and major DNA repair pathways. Most often encountered forms of DNA damage and the repair systems responsible for their removal. Abbreviations used: Non-Homologous End-Joining (NHEJ), Homologous Recombination (HR), Base Excision Repair (BER), Transcription Coupled Repair (TCR), Transcription Coupled-Nucleotide Excision Repair (TC-NER), Global Genome-Nucleotide Excision Repair (GG-NER), TransLesion Synthesis (TLS), MisMatch Repair (MMR). Figure adapted from the New England Journal of Medicine. 2009 Nov 5;361(19):1914.

1

DNA Double Strand Breaks (DSBs)

Although they do not present the most often encountered form of DNA damage, DSBs pose the most challenging threat for repair systems, due to the simultaneous loss of information on both DNA strands. Though usually grouped altogether, DSBs vary significantly in their nature (Fig. 3). Depending on their structure, DSBs can be categorised into one-ended, such as those occurring during replication fork stalling or collapse, or two-ended (pretty much everything else). Alternatively, the covalent attachment of a protein adjacent to the DSB, such as SPO11 during meiosis or TOPO-I upon treatment with camptothecin, or the synchronous emergence of several different lesions within a small DNA region, such as the IR-induced "clustered" damage, would render it a "dirty" break. On the contrary, a break not limited by nearby damage or masked by an attached protein would be assigned as "clean" [21]. The nature of a DSB, in combination with the cell-cycle stage, determines the DSB repair pathway that will be put into effect [24] and the potential requirement of additional repair pathways such as BER [18].

The importance of repairing DSBs is evident by the plethora of pathways that have evolutionarily arisen to contend them. Based on the amount of homology that these pathways utilise to restore the original information, they can be divided into those using no, little or full homology (Fig. 3). More specifically, NHEJ tethers clean or minimally processed DSBs together, employing no homology, thus often deviating from the initial sequence after repair [25]. On the other end of the spectrum, Homologous Recombination exploits the presence of the sister chromatid, or less frequently the homologue, in order to precisely reinstate the original DNA sequence [26]. Finally, Theta-Mediated End-Joining (TMEJ) [27], Microhomology-Mediated End-Joining (MMEJ) [28] and Single-Strand Annealing (SSA) [29] utilise increasing amounts of homology respectively, so as to inaccurately correct the DNA damage. Though the significance of the three latter pathways is undisputed, their role in DSB repair is secondary to NHEJ and HR, hence I shall focus on those in more detail. NHEJ constitutes the principal repair pathway of DSBs in mammals, primarily because of its availability during the entirety of the cell cycle and its straightforwardness. Though such characteristics render it

1

fast and ubiquitous, the absence of homology-use creates a caveat; NHEJ is error-prone [25]. On the contrary, HR is error-free, being restricted to the cell-cycle stages in which sister chromatids are present, hence late-S or G2 phase [30]. HR is a relatively slow, yet high-fidelity, process [26].
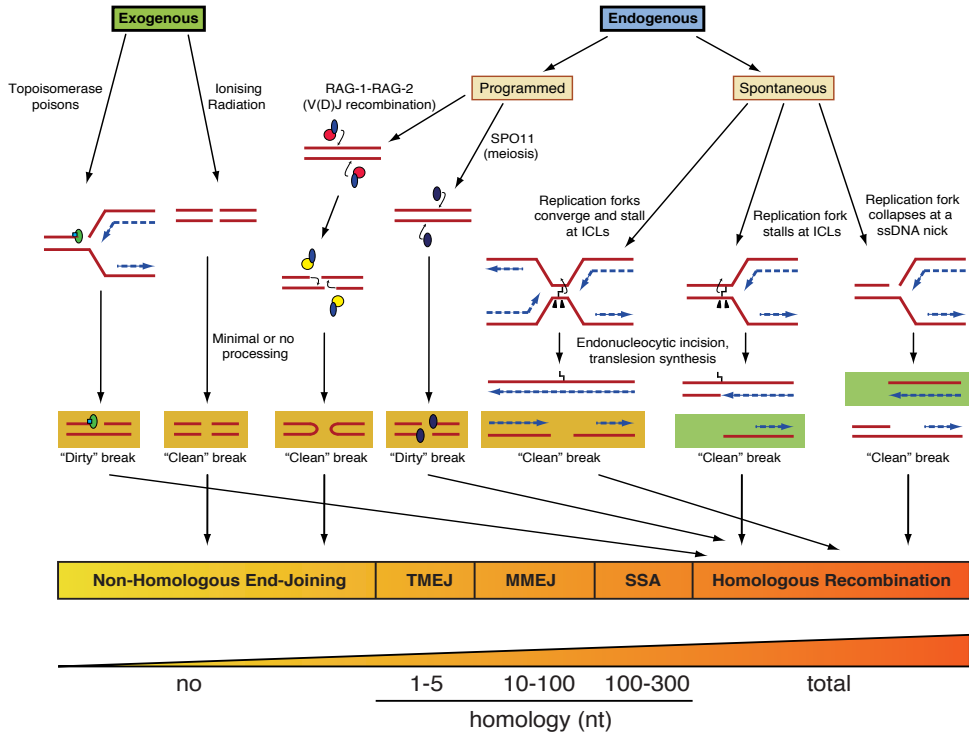
Figure 3. Different origins and nature of DSBs. DSBs come in many different forms, one-ended (depicted in light-green background) or two-ended (depicted in light-orange background), "dirty" or "clean". The nature of the DSB, in combination with the cell-cycle stage it occurs, determines the repair pathway used to reverse it. Different DSB repair pathways utilise different amounts of homology. Here homology-use is illustrated on a coloured scale, ranging from no homology (yellow) to total homology (dark orange). Abbreviations used: Theta-Mediated End-Joining (TMEJ), Microhomology Mediated End-Joining (MMEJ), Single Strand Annealing (SSA), nucleotide (nt). Figure adapted from Molecular Cell. 2012 Aug 24;47(4):497-510.

Non-Homologous End-Joining

The core reaction of NHEJ commences with the recognition of the break by the KU70-KU80 heterodimer, which creates a scaffolding dock for the accrual of downstream factors (Fig. 4a) [19]. The assembly of the KU-complex ensures that the two ends of the DSB stay tethered, therefore being protected from excessive processing by nucleases. The concomitant recruitment of the kinase DNA-PKcs results in the phosphorylation of several chromatin targets, including XRCC4, Ligase 4, DNA-PKcs itself and histone variant H2AX. Although the functional significance of some of these targets has remained elusive, the formation of γH2AX culminates in the accumulation of 53BP1, which in tandem with the KU-complex, protects the DSB ends from nucleolytic editing by MRE11, DNA2 and EXO1. Subsequently to DNA-PKcs activation, limited processing of the broken ends by ARTEMIS and other enzymes creates ligatable ends, which possess a 5' phosphate and a 3' hydroxyl. Finally, the heterotrimeric complex of DNA Ligase IV-XRCC4-XLF joins the two ends together, successfully sealing the gap and restoring the double-stranded helix structure [25].

Homologous recombination

HR is a multistep process entailing in a sequential manner, extensive processing of the DSB, search for homology and resolution/dissolution of formed Holliday junctions (Fig. 4b) [20]. More explicitly, DSBs initially attract both the KU-complex and the Mre11-Rad50-Nbs1 (MRN) complex. DNA nicking by the Mre11 nuclease and limited DNA resection towards the break (3'-5' resection), by the combined action of Mre11 and CTIP, removes the KU-complex and commits the DSB to repair by HR [31]. Subsequent longer resection away from the DSB ensues (5'-3' resection), creating extensive regions of 3'-single strand DNA (ssDNA). Long-range resection is executed by either of two nucleases EXO1 or DNA2 associating with the DNA-unwinding complex of BLM-TOPO3-RMI1 [24]. Resected DNA is immediately coated by the ssDNA-binding protein RPA, which forms a stable complex and protects the DNA from further degradation. In order for homology search to begin,

1

RPA must be exchanged for the RAD51 recombinase. This exchange step occurs in multiple non-redundant ways, involving either complexes formed by RAD51 with RAD52 and RAD54 [32] or more predominantly the BRCA1-PALB2-BRCA2-RAD51 complex (more details in the following sections) [33]. Upon being loaded on DNA, RAD51 forms nucleofilaments, initially probing neighbouring and subsequently more distant chromatin for homology [34]. When homology is detected, the DNA-RAD51 nucleofilament invades the homologous DNA and the correct information is copied. The result of this strand invasion is the creation of a D-loop which occasionally is resolved by strand-displacement, in a mechanism termed Synthesis-Dependent Strand Annealing (SDSA). However, the second DNA end of the D-loop is more frequently captured, culminating in the formation of a double Holliday Junction (dHJ). dHJs are subjected to processing by different complexes of endonucleases and helicases, leading to either their resolution or their dissolution [20] (Fig. 4) The net result of this laborious process is the error-free restoration of the original DNA sequence. In the work presented in this thesis (Chapter 4), we have uncovered a novel regulatory level in the formation of the BRCA1-PALB2-BRCA2 complex, which is responsible for the RPA-RAD51 exchange, hence I provide a more detailed overview of these proteins' functions.
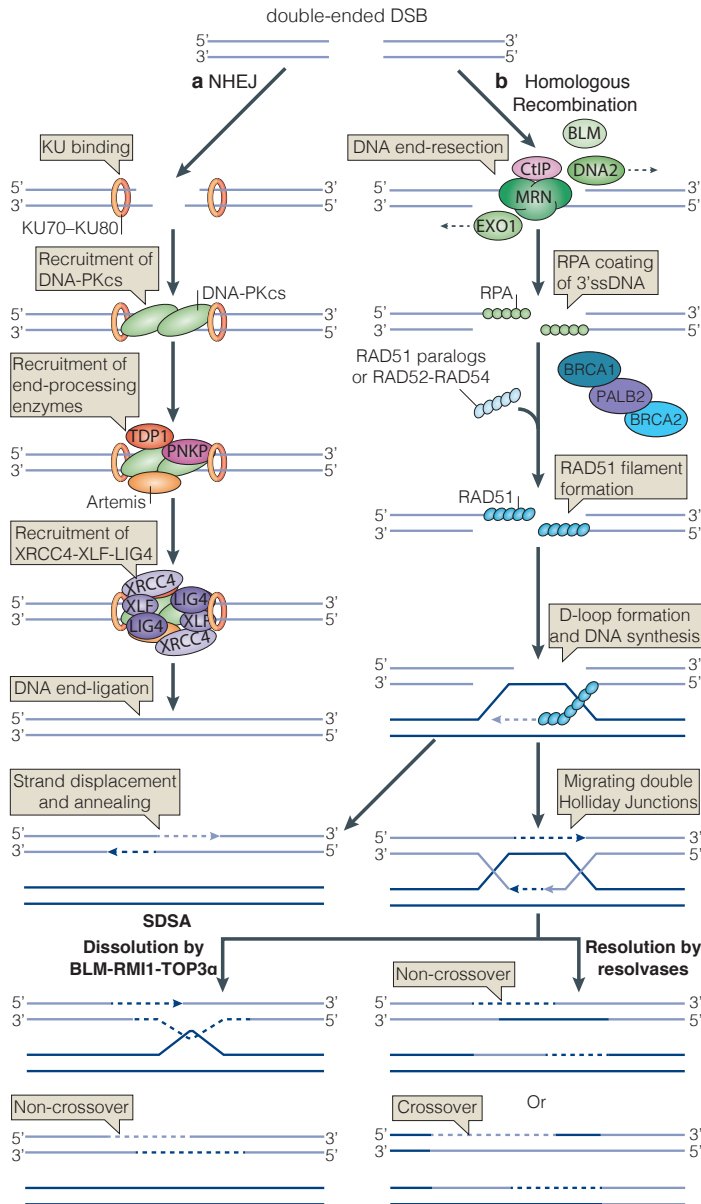
Figure 4. Main DNA DSB repair pathways. (A) Non-Homologous End-Joining (NHEJ) involves (i) KU binding, (ii) DNA PK-cs activation, (iii) End-processing enzymes modifying the DNA-ends, (iv) XRCC4-XLF-LIG4 recruitment and (v) DNA religation. (B) Homologous Recombination entails (i) DNA end-resection initially by CTIP and the MRN complex, subsequently by EXO1 or DNA2 in concert with the BLM, RMI1, TOPO3 complex, (ii) RPA coating of 3'single stranded DNA (3'ssDNA), (iii) RPA-RAD51 exchange and RAD51-filament formation, (iv) RAD51-mediated search of homology, (v) D-loop formation and DNA synthesis, (vi-a) strand displacement and annealing or (vi-b) Holliday Junction formation and resolution/dissolution. Figure adapted from Nature Reviews Molecular Cell Biology. 2014 Jan;15(1):7-18.

1

BRCA1

BRCA1 (BReast CAncer gene 1) is a paramount genome-caretaker, responsible for a wide array of protective mechanisms that guard genome integrity [35, 36]. Its importance becomes evident by the embryonic lethality observed upon homozygous BRCA1 deletion and the highly increased risk of tumour formation upon numerous pathogenic germline mutations or haploinsufficiency in the BRCA1 gene [35, 37-39].

BRCA1 forms a core complex with BARD1. This union shelters both partners from proteasomal degradation. Furthermore, this heterodimeric complex constitutes an E3-ubiquitin ligase [40-42] with several identified targets [43-45], whose catalytic activity however is not essential for tumour suppression [46, 47]. Though BRCA1-induced ubiquitylation may be of secondary importance, the ability of BRCA1 to recognise and bind phosphorylated proteins via its tandem BRCT domains makes it an excellent docking platform for several HR proteins. Importantly, phosphorylation-dependent interactions between BRCA1 and factors such as ABRAXAS, FANCJ, CTIP are mutually exclusive. Abrogation of all these interactions by mutating a key residue in the BRCT domain of BRCA1 results in proliferation defects, chromosomal instability and reduced formation of functional HR complexes [46, 48].

Complex	Function	Composition	HR effect	Interaction
Core	BRCA1 stabilisation and ubiquitin ligase activiy	BRCA1-BARD1	promotes	protein-protein
BRCA1A	G2-M checkpoint regulation and BRCA1 sequestration from the ssDNA compartment	BRCA1-ABRAXAS-RAP80-BRCC36-BRCC45-MERIT40	inhibits	phosphorylation dependent
BRCA1B	S phase progression and repair of replication associated DSBs	BRCA1-FANCJ-TOPBP1	promotes	phosphorylation dependent
BRCA1C	G2-M checkpoint regulation and DNA end-resection (?)	BRCA1-CTIP-MRE11-NBS1-RAD50	unclear	phosphorylation dependent
BRCC	RPA-RAD51 exchange and RAD51 loading onto ssDNA	BRCA1-PALB2-BRCA2-RAD51	promotes	protein-protein

Table 1. Different BRCA1 complexes. BRCA1 forms several complexes with different partners in either a phosphorylation-depedent manner or a direct protein-protein interaction fashion. Those complexes have opposing effects on error-free repair by HR. Table adapted from Nature Reviews Molecular Cell Biology. 2010 Feb;11(2):138-48.

To further elaborate, BRCA1 forms two phosphorylation-independent and 3 phosphorylation-dependent complexes (Table 1):

1. BRCA1 interacts with phosphorylated ABRAXAS to form a complex comprising additionally RAP80, BRCC36 and MERIT40 [49, 50]. This so-called BRCA1A complex is targeted to DSB-neighbouring chromatin thanks to the RAP80-dependent binding of RNF8/RNF168-ubiquitylated substrates [51, 52]. Though recruited at sites adjacent to the DSB, the BRCA1A complex is inhibitory to repair by HR, as it appears to limit DNA end-resection and to sequester BRCA1 from the single-stranded DNA compartment [53, 54], therefore limiting the association of BRCA1 with PALB2 and BRCA2 (Chapter 4), which facilitate RAD51 loading and HR. The BRCA1A complex also appears to be necessary for efficient regulation of the G2/M checkpoint [51, 55, 56].

2. BRCA1 binds phosphorylated FANCJ (also known as BACH1 or BRIP1) [57, 58] to form the BRCA1B complex along with TOPBP1. When bound to BRCA1 in a functional BRCA1B complex, the FANCJ helicase promotes repair of replication-associated DSBs by HR, therefore assisting timely progression through S phase [59]. However, excessive amounts of FANCJ or loss of its ability to interact with BRCA1, by mutation of its phoshorylation-acceptor site, hinder HR and instead promote error-prone DNA damage bypass [60].

3. BRCA1 interacts with phosphorylated CTIP and the MRN-complex [61-63] to build the BRCA1C complex. Though the CDK-dependent phosphorylation of CTIP promotes the assembly of this complex and has a functional relevance in DT40 chicken cells [63], recent studies have indicated that the BRCA1-CTIP interaction is less important for DNA end-resection in human cells [48], as CTIP deficient cells complemented with the non-phosphorylatable mutant that cannot interact with BRCA1 display an unperturbed phenotype.

4. BRCA1 interacts with PALB2 by means of a direct protein-protein interaction, mediated by its C-terminal coiled-coil domain and the

1

namesake domain in the N-terminus of PALB2 [33, 64, 65]. As it will be described in more detail later, PALB2 bridges the functions of BRCA1 and BRCA2, eventually promoting the formation of the BRCC complex which is responsible for the loading of RAD51 on ssDNA.

PALB2

Partner And Localiser of BRCA2 (PALB2) was originally identified as a protein interacting with BRCA2 and facilitating the latter's nuclear functions, namely its recruitment and retention at sites of DNA damage [66, 67]. Further studies established that PALB2 is a tumour suppressor gene, evident by the phenotypes observed upon pathogenic PALB2 mutations or heterozygosity, namely increased cancer predisposition [68, 69], premature G2 checkpoint abrogation [70], aberrant DNA replication and defective DDR [71]. PALB2 is a scaffold protein, mediating interactions between various HR factors that culminate in the loading of the RAD51 recombinase on ssDNA. Most notably, PALB2 promotes the indirect association of BRCA1 and BRCA2 into a functional complex, therefore bridging ssDNA with 3' overhangs, the product of early HR, to the latter HR step of homology search which is mediated by RAD51.

PALB2 accumulates at DSBs in a predominantly BRCA1-dependent manner, even though there is minimal accrual in the latter's absence [65, 72]. BRCA1 depleted cells reconstituted with a BRCA1 form that is unable to bind PALB2 cannot restore HR efficiency to normal levels [33], indicating that BRCA1 promotes HR primarily via PALB2. Though PALB2 recruitment at DSB occurs downstream of BRCA1, its chromatin retention is also mediated by its Chromatin Association Motif (ChAM) [73]. Interestingly, complementation of PALB2 cells with PALB2 lacking the ChAM domain fails to reinstate mitomycin C and olaparib survival rates to the wild-type situation [73], indicating that this motif is indeed necessary for the physiological function of PALB2.

As mentioned earlier, PALB2 additionally interacts with BRCA2 via its C-terminal-WD40 domain [67, 74]. This interaction is crucial for BRCA2 recruitment at sites of damage, evident by the disappearance of BRCA2 foci upon disruption of its association with PALB2 or loss of PALB2 [74].

PALB2 depletion also impairs RAD51 assembly at DSBs, although residual, RAD52-dependent RAD51 foci formation is still obvious [32]. Furthermore, PALB2 itself promotes HR by binding ssDNA and stimulating nucleofilament formation via direct interaction with RAD51 [75, 76]. It is worth mentioning that PALB2 can also multimerise, an event mediated by the same domain that interacts with BRCA1. Over-expression of a small polypeptide containing solely this NT-coiled-coil domain acts in a dominant negative manner, effectively sequestering endogenous PALB2 from its physiological partners and therefore reducing HR efficiency [77]. A plausible scenario arising from this observation is that excessive levels of PALB2, unless accompanied by elevated amounts of BRCA1, might lead to increased self-association and inhibition of its role in HR. Finally, PALB2 in tandem with BRCA2, but independently of RAD51, has been shown to promote replication fork restart after the induction of replication stress, by specifically recognising and interacting with phosphorylated RPA [78].

BRCA2

The final key player of the BRCC complex is BRCA2 (BReast CAncer gene 2), the actual culprit of RPA-RAD51 exchange. Rather similarly to BRCA1, BRCA2 is a prominent guardian of genome integrity, thus earning the nickname "chromosome custodian" [35]. Loss or pathogenic mutations of BRCA2 notably increase cellular genomic instability, promote malignant transformation and predispose to several different forms of cancer [39, 79].

BRCA2 binds ssDNA-dsDNA junctions [80] and facilitates RPA displacement [81], while at the same time it associates with RAD51 [82, 83] and promotes RAD51 filament formation specifically on ssDNA [84, 85]. BRCA2 accrual at double-ended DSBs is entirely dependent on its upstream partners BRCA1 and PALB2. However, besides its established role in RAD51 loading, BRCA2 was recently shown to hold a crucial role in the initial stabilisation of stalled replication forks and the subsequent error-free restart by HR. BRCA2 fulfils this exceptional role in two different ways, either by interacting with Polη [86] or by physically inhibiting MRE11-dependent degradation of the nascent DNA strand [87].

1

DNA damage and translational reprogramming

One important response that cells launch upon the induction of DNA damage is translational reprogramming, entailing a temporary halt in protein synthesis and a shift towards the expression of specific transcripts [10, 88, 89](Chapter 5). The translational arrest ensures energy preservation, given that normal protein synthesis consumes up to 40% of cellular ATP [90], while the translational switch promotes the synthesis of pro-survival proteins [11]. The importance of this translational response becomes further apparent by several unbiased genetic screens, showing that proteins involved in translation either constitute primary targets of DNA damage induced phosphorylation [91] or play a significant role in protecting against spontaneously induced DNA damage, evident by γH2AX formation [92]. Last but not least, several studies have now established that excessive protein synthesis fosters oncogenic transformation and tumourigenesis [11, 93], channeling new lines of research into the development of specific translation inhibitors that halt tumour progression [11, 94] or reverse chemoresistance [95].

The process of translation can be roughly divided into three stages: initiation, elongation and termination, with most of protein-synthesis regulation taking place at the rate-limiting step of initiation [11]. Cap-dependent translation-initiation begins with the formation of a heterotrimeric complex called eIF4F. This complex interacts with the mRNA-stabilising protein PABP and in concert with the 43S Pre-Initiation Complex (PIC) scans the 5'UTR of mRNAs for the first AUG codon [96]. eIF4F is comprised of a scaffolding protein (eIF4G), a helicase responsible for RNA unwinding (eIF4A) and a protein recognising the m^7GTP-modified 5'-end of the mRNA (eiF4E), the so-called mRNA cap [93] (Fig. 5a). The latter protein, eIF4E, is the least abundant and most diversely controlled, constituting the bottleneck in eIF4F formation and thus translation initiation [94].

Given its rate-limiting status, several proteins have evolved to antagonise the interaction of eIF4E with either the rest of the eIF4F complex or the mRNA cap, therefore hindering translation initiation. A prime example of the prior form of inhibition is the appropriately termed eIF4E-Binding Proteins

1

(4E-BPs). 4E-BPs share extensive homology with eIF4G and thus vie for the same binding places on eIF4E [95]. 4E-BP association with eIF4E sequesters it from the eIF4F, abrogating eIF4E binding to eIF4G [93] (Fig. 5B). Adding an extra regulatory layer, the eIF4E interaction with 4E-BP depends on the latter's phosphorylation status. Hypophosphorylated 4E-BPs readily bind and sequester eIF4E while mTOR-induced 4E-BP hyperphosporylation abrogates this interaction [96]. Besides eIF4E sequestration, cells inhibit translation initiation by expressing a structural analog of eIF4E, a protein called 4EHP. While 4EHP retains the ability to bind the mRNA cap, it cannot form a productive complex with eIF4G [96], effectively rendering 4EHP-bound transcripts secluded from the translation machinery (Fig. 5C). As with 4E-BPs, 4EHP is modulated by PTMs, namely ubiquitination [97] (Chapter 5) and ISGylation [98]. Both of these modifications appear to facilitate 4EHP binding to the cap structure and therefore translation inhibition.
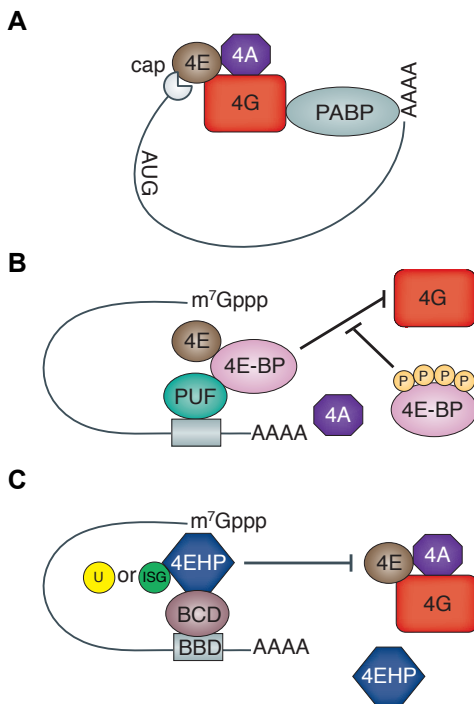
Figure 5. Inhibition of the cap-dependent translation initiation complex. (A) The eIF4F complex regulates cap-dependent translation initiation, binding upstream of the first AUG codon and scanning the 5'UTR of the translated mRNA. eIF4F consists of scaffolding protein eIF4G, RNA helicase eiF4A and m7cap-mRNA-binding protein eIF4E. PABP binds the poly-adenylated tail of the mRNA, creating a circular fold. (B) Inhibition of the eIF4E-eIF4G interaction by 4E-Binding Proteins (4E-BPs). 4E-BP hyperphosphorylation lifts the inhibitory effect. (C) Competitive inhibition of eIF4E binding to the cap of the mRNA by 4EHP. 4EHP is a structural analog of eIF4E binding the cap but not interacting with the rest of the eIF4F complex. 4EHP ubiquitylation or ISGylation promotes its binding to the cap. Abbreviations used: eukaryotic Initiation Factor (eIF), Poly-(A) Binding Protein (PABP), Ubiquitin (U), Interferon Stimulated Gene 15 (ISG). Figure adapted from Nature Reviews Genetics. 2012 Jun;13(6):383-94.

1

A breakthrough in scientific tools allows investigating gene interactions in genome-wide scale

The last decade has brought huge strides in science-related technology, enabling the detailed study of cellular processes such as the DDR. Firstly, ever-improving Mass Spectrometry facilities have allowed the meticulous study of changes upon DNA damage in the proteome and in the various protein PTMs, especially phosphorylation [99, 100] and ubiquitylation [101]. Furthermore, the field of transcriptomics has been revolutionised by the advances in sequencing techniques [102], dictating a *de facto* change from micro-arrays to Next Generation Sequencing (NGS). The latter not only provides an unprecedented, in-depth analysis of the transcriptome upon genotoxic stress, but also a comprehensive grasp of the mutational signatures in human cancers [103, 104] and repair-pathway-balance after DNA damage induction [27, 105]. Finally, it has never been easier to manipulate genomes, whether in the conventional way of creating mutants in model organisms [106], in the form of siRNA- or shRNA-mediated protein depletion [12, 107] or Crisper/Cas9-modification of endogenous loci [108, 109]. These tools have granted us the ability to perform functional genomics screens in protein-by-protein-reduced genomes and to investigate gene interactions in a genome-wide manner upon various forms of genotoxic stress [12, 110].

1

AIMS AND OUTLINE OF THIS THESIS

The meticulous study of the molecular mechanisms that cumulatively constitute the DDR is of the outmost importance for numerous reasons. Primarily, further elaboration on the interconnection of the processes comprising the DDR would enhance our chance of discovering drugable targets. The latter might prove useful for the never-ending battle against tumourigenesis and neurodegeneration. Furthermore, a better grasp on how the DDR works in the tissue or organism level would be undoubtedly beneficial for our strive to minimise the effects of ageing. Given their emerging role as central regulators of multiple facets of the DDR, the elucidation of protein PTMs and specifically ubiquitylation was chosen to be the focal point of my study.

In my thesis I put forward our most notable findings, which further elaborate the intricate role of PTMs in the regulation of the DDR at multiple levels. Initially, I provide a summary of the recent developments and our views on the modulation of NER **(Chapter 2)**. Subsequently, I present the results from a genetic screen we performed, showing that the De-Ubiquitylating (DUBs) enzymes USP26 and USP37 control both the DSB signalling cascade and DSB repair **(Chapter 3)**. In **Chapter 4** I introduce our unexpected finding that the RNF168 E3-ubiquitin ligase facilitates the error-free repair-pathway of HR by mediating PALB2 recruitment at the sites of damage. Illustrating the value of extensive, functional genomic screens in the elucidation of the DDR, in **Chapter 5** I present our results showing that the ARIH1 E3-ubiquitin ligase, one of the hits of our screen, orchestrates a DNA-damage induced translational arrest that promotes cell survival of both untransformed and cancer cells. In **Chapter 6**, I report our preliminary findings on the role of ARIH1 in directly mediating DSB repair. Finally, in **Chapter 7**, I discuss our discoveries under the spectrum of recent advancements in science-related technology and novel work in the DDR field. I also submit my thoughts on the perspective of the research-projects presented, hoping that further study on those will not only advance our understanding of the molecular mechanisms governing the DDR, but also provide potential targets for clinical applications.

1

REFERENCES

1.   Jensen, O.N., *Interpreting the protein language using proteomics.* Nat Rev Mol Cell Biol, 2006. **7**(6): p. 391-403.

2.   Panier, S. and D. Durocher, *Push back to respond better: regulatory inhibition of the DNA double-strand break response.* Nat Rev Mol Cell Biol, 2013. **14**(10): p. 661-72.

3.   Ulrich, H.D. and H. Walden, *Ubiquitin signalling in DNA replication and repair.* Nat Rev Mol Cell Biol, 2010. **11**(7): p. 479-89.

4.   Marechal, A. and L. Zou, *DNA damage sensing by the ATM and ATR kinases.* Cold Spring Harb Perspect Biol, 2013. **5**(9).

5.   Al-Hakim, A., et al., *The ubiquitous role of ubiquitin in the DNA damage response.* DNA Repair (Amst), 2010. **9**(12): p. 1229-40.

6.   Misteli, T. and E. Soutoglou, *The emerging role of nuclear architecture in DNA repair and genome maintenance.* Nat Rev Mol Cell Biol, 2009. **10**(4): p. 243-54.

7.   Carthew, R.W. and E.J. Sontheimer, *Origins and Mechanisms of miRNAs and siRNAs.* Cell, 2009. **136**(4): p. 642-55.

8.   Wang, Y. and T. Taniguchi, *MicroRNAs and DNA damage response: implications for cancer therapy.* Cell Cycle, 2013. **12**(1): p. 32-42.

9.   Wan, G., et al., *miRNA response to DNA damage.* Trends Biochem Sci, 2011. **36**(9): p. 478-84.

10.   Braunstein, S., et al., *Regulation of protein synthesis by ionizing radiation.* Mol Cell Biol, 2009. **29**(21): p. 5645-56.

11.   Silvera, D., S.C. Formenti, and R.J. Schneider, *Translational control in cancer.* Nat Rev Cancer, 2010. **10**(4): p. 254-66.

12.   Carreras Puigvert, J., et al., *Systems biology approach identifies the kinase Csnk1a1 as a regulator of the DNA damage response in embryonic stem cells.* Sci Signal, 2013. **6**(259): p. ra5.

13.   Kruse, J.J., et al., *A portrait of cisplatin-induced transcriptional changes in mouse embryonic stem cells reveals a dominant p53-like response.* Mutat Res, 2007. **617**(1-2): p. 58-70.

14.   Kamileri, I., I. Karakasilioti, and G.A. Garinis, *Nucleotide excision repair: new tricks with old bricks.* Trends Genet, 2012. **28**(11): p. 566-73.

15.   Scharer, O.D., *Nucleotide excision repair in eukaryotes.* Cold Spring Harb Perspect Biol, 2013. **5**(10): p. a012609.

16.   Marteijn, J.A., et al., *Understanding nucleotide excision repair and its roles in cancer and ageing.* Nat Rev Mol Cell Biol, 2014. **15**(7): p. 465-81.

17.   Barnes, D.E. and T. Lindahl, *Repair and genetic consequences of endogenous DNA base damage in mammalian cells.* Annu Rev Genet, 2004. **38**: p. 445-76.

18.   Caldecott, K.W., *Single-strand break repair and genetic disease.* Nat Rev Genet, 2008. **9**(8): p. 619-31.

19.   Deriano, L. and D.B. Roth, *Modernizing the nonhomologous end-joining repertoire: alternative and classical NHEJ share the stage.* Annu Rev Genet, 2013. **47**: p. 433-

55.

20. Moynahan, M.E. and M. Jasin, *Mitotic homologous recombination maintains genomic stability and suppresses tumorigenesis.* Nat Rev Mol Cell Biol, 2010. **11**(3): p. 196-207.

21. Chapman, J.R., M.R. Taylor, and S.J. Boulton, *Playing the end game: DNA double-strand break repair pathway choice.* Mol Cell, 2012. **47**(4): p. 497-510.

22. Pena-Diaz, J. and J. Jiricny, *Mammalian mismatch repair: error-free or error-prone?* Trends Biochem Sci, 2012. **37**(5): p. 206-14.

23. Andersen, P.L., F. Xu, and W. Xiao, *Eukaryotic DNA damage tolerance and translesion synthesis through covalent modifications of PCNA.* Cell Res, 2008. **18**(1): p. 162-73.

24. Symington, L.S. and J. Gautier, *Double-strand break end resection and repair pathway choice.* Annu Rev Genet, 2011. **45**: p. 247-71.

25. Betermier, M., P. Bertrand, and B.S. Lopez, *Is non-homologous end-joining really an inherently error-prone process?* PLoS Genet, 2014. **10**(1): p. e1004086.

26. Jasin, M. and R. Rothstein, *Repair of strand breaks by homologous recombination.* Cold Spring Harb Perspect Biol, 2013. **5**(11): p. a012740.

27. Koole, W., et al., *A Polymerase Theta-dependent repair pathway suppresses extensive genomic instability at endogenous G4 DNA sites.* Nat Commun, 2014. **5**: p. 3216.

28. McVey, M. and S.E. Lee, *MMEJ repair of double-strand breaks (director's cut): deleted sequences and alternative endings.* Trends Genet, 2008. **24**(11): p. 529-38.

29. Mimitou, E.P. and L.S. Symington, *DNA end resection--unraveling the tail.* DNA Repair (Amst), 2011. **10**(3): p. 344-8.

30. Karanam, K., et al., *Quantitative live cell imaging reveals a gradual shift between DNA repair mechanisms and a maximal use of HR in mid S phase.* Mol Cell, 2012. **47**(2): p. 320-9.

31. Stracker, T.H. and J.H. Petrini, *The MRE11 complex: starting from the ends.* Nat Rev Mol Cell Biol, 2011. **12**(2): p. 90-103.

32. Lok, B.H., et al., *RAD52 inactivation is synthetically lethal with deficiencies in BRCA1 and PALB2 in addition to BRCA2 through RAD51-mediated homologous recombination.* Oncogene, 2013. **32**(30): p. 3552-8.

33. Sy, S.M., M.S. Huen, and J. Chen, *PALB2 is an integral component of the BRCA complex required for homologous recombination repair.* Proc Natl Acad Sci U S A, 2009. **106**(17): p. 7155-60.

34. Renkawitz, J., et al., *Monitoring homology search during DNA double-strand break repair in vivo.* Mol Cell, 2013. **50**(2): p. 261-72.

35. Venkitaraman, A.R., *Cancer suppression by the chromosome custodians, BRCA1 and BRCA2.* Science, 2014. **343**(6178): p. 1470-5.

36. Huen, M.S., S.M. Sy, and J. Chen, *BRCA1 and its toolbox for the maintenance of genome integrity.* Nat Rev Mol Cell Biol, 2010. **11**(2): p. 138-48.

37. Bartek, J., J. Lukas, and J. Bartkova, *DNA damage response as an anti-cancer barrier: damage threshold and the concept of 'conditional haploinsufficiency'.* Cell Cycle, 2007. **6**(19): p. 2344-7.

1

38.   Hakem, R., et al., *The tumor suppressor gene Brca1 is required for embryonic cellular proliferation in the mouse.* Cell, 1996. **85**(7): p. 1009-23.

39.   Evers, B. and J. Jonkers, *Mouse models of BRCA1 and BRCA2 deficiency: past lessons, current understanding and future prospects.* Oncogene, 2006. **25**(43): p. 5885-97.

40.   Chen, A., et al., *Autoubiquitination of the BRCA1*BARD1 RING ubiquitin ligase.* J Biol Chem, 2002. **277**(24): p. 22085-92.

41.   Wu, L.C., et al., *Identification of a RING protein that can interact in vivo with the BRCA1 gene product.* Nat Genet, 1996. **14**(4): p. 430-40.

42.   Brzovic, P.S., et al., *Structure of a BRCA1-BARD1 heterodimeric RING-RING complex.* Nat Struct Biol, 2001. **8**(10): p. 833-7.

43.   Starita, L.M., et al., *BRCA1-dependent ubiquitination of gamma-tubulin regulates centrosome number.* Mol Cell Biol, 2004. **24**(19): p. 8457-66.

44.   Morris, J.R. and E. Solomon, *BRCA1 : BARD1 induces the formation of conjugated ubiquitin structures, dependent on K6 of ubiquitin, in cells during DNA replication and repair.* Hum Mol Genet, 2004. **13**(8): p. 807-17.

45.   Nishikawa, H., et al., *Mass spectrometric and mutational analyses reveal Lys-6-linked polyubiquitin chains catalyzed by BRCA1-BARD1 ubiquitin ligase.* J Biol Chem, 2004. **279**(6): p. 3916-24.

46.   Shakya, R., et al., *BRCA1 tumor suppression depends on BRCT phosphoprotein binding, but not its E3 ligase activity.* Science, 2011. **334**(6055): p. 525-8.

47.   Reid, L.J., et al., *E3 ligase activity of BRCA1 is not essential for mammalian cell viability or homology-directed repair of double-strand DNA breaks.* Proc Natl Acad Sci U S A, 2008. **105**(52): p. 20876-81.

48.   Reczek, C.R., et al., *The interaction between CtIP and BRCA1 is not essential for resection-mediated DNA repair or tumor suppression.* J Cell Biol, 2013. **201**(5): p. 693-707.

49.   Wang, B., et al., *Abraxas and RAP80 form a BRCA1 protein complex required for the DNA damage response.* Science, 2007. **316**(5828): p. 1194-8.

50.   Shao, G., et al., *MERIT40 controls BRCA1-Rap80 complex integrity and recruitment to DNA double-strand breaks.* Genes Dev, 2009. **23**(6): p. 740-54.

51.   Kim, H., J. Chen, and X. Yu, *Ubiquitin-binding protein RAP80 mediates BRCA1-dependent DNA damage response.* Science, 2007. **316**(5828): p. 1202-5.

52.   Wang, B. and S.J. Elledge, *Ubc13/Rnf8 ubiquitin ligases control foci formation of the Rap80/Abraxas/Brca1/Brcc36 complex in response to DNA damage.* Proc Natl Acad Sci U S A, 2007. **104**(52): p. 20759-63.

53.   Coleman, K.A. and R.A. Greenberg, *The BRCA1-RAP80 complex regulates DNA repair mechanism utilization by restricting end resection.* J Biol Chem, 2011. **286**(15): p. 13669-80.

54.   Hu, Y., et al., *RAP80-directed tuning of BRCA1 homologous recombination function at ionizing radiation-induced nuclear foci.* Genes Dev, 2011. **25**(7): p. 685-700.

55.   Kim, H., J. Huang, and J. Chen, *CCDC98 is a BRCA1-BRCT domain-binding protein involved in the DNA damage response.* Nat Struct Mol Biol, 2007. **14**(8): p. 710-5.

1

56.   Sobhian, B., et al., *RAP80 targets BRCA1 to specific ubiquitin structures at DNA damage sites.* Science, 2007. **316**(5828): p. 1198-202.

57.   Cantor, S.B., et al., *BACH1, a novel helicase-like protein, interacts directly with BRCA1 and contributes to its DNA repair function.* Cell, 2001. **105**(1): p. 149-60.

58.   Yu, X., et al., *The BRCT domain is a phospho-protein binding domain.* Science, 2003. **302**(5645): p. 639-42.

59.   Kumaraswamy, E. and R. Shiekhattar, *Activation of BRCA1/BRCA2-associated helicase BACH1 is required for timely progression through S phase.* Mol Cell Biol, 2007. **27**(19): p. 6733-41.

60.   Xie, J., et al., *Targeting the FANCJ-BRCA1 interaction promotes a switch from recombination to poleta-dependent bypass.* Oncogene, 2010. **29**(17): p. 2499-508.

61.   Yu, X., et al., *The C-terminal (BRCT) domains of BRCA1 interact in vivo with CtIP, a protein implicated in the CtBP pathway of transcriptional repression.* J Biol Chem, 1998. **273**(39): p. 25388-92.

62.   Chen, L., et al., *Cell cycle-dependent complex formation of BRCA1.CtIP.MRN is important for DNA double-strand break repair.* J Biol Chem, 2008. **283**(12): p. 7713-20.

63.   Yun, M.H. and K. Hiom, *CtIP-BRCA1 modulates the choice of DNA double-strand-break repair pathway throughout the cell cycle.* Nature, 2009. **459**(7245): p. 460-3.

64.   Dong, Y., et al., *Regulation of BRCC, a holoenzyme complex containing BRCA1 and BRCA2, by a signalosome-like subunit and its role in DNA repair.* Mol Cell, 2003. **12**(5): p. 1087-99.

65.   Zhang, F., et al., *PALB2 links BRCA1 and BRCA2 in the DNA-damage response.* Curr Biol, 2009. **19**(6): p. 524-9.

66.   Xia, B., et al., *Fanconi anemia is associated with a defect in the BRCA2 partner PALB2.* Nat Genet, 2007. **39**(2): p. 159-61.

67.   Xia, B., et al., *Control of BRCA2 cellular and clinical functions by a nuclear partner, PALB2.* Mol Cell, 2006. **22**(6): p. 719-29.

68.   Rahman, N., et al., *PALB2, which encodes a BRCA2-interacting protein, is a breast cancer susceptibility gene.* Nat Genet, 2007. **39**(2): p. 165-7.

69.   Tischkowitz, M., et al., *Analysis of PALB2/FANCN-associated breast cancer families.* Proc Natl Acad Sci U S A, 2007. **104**(16): p. 6788-93.

70.   Menzel, T., et al., *A genetic screen identifies BRCA2 and PALB2 as key regulators of G2 checkpoint maintenance.* EMBO Rep, 2011. **12**(7): p. 705-12.

71.   Nikkila, J., et al., *Heterozygous mutations in PALB2 cause DNA replication and damage response defects.* Nat Commun, 2013. **4**: p. 2578.

72.   Zhang, F., et al., *PALB2 functionally connects the breast cancer susceptibility proteins BRCA1 and BRCA2.* Mol Cancer Res, 2009. **7**(7): p. 1110-8.

73.   Bleuyard, J.Y., et al., *ChAM, a novel motif that mediates PALB2 intrinsic chromatin binding and facilitates DNA repair.* EMBO Rep, 2012. **13**(2): p. 135-41.

74.   Sy, S.M., et al., *PALB2 regulates recombinational repair through chromatin association and oligomerization.* J Biol Chem, 2009. **284**(27): p. 18302-10.

1

75. Buisson, R., et al., *Cooperation of breast cancer proteins PALB2 and piccolo BRCA2 in stimulating homologous recombination.* Nat Struct Mol Biol, 2010. **17**(10): p. 1247-54.

76. Dray, E., et al., *Enhancement of RAD51 recombinase activity by the tumor suppressor PALB2.* Nat Struct Mol Biol, 2010. **17**(10): p. 1255-9.

77. Buisson, R. and J.Y. Masson, *PALB2 self-interaction controls homologous recombination.* Nucleic Acids Res, 2012. **40**(20): p. 10312-23.

78. Murphy, A.K., et al., *Phosphorylated RPA recruits PALB2 to stalled DNA replication forks to facilitate fork recovery.* J Cell Biol, 2014. **206**(4): p. 493-507.

79. Roy, R., J. Chun, and S.N. Powell, *BRCA1 and BRCA2: different roles in a common pathway of genome protection.* Nat Rev Cancer, 2012. **12**(1): p. 68-78.

80. Yang, H., et al., *BRCA2 function in DNA binding and recombination from a BRCA2-DSS1-ssDNA structure.* Science, 2002. **297**(5588): p. 1837-48.

81. Yang, H., et al., *The BRCA2 homologue Brh2 nucleates RAD51 filament formation at a dsDNA-ssDNA junction.* Nature, 2005. **433**(7026): p. 653-7.

82. Chen, P.L., et al., *The BRC repeats in BRCA2 are critical for RAD51 binding and resistance to methyl methanesulfonate treatment.* Proc Natl Acad Sci U S A, 1998. **95**(9): p. 5287-92.

83. Wong, A.K., et al., *RAD51 interacts with the evolutionarily conserved BRC motifs in the human breast cancer susceptibility gene brca2.* J Biol Chem, 1997. **272**(51): p. 31941-4.

84. Carreira, A., et al., *The BRC repeats of BRCA2 modulate the DNA-binding selectivity of RAD51.* Cell, 2009. **136**(6): p. 1032-43.

85. Shivji, M.K., et al., *The BRC repeats of human BRCA2 differentially regulate RAD51 binding on single- versus double-stranded DNA to stimulate strand exchange.* Proc Natl Acad Sci U S A, 2009. **106**(32): p. 13254-9.

86. Buisson, R., et al., *Breast cancer proteins PALB2 and BRCA2 stimulate polymerase eta in recombination-associated DNA synthesis at blocked replication forks.* Cell Rep, 2014. **6**(3): p. 553-64.

87. Schlacher, K., et al., *Double-strand break repair-independent role for BRCA2 in blocking stalled replication fork degradation by MRE11.* Cell, 2011. **145**(4): p. 529-42.

88. Lu, X., et al., *Radiation-induced changes in gene expression involve recruitment of existing messenger RNAs to and away from polysomes.* Cancer Res, 2006. **66**(2): p. 1052-61.

89. Reinhardt, H.C., et al., *Is post-transcriptional stabilization, splicing and translation of selective mRNAs a key to the DNA damage response?* Cell Cycle, 2011. **10**(1): p. 23-7.

90. Buttgereit, F. and M.D. Brand, *A hierarchy of ATP-consuming processes in mammalian cells.* Biochem J, 1995. **312 (Pt 1)**: p. 163-7.

91. Matsuoka, S., et al., *ATM and ATR substrate analysis reveals extensive protein networks responsive to DNA damage.* Science, 2007. **316**(5828): p. 1160-6.

92. Paulsen, R.D., et al., *A genome-wide siRNA screen reveals diverse cellular processes and pathways that mediate genome stability.* Mol Cell, 2009. **35**(2): p. 228-39.

93. Sonenberg, N. and A.G. Hinnebusch, *Regulation of translation initiation in eukaryotes: mechanisms and biological targets.* Cell, 2009. **136**(4): p. 731-45.

94. Graff, J.R., et al., *Targeting the eukaryotic translation initiation factor 4E for cancer therapy.* Cancer Res, 2008. **68**(3): p. 631-4.

95. Cencic, R., et al., *Reversing chemoresistance by small molecule inhibition of the translation initiation complex eIF4F.* Proc Natl Acad Sci U S A, 2011. **108**(3): p. 1046-51.

96. Kong, J. and P. Lasko, *Translational control in cellular and developmental processes.* Nat Rev Genet, 2012. **13**(6): p. 383-94.

97. Tan, N.G., et al., *Human homologue of ariadne promotes the ubiquitylation of translation initiation factor 4E homologous protein, 4EHP.* FEBS Lett, 2003. **554**(3): p. 501-4.

98. Okumura, F., W. Zou, and D.E. Zhang, *ISG15 modification of the eIF4E cognate 4EHP enhances cap structure-binding activity of 4EHP.* Genes Dev, 2007. **21**(3): p. 255-60.

99. Olsen, J.V., et al., *Quantitative phosphoproteomics reveals widespread full phosphorylation site occupancy during mitosis.* Sci Signal, 2010. **3**(104): p. ra3.

100. Pines, A., et al., *Global phosphoproteome profiling reveals unanticipated networks responsive to cisplatin treatment of embryonic stem cells.* Mol Cell Biol, 2011. **31**(24): p. 4964-77.

101. Povlsen, L.K., et al., *Systems-wide analysis of ubiquitylation dynamics reveals a key role for PAF15 ubiquitylation in DNA-damage bypass.* Nat Cell Biol, 2012. **14**(10): p. 1089-98.

102. van Dijk, E.L., et al., *Ten years of next-generation sequencing technology.* Trends Genet, 2014. **30**(9): p. 418-26.

103. Alexandrov, L.B., et al., *Signatures of mutational processes in human cancer.* Nature, 2013. **500**(7463): p. 415-21.

104. Helleday, T., S. Eshtad, and S. Nik-Zainal, *Mechanisms underlying mutational signatures in human cancers.* Nat Rev Genet, 2014. **15**(9): p. 585-98.

105. Roerink, S.F., R. van Schendel, and M. Tijsterman, *Polymerase theta-mediated end joining of replication-associated DNA breaks in C. elegans.* Genome Res, 2014. **24**(6): p. 954-62.

106. Guenole, A., et al., *Dissection of DNA damage responses using multiconditional genetic interaction maps.* Mol Cell, 2013. **49**(2): p. 346-58.

107. Adamson, B., et al., *A genome-wide homologous recombination screen identifies the RNA-binding protein RBMX as a component of the DNA-damage response.* Nat Cell Biol, 2012. **14**(3): p. 318-28.

108. Doudna, J.A. and E. Charpentier, *Genome editing. The new frontier of genome engineering with CRISPR-Cas9.* Science, 2014. **346**(6213): p. 1258096.

109. Ochi, T., et al., *DNA repair. PAXX, a paralog of XRCC4 and XLF, interacts with Ku to promote DNA double-strand break repair.* Science, 2015. **347**(6218): p. 185-8.

110. Bandyopadhyay, S., et al., *Rewiring of genetic networks in response to DNA damage.* Science, 2010. **330**(6009): p. 1385-9.

2

Insight in the multilevel regulation of NER

Madelon Dijk, Dimitris Typas, Leon H. Mullenders and Alex Pines

ABSTRACT

Nucleotide excision repair (NER) is a key component of the DNA damage response (DDR) and it is essential to safeguard genome integrity against genotoxic insults. The regulation of NER is primarily mediated by protein Post-Translational Modification (PTMs). The NER machinery removes a wide spectrum of DNA helix distorting lesions, including those induced by solar radiation, through two sub-pathways: Global Genome-NER (GG-NER) and Transcription Coupled-NER (TC-NER). Severe clinical consequences associated with inherited NER defects, including premature ageing, neurodegeneration and extreme cancer susceptibility, underscore the biological relevance of NER. In the last two decades most of the core NER machinery has been elaborately described, shifting attention to molecular mechanisms that either facilitate NER in the context of chromatin or promote the timely and accurate interplay between NER factors and various PTMs. In this review, we summarise and discuss the latest findings in NER. In particular, we focus on emerging factors and novel molecular mechanisms by which NER is regulated.

2

INTRODUCTION

A wide variety of genome-caretaking mechanisms, collectively referred to as the DNA damage response (DDR), neutralise the deleterious effects of DNA damage and prevent toxicity, mutagenesis and genomic instability. The DDR entails both initial sensing of DNA damage and subsequent signalling cascades, which activate cell cycle checkpoints and distinct repair pathways, depending on the type of damage. Among the various human repair pathways, Nucleotide Excision Repair (NER) is the only repair system capable of counteracting ultraviolet (UV)-light-induced genotoxic insults. NER eliminates DNA photolesions i.e. 6–4 pyrimidine-pyrimidone photoproducts (6–4PPs) and Cyclo-butane Pyrimidine Dimers (CPDs). The importance of NER in protecting organisms against the carcinogenic effects of solar-UV-induced DNA damage is underscored by the hereditary disease Xeroderma Pigmentosum (XP). XP patients are clinically characterised by hypersensitivity to sunlight, predisposition to skin cancer and, in a minority of cases (25%), premature ageing accompanied by severe neurological and developmental problems [1]. XP has been linked to defects in seven NER genes (XP-A through XP-G) and in a gene encoding DNA polymerase eta (XP variant).

NER removes bulky DNA lesions through two distinct sub-pathways: Global Genome-NER (GG-NER) and Transcription Coupled-NER (TC-NER). GG-NER corrects DNA damage occurring in the entire genome, whereas TC-NER specifically acts on DNA damage in the transcribed strand of transcriptionally active genes. The two sub-pathways primarily differ in the recognition of DNA lesions in chromatin. GG-NER commences with the concerted action of two heterodimeric complexes, namely UV-DDB and XPC–RAD23, that encompass two XP factors (XPE and XPC), whereas TC-NER is initiated by stalling of RNA polymerase II at UV-induced DNA lesions that triggers the recruitment of TC-NER specific, non-XP factors. After damage recognition, both pathways converge into a common pathway that involves DNA unwinding, lesion verification, dual incision, DNA re-synthesis and finally ligation. In the last two decades, the core NER machinery has been meticulously studied and accurately portrayed, shifting attention to molecular

mechanisms that either regulate NER in the chromatin-context or promote the spatiotemporally accurate interplay between NER factors and various PTMs (Fig.1 and 2). In this review, we summarise the newest findings in the field and discuss emerging regulatory mechanisms ensuring NER efficiency.

Transcription Coupled-NER (TC-NER)

Stalling of elongating RNA polymerase by DNA lesions in the transcribed strand of active genes initiates fast repair of the blocking DNA damage. This process is referred to as Transcription Coupled-NER. Defects in TC-NER are associated with the severe developmental and neurological disorder Cockayne Syndrome (CS) and the much milder disorder UV sensitive syndrome (UVsS), which is primarily characterised by skin photosensitivity. Classic CS results from mutations in the Cockayne Syndrome complementation group A or B genes (CSA and CSB). A distinct, though much smaller, set of mutations in these genes underlies UVsS. Intriguingly, it was recently shown that UVsS most often relates to mutations in the KIAA1530 gene, which was subsequently renamed to UVSSA (encoding UV-stimulated scaffold protein A) [2-4]. As both disorders are characterised by impaired TC-NER, but with substantially different clinical outcomes, it is possible that the TC-NER defect only explains the common hypersensitivity to sunlight, while the neurodevelopmental abnormalities observed for CS patients may arise largely due to a defect in the CSA/CSB function in other cellular processes [5-7]. In line with this scenario, CS proteins have been implicated in other processes such as transcription [8, 9], oxidative damage repair [10, 11] and maintenance of mitochondrial DNA stability [12-14]. Whether UVSSA exerts a role in the aforementioned processes has yet to be determined.

UVSSA: a novel regulator of TC-NER

Current models describe the recruitment of the SNF2/SWI2 ATPase CSB upon stalling of elongating RNA polymerase II (RNAPIIo) to the site of damage, their transient interaction being stabilised in an ATP-dependent manner [15-17]. This step is followed by the CSB-dependent recruitment of CSA, which functions as a DCAF adaptor in the E3 ubiquitin ligase complex consisting of Cullin4A, DDB1 and Rbx1/ROC1 (CRL4[CSA]).

This complex has common architectural features with the CRL4[DDB2] complex responsible for damage recognition in GG-NER [18].

Upon identification of UVSSA as the causative gene for UVsS by whole-exome sequencing [2], microcell-mediated transfer [4] and SILAC- based proteomic approaches [3, 19], the role for the UVSSA protein in TC-NER was manifested by four research groups. Schwertman et al. and Nakazawa et al. showed that, upon UVSSA depletion, the recovery of RNA synthesis after damage induction was diminished, while unscheduled DNA synthesis was unaffected [2, 3]. In line with these results, immunostaining of UV-induced CPDs and 6–4PPs further indicated that UVSSA is dispensable for GG-NER, as UVSSA knockdown did not change the overall repair efficiency in either wild-type or CSA-deficient cells, confirming its specific role in TC-NER [4, 19]. In addition, by either mass spectrometry, or immunoprecipitations combined with western blot analyses [2-4, 19], several groups not only recognised DDB1, CSA and several TFIIH subunits as UVSSA-interacting proteins in the absence of damage, but also showed a UV- and CSA-dependent interaction with CSB and RNA polymerase II.

Three-dimensional structure prediction identified a domain of unknown function (DUF20430) near the C-terminus of UVSSA and a domain with substantial homology to the Vps-27, Hrs and STAM (VHS) domain close to the N-terminus of UVSSA. The presence of both domains is required for TC-NER activity, as shown by the lack of RNA synthesis recovery by reconstitution of several deletion mutants in UV-irradiated UVSSA-deficient cells [2]. The VHS domain has been shown to contain the CSA binding site and is likely also important for strengthening the UVSSA interaction with CSB or (other) ubiquitylated proteins. The CSA binding domain was mapped to a different region than the domain required for interaction with TFIIH, but deletion of the latter rendered HEK293T cells equally sensitive to UV-irradiation as those lacking the CSA interacting domain [19]. In contrast, ChIP experiments employing chromatin from cross-linked cells [3] indicate that UVSSA might as well be recruited to the repair complex via a RNA polymerase-dependent, but UV- and CSA/CSB-independent interaction. The latter scenario is also in agreement with the observation of GFP-UVSSA accumulation at sites of

2

local UV-C DNA damage in CSA- and CSB-deficient cells [3], suggesting that it is not the recruitment per se, but merely the stabilisation of UVSSA within the repair complex that depends on the CS proteins [3, 4, 7]. In addition, UVSSA was implicated in the dephosphorylation of elongating RNAPIIo upon stalling at a UV-induced lesion. In KPS3 cells that lack UVSSA, the hypo-phosphorylated, initiating form of RNAPII after an initial decrease upon UV-irradiation does not reappear. Such an effect is also observed in CSA- or CSB deficient cells and certain XP mutants, indicating impaired restoration of RNAPII levels, which in repair proficient cells ensures transcription re-initiation [2, 4, 20].

Interestingly, the deubiquitylating enzyme Ubiquitin-Specific Protease 7 (USP7) was also picked up as a UVSSA interaction partner, irrespectively of its cellular localisation or the presence of DNA damage [3, 19]. USP7 has been reported to target several proteins involved in the DNA damage response, as well as tumour suppressors, DNA replication proteins, viral proteins and epigenetic modulators [21-23]. USP7 depletion led to diminished RNA synthesis recovery and cell survival after UV-damage induction, at levels comparable to those observed upon UVSSA-depletion [2, 4]. UVSSA and USP7 were found to interact with the same set of TC-NER proteins. Moreover, a proteasome- and UV-dependent decrease in CSB levels was shown to depend on both UVSSA and USP7 [2]. Taken together, this data indicates the formation of a stable UVSSA-USP7 complex, which likely explains the common role for both proteins in CSB stabilisation upon DNA damage induction. A plausible model for the function of the UVSSA-USP7 complex in CSB stabilisation would require UVSSA to bring USP7 in close proximity to CSB in the TC-NER complex, thus enabling it to exert its deubiquitylating activity on CSB, eventually preventing proteasomal degradation of CSB.

Elongating RNA Polymerase degradation

Several studies have demonstrated that the UV-induced degradation of RNA polymerase is dependent on CSA and CSB, although different E3 ubiquitin ligases have been suggested to be responsible for the actual K48-linked ubiquitylation. A UV-dependent decrease in elongating RNA polymerase in is apparent in both repair-proficient and UVSSA-deficient cells [2]. Current

evidence, regarding RNAPIIo processing by UVSSA and the CS proteins, would fit into a model that supports various events upon stalling of RNA polymerase at a lesion. UV-irradiated cells lacking one of the CS proteins would initiate a signalling cascade, likely prompted by the prolonged stalling of RNAPIIo, that eventually would lead to apoptosis. This signalling response would most likely be mediated by defective TC-NER in concert with the inability to degrade RNA polymerase. However, in UVSSA-deficient cells, although TC-NER is defective, CSB- and CSA-dependent removal of RNA polymerase is still possible. The net result is not only avoiding persistently stalled RNA polymerase at the site of damage but also enabling repair via alternative pathways [2, 3]. Although it is postulated that the lesion-shielding RNA polymerase needs to be displaced from the site of damage, in order to increase the accessibility by repair factors and to allow repair, UV-mediated degradation of RNA polymerase might only be a last resort, in case the impaired transcription elongation becomes detrimental to the cell. A mechanism of backtracking of transcribing RNA polymerase would enable resumption of transcription after repair, by sliding backward along the DNA and RNA. This appears to be a more efficient process than transcription termination as a prerequisite for NER.

Backtracking of elongating RNA Polymerase and transcriptional restart

RNA polymerase backtracking has been implicated in many processes, including maintenance of genome stability, control of transcription elongation/ termination; additionally, backtracking has been suggested to possess a proofreading function [24, 25]. As opposed to backtracking, the forward translocation of RNA polymerase promoted by the DNA translocase Mfd has been shown to drive TC-NER in prokaryotes [26-28]. Subsequently to displacing stalled bacterial RNA polymerase, Mfd also recruits UvrA, which along UvrB initiates repair by attracting the incision factor UvrC. However, evidence for an essential role of backtracking in TC-NER in Escherichia coli was recently presented [29]. In an in vitro single-round runoff elongation assay, ATP-dependent pausing of RNA polymerase was shown to result from backtracking mediated by the UvrD helicase, as the extruding RNA was susceptible to cleavage by GreB and this stimulated transcription reactivation.

2

Deficiency in the transcript cleavage factors GreA and GreB, that would normally counteract backtracking by UvrD, appeared to increase the lesion repair rate and also rendered UvrD-deficient cells less sensitive to several DNA damage inducing agents. Moreover, in vitro CPD excision by UvrC appeared to be severely inhibited in the absence of UvrD, when the elongation complex was positioned in a lesion-shielding manner, compared to either the presence of UvrD or the assembly of RNA polymerase at a position upstream to the CPD. Based on this data, UvrD-induced backtracking was suggested to be the main mechanism to displace RNA polymerase from the damage during TC-NER in prokaryotes, while stimulation of its forward movement by Mfd was proposed to be mainly important for transcription reactivation after repair [29]. Whether TC-NER is also driven in eukaryotes by backtracking remains to be elucidated. Given the evolutionary conservation of TC-NER and the frequent occurrence of backtracking as a regulatory mechanism at transcription pausing sites, this scenario is not unlikely [25, 29].
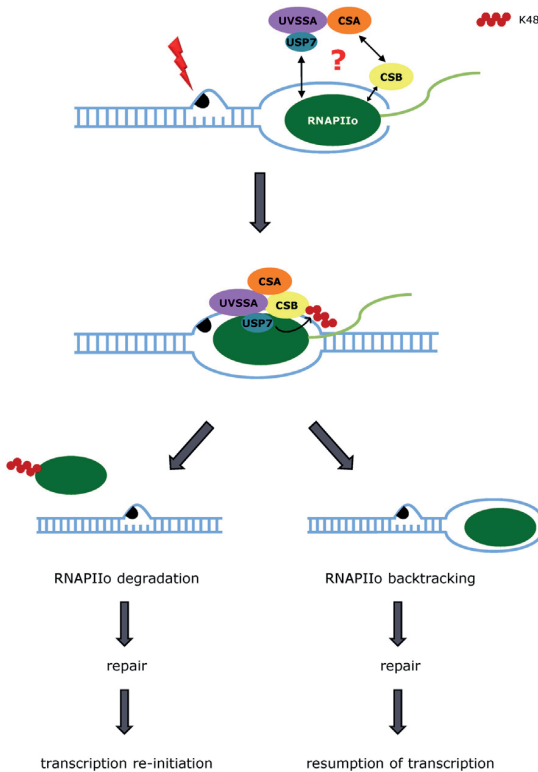

Figure 1. Upon damage-induced stalling of elongating RNA Polymerase II (RNAPIIo), the formation of the pre-incision complex is initiated by stabilisation of the RNAPIIo-CSB interaction and subsequent recruitment of CSA. UVSSA becomes part of the TC-NER complex in either a CSB/CSA-dependent interaction or by its interaction with RNAPIIo. UVSSA recruits the de-ubiquitinating protein USP7 in the vicinity of CSB, thereby removing ubiquitin chains from CSB and protecting it from degradation. Displacement of RNAPIIo from the site of damage by either its proteasomal degradation or backtracking increases accessibility to other NER factors. RNAPIIo degradation, which depends on CSA and CSB, implicates transcription termination as a requirement for repair, while backtracking enables a resumption of transcription after repair from a site relatively close to the damage. In both cases, specific chromatin remodeling is required for continuation of transcription and restoration of gene expression to original levels.

Transcription restart upon repair completion

At the cellular level, impaired TC-NER in CS or UVSSA-deficient cells results in inability to resume RNA synthesis after DNA damage. Recently, several groups demonstrated that completion of damage repair itself is not sufficient to restart the transcription machinery. Instead, recovery of transcription seems to require chromatin reorganisation so as to establish pre-damaged levels of gene expression. For example, in addition to the contribution of the histone chaperones CAF1 and ASF1 [30], the restart of stalled RNA polymerase was shown to be promoted by the SPT16 subunit of FACT (FAcilitates Chromatin Transcription), which accelerates the damage-induced exchange of histones H2A and H2B [31]. Moreover, a role in transcriptional restart upon DNA repair was recently described for the histone chaperone HIRA and the methyltransferase Dot1L, which act by stimulating H3.3 incorporation and H3K79 dimethylation, respectively [32-34]. In parallel to the chromatin relaxation required for early NER events, specific chromatin remodelling and PTMs appear to be essential for NER-completion and transcription continuation.

Global Genome NER (GG-NER)

Elaborating on the handoff between the two GG-NER sensor complexes

Given the fact that UV-damage recognition appears to be one of the rate-limiting steps in NER [35], the intricate interplay between the two sensor complexes, UV-DDB and XPC-Rad23-Centrin, is paramount. Although DDB2 is dispensable for the in vitro reconstitution of the NER reaction [36], its in vivo presence has been demonstrated to significantly stimulate XPC binding to UV-damaged chromatin [37, 38], especially at lesions otherwise intractable by XPC, such as CPDs [39].

Several hypotheses have been raised to exemplify the DDB2-to-XPC handover. It was initially postulated that a direct interaction between these two proteins might exist. Though there have been reports supporting this scenario [40, 41], mapping specific interaction-domains and validation of this interaction by means of mass spectrometry have remained elusive,

2

indicating that if DDB2 and XPC indeed interact, they do so very transiently. On the other hand, it is by now well understood that DDB2 regulates the retention time of both UV damage-recognition complexes, as part of the CUL4A-DDB1-RBX1 ubiquitin ligase (CRL[DDB2]) [42]. CRL[DDB2] promotes the ubiquitylation of XPC and itself upon UV irradiation [41] with the kinetics of this modification, not coincidentally, being very similar to the association with photo-lesions [43]. Whilst DDB2 poly-ubiquitylation leads to its dissociation from the sites of UV damage and its proteasomal degradation [41, 44], the atypical poly-ubiquitylation of XPC increases its stability at photo-lesions [41, 43]. Although the swift, UV-mediated proteasomal degradation of DDB2 is counterintuitive, recent reports have sought to elucidate its significance. On first instance, it was demonstrated that the residence time of DDB2 at photo-lesions is regulated by competing PTMs. DDB2 poly-ADP ribosylation (PARylation) and ubiquitylation occur at the same region, with the former inhibiting the latter, therefore increasing the half-life of DDB2 [45]. Moreover, it has become clear that the timely removal of DDB2, and later XPC, is controlled by its ubiquitylation status and its segregation by VCP [46], forming an additional regulatory level exerted by ubiquitylation of UV-damage sensor complexes.

Intriguingly, XPC too appears to be tightly modulated by multiple PTMs upon UV irradiation, as it was shown not only to be ubiquitylated at several sites [47] but also SUMOylated [48]. These two modifications, in contrast to the competitive nature of PARylation and ubiquitylation of DDB2, appear to behave cooperatively. More explicitly, XPC SUMOylation promotes the accumulation of the SUMO-targeted E3 ubiquitin ligase RNF111, which in turn further decorates XPC with non-proteolytic K63-ubiquitin chains [43]. Given the fact that XPC is intrinsically unstable as a monomer, necessitating its association with stabilising partners hRad23A/B [49, 50], it is striking that upon UV irradiation and XPC binding to damaged chromatin, hRad23A/B dissociates [49]. Concomitantly, XPC ubiquitylation reaches its peak [43], raising the possibility that non-canonical XPC ubiquitylation might be initially read by downstream effectors in a protective manner that will stabilise XPC at the sites of damage. Following UV-damage recognition and verification, ubiquitylated XPC is removed by VCP in order to promote the build-up of the
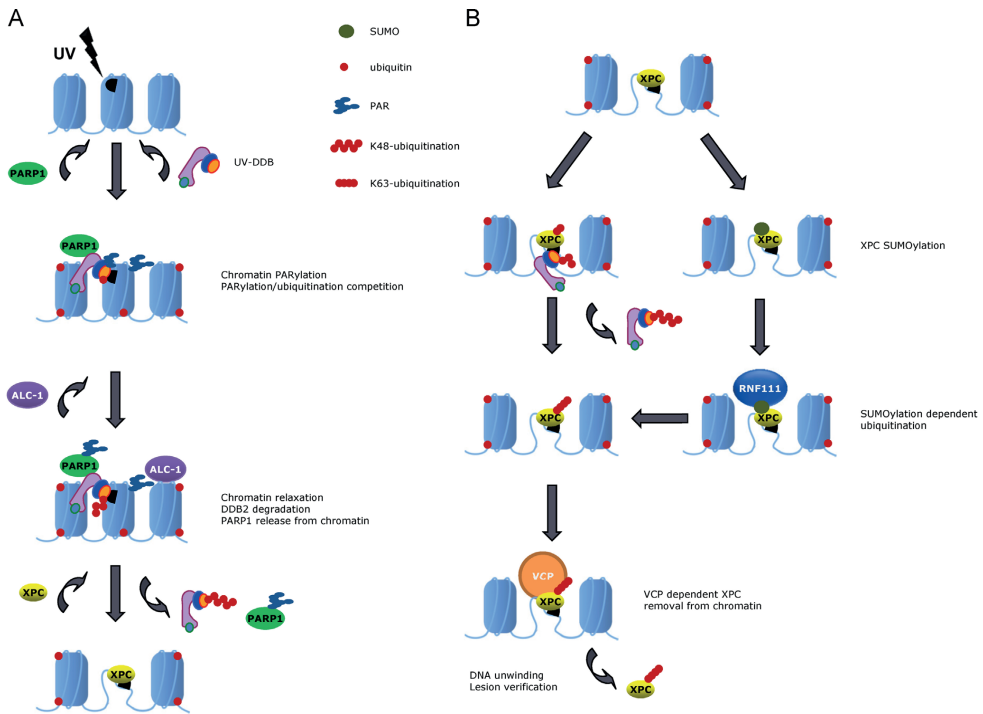
downstream repair complex [46].

Figure 2. (A) UV-DDB is the first NER factor to accumulate at UV damage, as part of the Cullin-RING-E3 ubiquitin ligase complex CUL4A- DDB1-RBX1. This complex binds to UV damage and, in concert with PARP1, tightly regulates the steady-state levels and retention time of DDB2 by opposing modifications (PARylation and ubiquitylation). PARP1 creates accessibility for recruitment of NER factors by its ability to disrupt chromatin structure and by promoting the recruitment of Swi2/Snf2 chromatin remodeler ALC1, thereby stimulating the recruitment of XPC to assemble a functional repair complex. (B) XPC ubiquitylation is mediated by the UV-DDB complex and by its SUMOylation that promotes the assembly of the SUMO-targeted E3 ubiquitin ligase RNF111, which in turn further decorates XPC with non-proteolytic K63-ubiquitin chains. Following UV-damage recognition and verification, ubiquitylated XPC is removed by VCP to promote the build-up of the downstream repair complex.

Restructuring chromatin around UV damage

Like other DNA metabolism processes, NER is to a great extent regulated by chromatin status. Highly compacted heterochromatin poses a challenge for efficient NER, manifested by the relatively slow repair of bulky DNA lesions [51], most likely necessitating carefully modulated and spatiotemporally precise chromatin remodeling events. Such events usually promote transient

2

chromatin decompaction, therefore granting access to the repair machinery at sites of damage. Although such open chromatin conformation is beneficial at early stages, upon completion of DNA repair, chromatin environment needs to be restored to its original state so that epigenetic marks and transcriptional status can be maintained [52].

While it has been demonstrated that UV damage per se results in histone eviction [53], local chromatin de-condensation is more commonly achieved by PTMs on core histones and the incorporation of histone variants. Alternatively, nucleosome sliding or nucleosome disassembly can take place, usually modulated by ATP-dependent chromatin remodelers. As the first factor to identify UV photo- lesions, DDB2 facilitates local chromatin unfolding in all the aforementioned ways. Independently of its association in the CRL ubiquitin ligase complex, DDB2 was shown to promote chromatin decompaction, histone eviction and, therefore, the assembly of the NER machinery [49]. Recent reports have reinforced this notion by showing that DDB2 can promote PARP1-dependent chromatin poly-ADP ribosylation [45, 54]. PARylation of histones and other chromatin proteins usually leads to a less rigid, looser chromatin environment. In addition, DDB2-induced chromatin PARylation facilitates the recruitment of the chromatin remodeler ALC1 [45], which can further restructure UV-damage containing nucleosomes. As part of the CRL E3 ligase complex, DDB2 induces the ubiquitylation of all core histones [55-57], resulting in nucleosome destabilisation, H2A-H2B dimer loss and decreased histone-DNA interaction, all hallmarks of accessible chromatin.

Regulation of incision events

Although NER recognition complexes dictate to a great extent the rate of the NER reaction, the spatiotemporal coordination of the pre-and post-incision stages of NER also appears to be of paramount importance. Tight regulation of new repair events (incision), when gap-filling/sealing has not been completed, is essential to prevent generation of DNA strand-breaks that could lead to illegitimate recombinogenic events. Indeed, generation of repair gaps by inhibition of DNA repair synthesis leads to saturation of incision events at very low UV doses [34]. Surprisingly, RPA appears to exert

2

a key role in surveilling incision events, being the sole NER protein thus far reported to be present both pre- and post-incision [58, 59]. More specifically, RPA is recruited prior to incision and remains associated at the repair-site after recruitment of post-incision factors, until the gap-filling and ligation steps take place. In UV-irradiated, non-cycling cells this RPA-coordination is independent of phosphorylation by the related ATR kinase [58, 60]. In contrast, in UV-irradiated, cycling cells RPA is released from PML bodies in an ATR dependent manner, most likely to compensate for RPA accumulation at stalled replication forks. Supporting the notion that RPA availability constitutes a NER-bottleneck is the fact that persistently stalled replication forks inhibit NER in trans by sequestering RPA from sites of damage [59]. Furthermore, in line with a limited RPA pool is the recent finding that excessive amounts of ssDNA in replicating cells lead to RPA depletion, particularly in the absence of ATR [61].

CONCLUSIONS

Although an extraordinarily broad range of proteins has been implicated in NER, strides in our current understanding of the chromatin micro-environment make it safe to assume that more factors remain yet unidentified. The recent discovery of UVSSA and USP7 in TC-NER certainly point towards that direction. Despite the fact that the core NER reaction is well studied, we are just beginning to comprehend how NER-related factors are spatiotemporally modulated in the restrictive chromatin environment. Recent studies have begun to shed more light on the importance of post-translational modifications in orchestrating NER, ensuring its efficient "wiring' with other concomitant events, such as signalling cascades and transcriptional responses. Furthermore, the potential of competitive or cooperative action between PTMs during DNA damage, as shown for DDB2 and XPC, raises the possibility of elaborate crosstalk between NER factors. This additionally hints towards the assumption that several regulatory levels, having thus far received little attention, safeguard the efficacy of NER. Data obtained by live imaging, screening assays and mass-spectrometry, along with the ever-more effective bio-informatical integration of this data, will help us elucidate further this intricate choreography of NER proteins in the near future.

REFERENCES

1. DiGiovanna, J.J. and K.H. Kraemer, Shining a light on xeroderma pigmentosum. J Invest Dermatol, 2012. 132(3 Pt 2): p. 785-96.

2. Nakazawa, Y., et al., Mutations in UVSSA cause UV-sensitive syndrome and impair RNA polymerase IIo processing in transcription-coupled nucleotide-excision repair. Nat Genet, 2012. 44(5): p. 586-92.

3. Schwertman, P., et al., UV-sensitive syndrome protein UVSSA recruits USP7 to regulate transcription-coupled repair. Nat Genet, 2012. 44(5): p. 598-602.

4. Zhang, X., et al., Mutations in UVSSA cause UV-sensitive syndrome and destabilize ERCC6 in transcription-coupled DNA repair. Nat Genet, 2012. 44(5): p. 593-7.

5. Brooks, P.J., Blinded by the UV light: how the focus on transcription-coupled NER has distracted from understanding the mechanisms of Cockayne syndrome neurologic disease. DNA Repair (Amst), 2013. 12(8): p. 656-71.

6. Cleaver, J.E., Photosensitivity syndrome brings to light a new transcription-coupled DNA repair cofactor. Nat Genet, 2012. 44(5): p. 477-8.

7. Schwertman, P., W. Vermeulen, and J.A. Marteijn, UVSSA and USP7, a new couple in transcription-coupled DNA repair. Chromosoma, 2013. 122(4): p. 275-84.

8. Balajee, A.S., et al., Reduced RNA polymerase II transcription in intact and permeabilized Cockayne syndrome group B cells. Proc Natl Acad Sci U S A, 1997. 94(9): p. 4306-11.

9. van Gool, A.J., et al., The Cockayne syndrome B protein, involved in transcription-coupled DNA repair, resides in an RNA polymerase II-containing complex. Embo j, 1997. 16(19): p. 5955-65.

10. Menoni, H., J.H. Hoeijmakers, and W. Vermeulen, Nucleotide excision repair-initiating proteins bind to oxidative DNA lesions in vivo. J Cell Biol, 2012. 199(7): p. 1037-46.

11. Stevnsner, T., et al., The role of Cockayne Syndrome group B (CSB) protein in base excision repair and aging. Mech Ageing Dev, 2008. 129(7-8): p. 441-8.

12. Aamann, M.D., et al., Cockayne syndrome group B protein promotes mitochondrial DNA stability by supporting the DNA repair association with the mitochondrial membrane. Faseb j, 2010. 24(7): p. 2334-46.

13. Scheibye-Knudsen, M., D.L. Croteau, and V.A. Bohr, Mitochondrial deficiency in Cockayne syndrome. Mech Ageing Dev, 2013. 134(5-6): p. 275-83.

14. Stevnsner, T., et al., Mitochondrial repair of 8-oxoguanine is deficient in Cockayne syndrome group B. Oncogene, 2002. 21(57): p. 8675-82.

15. Fousteri, M., et al., Cockayne syndrome A and B proteins differentially regulate recruitment of chromatin remodeling and repair factors to stalled RNA polymerase II in vivo. Mol Cell, 2006. 23(4): p. 471-82.

16.   Lake, R.J. and H.Y. Fan, Structure, function and regulation of CSB: a multi-talented gymnast. Mech Ageing Dev, 2013. 134(5-6): p. 202-11.

17.   Lake, R.J., et al., UV-induced association of the CSB remodeling protein with chromatin requires ATP-dependent relief of N-terminal autorepression. Mol Cell, 2010. 37(2): p. 235-46.

18.   Fischer, E.S., et al., The molecular basis of CRL4DDB2/CSA ubiquitin ligase architecture, targeting, and activation. Cell, 2011. 147(5): p. 1024-39.

19.   Fei, J. and J. Chen, KIAA1530 protein is recruited by Cockayne syndrome complementation group protein A (CSA) to participate in transcription-coupled repair (TCR). J Biol Chem, 2012. 287(42): p. 35118-26.

20.   Rockx, D.A., et al., UV-induced inhibition of transcription involves repression of transcription initiation and phosphorylation of RNA polymerase II. Proc Natl Acad Sci U S A, 2000. 97(19): p. 10503-8.

21.   Jagannathan, M., et al., A role for USP7 in DNA replication. Mol Cell Biol, 2014. 34(1): p. 132-45.

22.   Nicholson, B. and K.G. Suresh Kumar, The multifaceted roles of USP7: new therapeutic opportunities. Cell Biochem Biophys, 2011. 60(1-2): p. 61-8.

23.   Sheng, Y., et al., Molecular recognition of p53 and MDM2 by USP7/HAUSP. Nat Struct Mol Biol, 2006. 13(3): p. 285-91.

24.   Nudler, E., RNA polymerase backtracking in gene regulation and genome instability. Cell, 2012. 149(7): p. 1438-45.

25.   Sahoo, M. and S. Klumpp, Backtracking dynamics of RNA polymerase: pausing and error correction. J Phys Condens Matter, 2013. 25(37): p. 374104.

26.   Ganesan, A., G. Spivak, and P.C. Hanawalt, Transcription-coupled DNA repair in prokaryotes. Prog Mol Biol Transl Sci, 2012. 110: p. 25-40.

27.   Park, J.S., M.T. Marr, and J.W. Roberts, E. coli Transcription repair coupling factor (Mfd protein) rescues arrested complexes by promoting forward translocation. Cell, 2002. 109(6): p. 757-67.

28.   Selby, C.P. and A. Sancar, Molecular mechanism of transcription-repair coupling. Science, 1993. 260(5104): p. 53-8.

29.   Epshtein, V., et al., UvrD facilitates DNA repair by pulling RNA polymerase backwards. Nature, 2014. 505(7483): p. 372-7.

30.   Polo, S.E., D. Roche, and G. Almouzni, New histone incorporation marks sites of UV repair in human cells. Cell, 2006. 127(3): p. 481-93.

31.   Dinant, C., et al., Enhanced chromatin dynamics by FACT promotes transcriptional restart after UV-induced DNA damage. Mol Cell, 2013. 51(4): p. 469-79.

32.   Adam, S., S.E. Polo, and G. Almouzni, Transcription recovery after DNA damage requires chromatin priming by the H3.3 histone chaperone HIRA. Cell, 2013. 155(1):

2

p. 94-106.

33. Mandemaker, I.K., W. Vermeulen, and J.A. Marteijn, Gearing up chromatin: A role for chromatin remodeling during the transcriptional restart upon DNA damage. Nucleus, 2014. 5(3): p. 203-10.

34. Oksenych, V., et al., Histone methyltransferase DOT1L drives recovery of gene expression after a genotoxic attack. PLoS Genet, 2013. 9(7): p. e1003611.

35. Luijsterburg, M.S., et al., Stochastic and reversible assembly of a multiprotein DNA repair complex ensures accurate target site recognition and efficient repair. J Cell Biol, 2010. 189(3): p. 445-63.

36. Aboussekhra, A., et al., Mammalian DNA nucleotide excision repair reconstituted with purified protein components. Cell, 1995. 80(6): p. 859-68.

37. Moser, J., et al., The UV-damaged DNA binding protein mediates efficient targeting of the nucleotide excision repair complex to UV-induced photo lesions. DNA Repair (Amst), 2005. 4(5): p. 571-82.

38. Nishi, R., et al., UV-DDB-dependent regulation of nucleotide excision repair kinetics in living cells. DNA Repair (Amst), 2009. 8(6): p. 767-76.

39. Sugasawa, K., et al., A multistep damage recognition mechanism for global genomic nucleotide excision repair. Genes Dev, 2001. 15(5): p. 507-21.

40. Fei, J., et al., Regulation of nucleotide excision repair by UV-DDB: prioritization of damage recognition to internucleosomal DNA. PLoS Biol, 2011. 9(10): p. e1001183.

41. Sugasawa, K., et al., UV-induced ubiquitylation of XPC protein mediated by UV-DDB-ubiquitin ligase complex. Cell, 2005. 121(3): p. 387-400.

42. Groisman, R., et al., The ubiquitin ligase activity in the DDB2 and CSA complexes is differentially regulated by the COP9 signalosome in response to DNA damage. Cell, 2003. 113(3): p. 357-67.

43. Poulsen, S.L., et al., RNF111/Arkadia is a SUMO-targeted ubiquitin ligase that facilitates the DNA damage response. J Cell Biol, 2013. 201(6): p. 797-807.

44. Rapic-Otrin, V., et al., Sequential binding of UV DNA damage binding factor and degradation of the p48 subunit as early events after UV irradiation. Nucleic Acids Res, 2002. 30(11): p. 2588-98.

45. Pines, A., et al., PARP1 promotes nucleotide excision repair through DDB2 stabilization and recruitment of ALC1. J Cell Biol, 2012. 199(2): p. 235-49.

46. Puumalainen, M.R., et al., Chromatin retention of DNA damage sensors DDB2 and XPC through loss of p97 segregase causes genotoxicity. Nat Commun, 2014. 5: p. 3695.

47. Povlsen, L.K., et al., Systems-wide analysis of ubiquitylation dynamics reveals a key role for PAF15 ubiquitylation in DNA-damage bypass. Nat Cell Biol, 2012. 14(10): p. 1089-98.

48.   Wang, Q.E., et al., DNA repair factor XPC is modified by SUMO-1 and ubiquitin fol-
       lowing UV irradiation. Nucleic Acids Res, 2005. 33(13): p. 4023-34.

49.   Luijsterburg, M.S., et al., DDB2 promotes chromatin decondensation at UV-induced
       DNA damage. J Cell Biol, 2012. 197(2): p. 267-81.

50.   Ng, J.M., et al., A novel regulation mechanism of DNA repair by damage-induced and
       RAD23-dependent stabilization of xeroderma pigmentosum group C protein. Genes
       Dev, 2003. 17(13): p. 1630-45.

51.   van Hoffen, A., et al., Nucleotide excision repair and its interplay with transcription.
       Toxicology, 2003. 193(1-2): p. 79-90.

52.   Green, C.M. and G. Almouzni, Local action of the chromatin assembly factor CAF-1
       at sites of nucleotide excision repair in vivo. Embo j, 2003. 22(19): p. 5163-74.

53.   Duan, M.R. and M.J. Smerdon, UV damage in DNA promotes nucleosome unwrap-
       ping. J Biol Chem, 2010. 285(34): p. 26295-303.

54.   Robu, M., et al., Role of poly(ADP-ribose) polymerase-1 in the removal of UV-in-
       duced DNA lesions by nucleotide excision repair. Proc Natl Acad Sci U S A, 2013.
       110(5): p. 1658-63.

55.   Guerrero-Santoro, J., et al., The cullin 4B-based UV-damaged DNA-binding protein
       ligase binds to UV-damaged chromatin and ubiquitinates histone H2A. Cancer Res,
       2008. 68(13): p. 5014-22.

56.   Kapetanaki, M.G., et al., The DDB1-CUL4ADDB2 ubiquitin ligase is deficient in xe-
       roderma pigmentosum group E and targets histone H2A at UV-damaged DNA sites.
       Proc Natl Acad Sci U S A, 2006. 103(8): p. 2588-93.

57.   Wang, H., et al., Histone H3 and H4 ubiquitylation by the CUL4-DDB-ROC1 ubiquitin
       ligase facilitates cellular response to DNA damage. Mol Cell, 2006. 22(3): p. 383-94.

58.   Overmeer, R.M., et al., Replication protein A safeguards genome integrity by con-
       trolling NER incision events. J Cell Biol, 2011. 192(3): p. 401-15.

59.   Tsaalbi-Shtylik, A., et al., Persistently stalled replication forks inhibit nucleotide exci-
       sion repair in trans by sequestering Replication protein A. Nucleic Acids Res, 2014.
       42(7): p. 4406-13.

60.   Auclair, Y., et al., ATR kinase is required for global genomic nucleotide excision repair
       exclusively during S phase in human cells. Proc Natl Acad Sci U S A, 2008. 105(46):
       p. 17896-901.

61.   Toledo, L.I., et al., ATR prohibits replication catastrophe by preventing global exhaus-
       tion of RPA. Cell, 2013. 155(5): p. 1088-103.

2

3

The de-ubiquitylating enzymes USP26 and USP37 regulate homologous recombination by counteracting RAP80

Dimitris Typas*, Martijn S. Luijsterburg*, Wouter W. Wiegant, Michaela Diakatou, Angela Helfricht, Peter E. Thijssen, Bram van de Broek, Leon H. Mullenders, and Haico van Attikum

* These authors contributed equally to this work

ABSTRACT

The faithful repair of DNA double-strand breaks (DSBs) is essential to safeguard genome stability. DSBs elicit a signalling cascade involving the E3 ubiquitin ligases RNF8/RNF168 and the ubiquitin-dependent assembly of the BRCA1-Abraxas-RAP80-MERIT40 complex. The association of BRCA1 with ubiquitin conjugates, which occurs in a RAP80-dependent manner, is known to be inhibitory to DSB repair by homologous recombination (HR). However, the precise regulation of this mechanism remains poorly understood. By performing genetic screens, we identified USP26 and USP37 as key de-ubiquitylating enzymes (DUBs) that limit the repressive impact of RNF8/RNF168 on HR. Both DUBs are recruited to bona fide DSBs where they actively remove RNF168-induced ubiquitin conjugates. Depletion of USP26 or USP37 disrupts the execution of HR and this effect is alleviated by the simultaneous depletion of RAP80. In addition, we demonstrate that these DUBs prevent the ubiquitin-dependent sequestration of BRCA1 via the BRCA1-Abraxas-RAP80-MERIT40 complex, allowing BRCA1 to form a complex and cooperate with PALB2-BRCA2-RAD51 in HR. These findings reveal a novel ubiquitin-dependent mechanism that orchestrates the spatial assembly of distinct BRCA1-containing complexes for efficient repair of DSBs by HR.

3

INTRODUCTION

DNA double-strand breaks (DSBs) pose a considerable threat to the stability of the human genome and their timely repair is essential to safeguard genome stability and counteract tumour development [1]. Cells activate robust signalling pathways in response to DSBs that coordinate cell cycle progression, changes in chromatin structure and DNA repair [2, 3]. Eukaryotic cells primarily utilise homologous recombination (HR) or non-homologous end-joining (NHEJ) to remove DSBs from their genomes.

A key feature of the DNA damage response (DDR) is the rapid assembly of signalling and repair factors in the vicinity of DSBs, by progressively modifying histones and DNA repair enzymes [4, 5]. An initial phosphorylation-dependent cascade of post-translational modifications in DSB-containing chromatin requires the ATM kinase and culminates into the association of MDC1 with phosphorylated histone H2A variant H2AX (γH2AX) [6]. The binding of the RNF8 E3 ubiquitin ligase to MDC1 subsequently initiates a ubiquitylation-dependent cascade, involving the recruitment of the E3 ubiquitin ligase RNF168 in cooperation with the E2 ubiquitin-conjugating enzyme UBC13 [7, 8]. The activity of these enzymes contributes to the ubiquitylation of K13/15 on histone H2A/H2AX [9, 10], as well as the ubiquitin-dependent assembly of 53BP1 [11], RAD18 [12] and the BRCA1-Abraxas-RAP80-MERIT40 (or BRCA1-A) complex [13-16] onto DSB-neighbouring chromatin.

This ubiquitylation cascade is tightly controlled by sophisticated mechanisms that entail chromatin remodelling enzymes [17-19] and additional ubiquitin ligases [20]. Furthermore, it has recently become clear that the removal of ubiquitin by specific de-ubiquitylating enzymes (DUBs) represents an equally important regulatory mechanism in the DDR [21-24]. The human genome contains ~90 potential DUBs that belong to five distinct subfamilies: ubiquitin-specific proteases (USPs), ubiquitin carboxy-terminal hydrolases (UCHs), ovarian tumour proteases (OTUs), Machado-Joseph disease enzymes (MJDs) and JAB1/MPN/MOV34 metalloenzymes (JAMMs). A number of DUBs have been linked to reversing RNF8/RNF168-mediated chromatin ubiquitylation during DNA damage signalling [21, 25] and a recent genetic

screening approach identified many DUBs with potential roles in the DDR [26].

Although the principles underlying the RNF8 signalling pathway are by now well understood, we are only beginning to comprehend how this pathway is linked to the actual repair of DSBs through the major repair pathways NHEJ [27] and HR [28-30]. During HR, the ends of a DSB are resected to expose 3' single-stranded DNA (ssDNA) overhangs, which are rapidly coated with the ssDNA-binding protein RPA. Following resection, the PALB2 protein is recruited by BRCA1 and subsequently facilitates the assembly of BRCA2 [31, 32]. This, in turn, promotes the exchange of RPA with RAD51, which drives the search for and pairing with a homologous sequence, as well as the exchange of homologous DNA during the final steps of HR [31-33]. BRCA1 is incorporated into distinct multi-protein complexes, including BRCA1-PALB2-BRCA2-RAD51 and BRCA1-Abraxas-RAP80-MERIT40 [34]. Strikingly, while the BRCA1-PALB2-BRCA2-RAD51 complex promotes HR, the BRCA1-Abraxas-RAP80-MERIT40 complex functionally antagonises this repair process by sequestering BRCA1 from HR sites by binding to RNF8/RNF168-ubiquitylated chromatin [16, 35-40]. These findings suggest that distinct BRCA1-containing complexes can differentially affect HR in a manner dependent on DNA damage-induced ubiquitylation. Remarkably, little is known about the involvement of DUBs in regulating BRCA1-dependent HR.

Through genetic screens we identified the de-ubiquitylating enzymes USP26 and USP37 as key factors critical for DSB repair by HR. Mechanistically, we show that by removing RNF168-induced ubiquitin conjugates distal from DSBs, these enzymes prevent the ubiquitin-dependent sequestration of BRCA1 through the BRCA1-Abraxas-RAP80-MERIT40 complex, ultimately allowing BRCA1 to form a complex with PALB2-BRCA2-RAD51 and execute HR. Thus, these enzymes promote HR by limiting the repressive impact of RAP80 on HR. These findings reveal a novel ubiquitin-dependent mechanism that orchestrates the spatial assembly and function of HR complexes at DSBs.

RESULTS

A screen for DUBs reveals novel regulators of 53BP1 and RAD51

The BRCA1 protein is incorporated into distinct multi-protein complexes that are not all competent in promoting HR. While the BRCA1-PALB2-BRCA2-RAD51 complex promotes HR, the BRCA1-Abraxas-RAP80-MERIT40 complex functionally antagonises this repair process by sequestering BRCA1 from HR sites by binding to RNF8/RNF168-ubiquitylated chromatin [16, 35-40]. These findings suggest that distinct BRCA1-containing complexes can differentially affect HR in a manner dependent on RNF8/RNF168 damage-induced ubiquitylation. Although the responsible E3 ubiquitin ligases RNF8 and RNF168 have been characterised [7, 8, 13-15], potential DUBs that play a role in this ubiquitin-dependent regulation of HR remain elusive. In order to identify such proteins, we performed an over-expression screen using a FLAG-tagged cDNA library of ~60 human DUBs (Supplemental Fig. 1A) in human U2OS cells (Fig. 1A). Specifically, we monitored if DUB over-expression simultaneously antagonises the ionising radiation (IR)-induced formation of 53BP1 foci, a read-out for RNF168-mediated ubiquitylation [11], as well as the IR-induced focal accumulation of RAD51, a measure of HR efficiency. Given that 53BP1 directly binds to RNF168-induced ubiquitin conjugates [9, 11], we reasoned that DUBs modulating both these processes are likely to regulate RNF168-mediated HR events.

Imaging-based analysis revealed that most DUBs did not appreciably alter the IR-induced accumulation of 53BP1 or RAD51 (Fig. 1B; black circles – see also Supplemental Fig. 1B,C). However, a subset of DUBs predominantly impinged on 53BP1 accrual (Fig. 1B; green circles), such as the earlier reported enzyme USP44, [21] (Supplemental Fig. 1D), while another set of DUBs mainly impacted RAD51 foci formation (Fig. 1B; blue circles), including the previously described USP1 [41]. Only a small number of DUBs affected both 53BP1 and RAD51 recruitment simultaneously (Fig. 1B; red circles), including USP29, an enzyme linked to H2A de-ubiquitylation [21], and the recently reported HR modulator DUB3 (Supplemental Fig. 1D,E) [42]. The

fact that we identified various published DUBs demonstrates the validity of our screen. Importantly, among the DUBs that suppressed both 53BP1 and RAD51 IRIF formation, USP26 and USP37 emerged as novel candidates (Fig. 1B and Supplemental Fig. 1D,E). We could not distinguish a common pattern in the impact of DUBs on 53BP1 or RAD51 foci formation within USP, UCH, MJD, JAMM, OTU or unclassified DUBs (Supplemental Fig. 1B-E), suggesting this is a unique property of the identified enzymes. Thus, via our screen, we identified USP26 and USP37 as potential novel regulators of 53BP1 and RAD51.
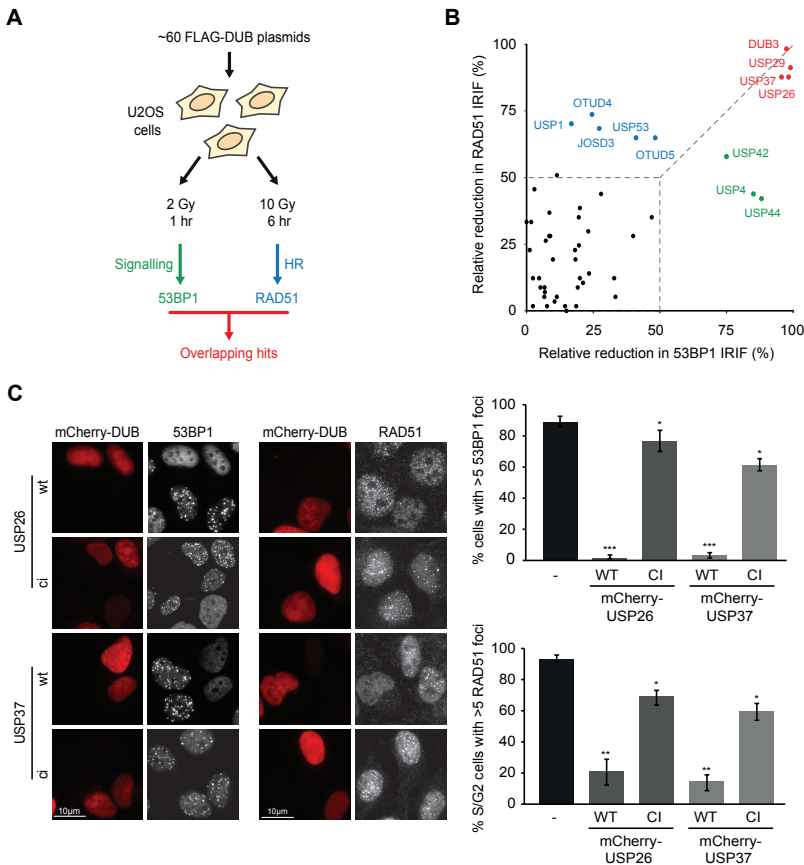

Figure 1. DUB screen for regulators of 53BP1 and RAD51 IRIF formation. (A) Experimental design of the DUB over-expression screens. (B) Bi-dimensional representation of the relative decrease in 53BP1 (x-axis) and RAD51 (y-axis) IRIF formation upon over-expression of FLAG-tagged DUBs. (C) Impact of the expression of wild-type (WT) or catalytic inactive (CI) mCherry-tagged DUBs (red) on 53BP1 (white; left panel) or RAD51 IRIF formation (white; right panel) in mAG-geminin-expressing (images not shown) S/G2 cells. Quantified data are represented as mean ± S.D. (n=3). *, P<0.05, **, P<0.01, ***, P<0.001 (student's t test). See also Supplementary Figure 1.

USP26 and USP37 reverse RNF168-induced ubiquitylation at DSBs

To validate and extend these findings, we generated mCherry- and GFP-tagged versions of USP26 and USP37. Over-expression of these DUBs did not change the accumulation of γH2AX, MDC1, and RNF8 (Supplemental Fig. 2A), yet abrogated ubiquitin conjugation and all events downstream of it, including the assembly of ubiquitin-binding factors RNF168, RAP80, BRCA1 and 53BP1 after IR in a catalytic-dependent manner (Fig. 1C and Supplemental Fig. 2B). Both DUBs were rapidly recruited to laser-induced DNA damage tracks (Supplemental Fig. 2C). Given the multitude of DNA lesions inflicted by laser micro-irradiation, we additionally used a U2OS cell line in which DSBs are specifically induced by targeting the LacR-tagged FokI nuclease to a genomic locus containing LacO repeats [43]. In line with the results obtained by laser micro-irradiation, both USP26 and USP37 accumulated at bona fide, FokI-induced DSBs marked by γH2AX (Fig. 2A,B). Importantly, USP26 and USP37 were able to remove ubiquitin conjugates at these DSBs in a manner dependent on their catalytic activity, as well as their C-terminal ubiquitin-binding domains (UIMs) (Fig. 2B,C and Supplemental Fig. 2B (FK2 foci), 2D-E). Strikingly, loss of these UIMs did not affect recruitment of the DUBs to FokI-induced DSBs (Supplemental Fig. 2E). This suggests that both DUBs can directly reverse RNF168-induced ubiquitin conjugation. Indeed, when mCherry-LacR-RNF8 or mCherry-LacR-RNF168 was tethered to a LacO array to induce local chromatin ubiquitylation [18, 44, 45], robust accumulation of both DUBs was observed (Fig. 2D), indicating that these DUBs can recognise RNF8/RNF168-induced ubiquitin moieties. Furthermore, we examined if our DUBs affect the ubiquitylation of chromatin substrates by RNF168 immobilsed at the LacO array or the subsequent recognition of ubiquitylated-H2A-type histones by 53BP1. Both USP26 and USP37 reduced FK2 (Supplemental Fig. 3A) and 53BP1 (Supplemental Fig. 3B) accumulation at the array, implying that they directly remove RNF168-induced ubiquitylation. RNF168 targets H2A-type histones for ubiquitylation [9, 10]. Interestingly, ectopic expression of USP37 moderately decreased RNF168-induced H2A ubiquitylation [9, 46], while expression of USP26 nearly eliminated such ubiquitylation (Fig. 2E). Thus, our results suggest that USP26 and USP37 are able to bind to chromatin modified by RNF8/RNF168

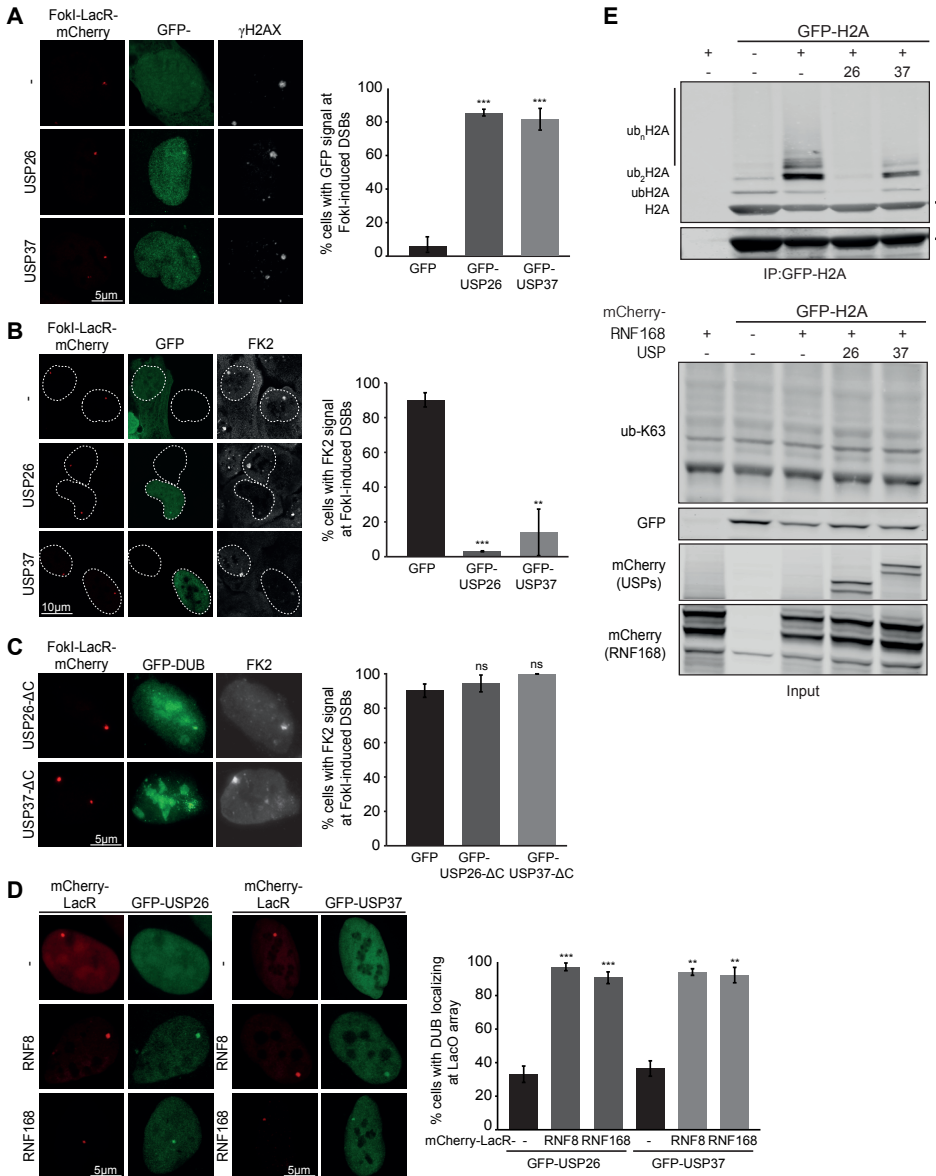and reverse ubiquitylation induced by these E3 ligases at DSBs.

Figure 2. USP26 and USP37 accumulate at DSBs and regulate chromatin ubiquitylation.
(A) Recruitment of the indicated GFP fusion proteins to FokI-mCherry-LacR-induced DSBs marked by γH2AX (white) in cells containing a LacO array. (B) As in A, but stained for ubiquitin-FK2 (white). (C) Recruitment of GFP-tagged DUBs lacking their C-termini (ΔC; green) and their impact on ubiquitin-FK2 at FokI-induced DSBs (white). (D) Recruitment of GFP-tagged DUBs upon tethering of the indicated mCherry-LacR fusion proteins in cells containing a LacO array. (E) IP of GFP-H2A under denaturing conditions in the absence or presence of mCherry-RNF168 and the indicated mCherry-tagged DUBs. Quantified data are represented as mean ± S.D. (n=3). *, P<0.05, **, P<0.01, ***, P<0.001 (student's t test).

Loss of USP26 or USP37 impairs DSB repair

To address if the identified DUBs play a role in HR under physiological conditions, USP26 and USP37 were depleted using independent siRNAs. Immunoblotting (Fig. 3A) and RT-qPCR (Supplemental Fig. 4A) analysis confirmed that the protein and mRNA levels of both DUBs were dramatically reduced. Loss of these DUBs led to a significant increase in IR-induced ubiquitin conjugates (Fig. 3B) and accumulation of the ubiquitin-binding protein 53BP1 (Supplemental Fig. 4B), suggesting that USP26 and USP37 control the levels of DSB-induced ubiquitylation. Surprisingly, however, depletion of either DUB also resulted in a clear reduction of IR-induced PALB2 and RAD51 (Fig. 3C) accumulation, indicating that excessive DSB-induced ubiquitylation disrupts HR. In further agreement with a physiological role of these DUBs in regulating HR, loss of USP26 or USP37 resulted in defective accumulation of the CtIP nuclease and moderately decreased DNA-end resection, assayed by RPA foci formation (Supplemental Fig. 4C).

Flow cytometric analysis of DR-GFP cells confirmed that USP26 or USP37 depletion leads to a significant defect in HR (Fig. 4A). Notably, over-expression of mCherry-tagged RNF8 or RNF168 also strongly inhibited HR (Fig. 4B). Thus, the over-expression of RNF8/168 phenocopied the depletion of USP26/37 as both conditions trigger excessive chromatin ubiquitylation. The effects on HR were not due to alterations in the cell cycle as cell cycle profiles were unchanged under these conditions (Supplemental Fig. 5A,B). Depletion of USP26 or USP37 also rendered cells highly sensitive to a poly(ADP-ribose) polymerase (PARP) inhibitor, which is a hallmark of HR-deficient cells such as those lacking BRCA2 (Fig. 4C) [47].

Having shown that USP26 and USP37 regulate HR, we next sought to address if these enzymes affect the other major DSB repair pathway, non-homologous end-joining (NHEJ). Using the flow cytometry-based EJ5-GFP reporter assay to monitor NHEJ efficiency [48], we found that USP26 or USP37 depletion substantially impaired this repair pathway (Fig. 4D). In line with a general defect in DSB repair, the combined knockdown of USP26 and USP37 led to a delay in the clearance of IR-induced γH2AX foci (Supplemental Fig. 5C), whereas depletion of either DUB rendered cells sensitive to IR (Fig.

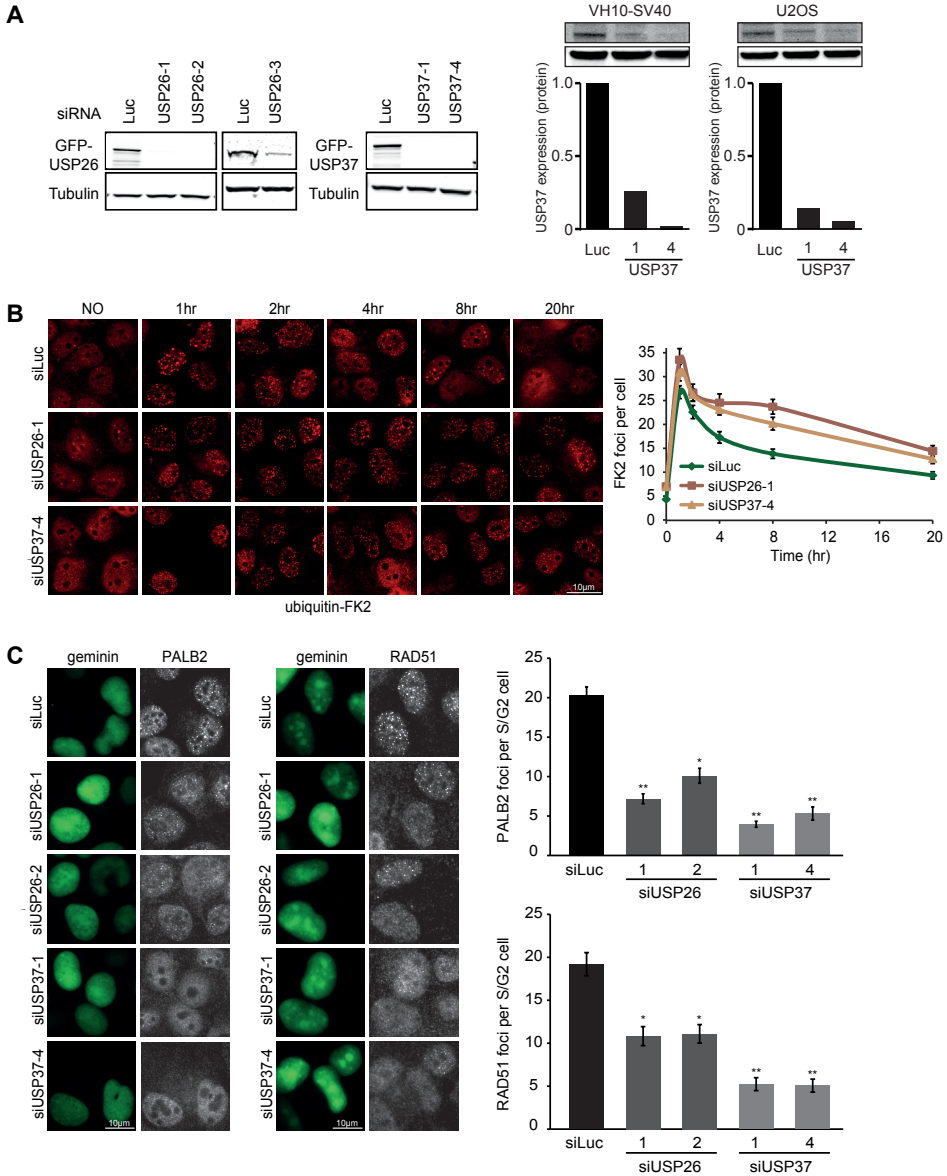4E). Collectively, this work reveals USP26 and USP37 as novel factors that are required for DSB repair.

Figure 3. USP26 or USP37 depletion abrogates the formation of PALB2-RAD51 complex at DSBs. (A) Western blot analysis of GFP-USP26, GFP- or endogenous-USP37 expression in cells treated with the indicated siRNAs. (B) Effect of DUB depletion on ubiquitin-FK2 IRIF formation in time. Note that 0 hr indicates non-irradiated cells. (C) Effect of DUB depletion on PALB2 (white; left panel) or RAD51 (white; right panel) IRIF formation in mAG-geminin-expressing (green) S/G2 cells. Quantified data are represented as mean ± S.E.M (n=3). *, P<0.05, **, P<0.01, ***, P<0.001 (student's t test).
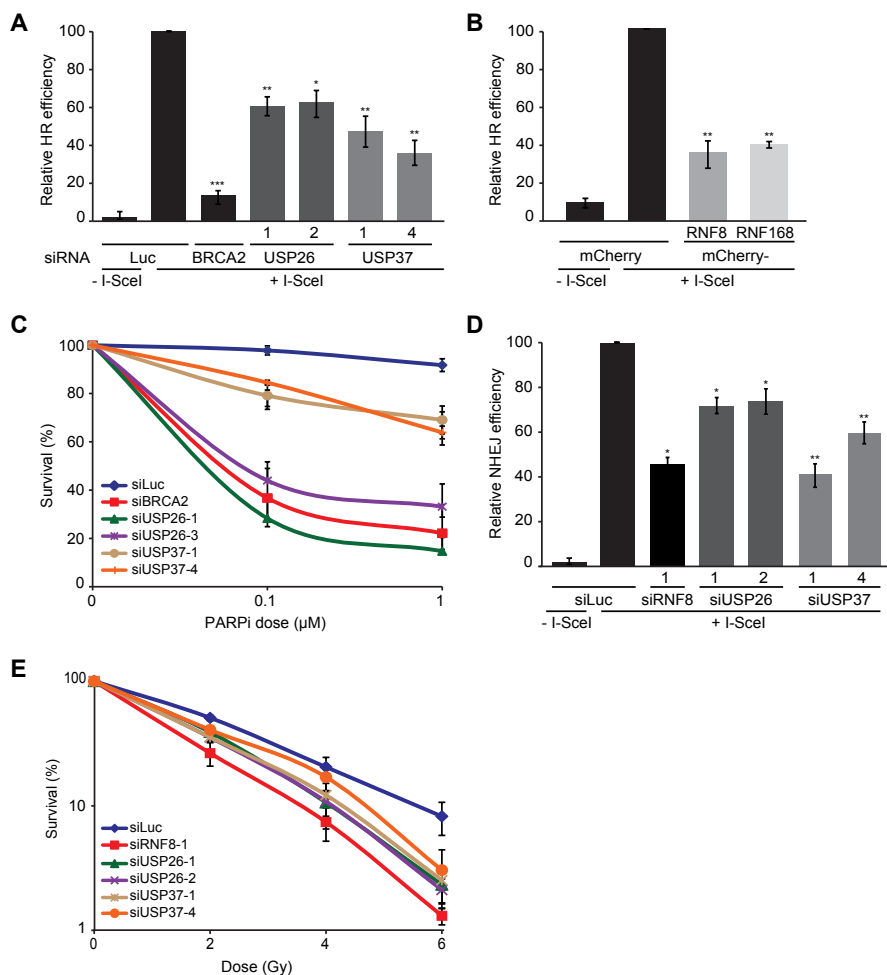
3

Figure 4. USP26 or USP37 depletion disrupts HR and NHEJ and sensitises cells to DNA damaging agents. (A) Impact of the indicated siRNAs on HR efficiency measured using the DR-GFP reporter. (B) Impact of the expression of the indicated mCherry-fusion proteins on HR efficiency using the DR-GFP reporter. (C) Clonogenic survival of VH10-SV40 cells that were transfected with the indicated siRNAs and exposed to PARP inhibitor (Olaparib). (D) Impact of the indicated siRNAs on NHEJ efficiency measured using the EJ5-GFP reporter. (E) Clonogenic survival of IR-exposed U2OS cells transfected with the indicated siRNAs. Quantified data are represented as mean ± S.D. (n=3). *, P<0.05, **, P<0.01, ***, P<0.001 (student's t test).

3

Loss of USP26 or USP37 impairs HR by antagonising RAP80-dependent sequestration of BRCA1

To gain insight into the mechanism that disrupts HR under conditions of excessive ubiquitylation, we turned our attention to the BRCA1-Abraxas-RAP80-MERIT40 complex, which through RAP80 drives the ubiquitin-dependent recruitment of BRCA1 to RNF8/RNF168-modified chromatin [7, 13-16, 35-37]. It was recently unveiled that RAP80-mediated recruitment of BRCA1 inhibits HR [38, 39], by sequestering BRCA1 from HR sites, thus hampering the formation of a BRCA1-PALB2-BRCA2-RAD51 complex, which is essential for HR [38, 40]. We reasoned that USP26 and USP37 may antagonise the RAP80-dependent sequestration of BRCA1 by removing RNF8/RNF168-mediated ubiquitylation and thereby promote HR. To address this, we established a quantitative, computer-assisted approach to measure BRCA1 foci size. In agreement with an earlier report [38], we found that BRCA1 foci were not reduced in number, but rather were considerably smaller in size following depletion of RAP80 (Fig. 5A). In contrast, depletion of either DUB had the opposite effect, leading to an increase in larger BRCA1 foci without affecting the total number of foci (Fig. 5B,C and Supplemental Fig. 5D). Remarkably, depletion of RAP80 in DUB knock-down cells completely rescued the shift towards larger foci and led to a reappearance of small BRCA1 foci (Fig. 5B,C). To test the functional relevance of these findings, we depleted RAP80 and examined if this would restore HR proficiency in USP26 or USP37-depleted cells. Indeed, we found that defective IR-induced accrual of both PALB2 and RAD51 in USP26- or USP37-depleted cells could be fully rescued by additional depletion of RAP80 (Fig. 6A,B). Similarly, HR efficiency was completely restored upon co-depletion of either DUB and RAP80, as measured in the DR-GFP reporter assay (Fig. 6C). Cell-cycle profiles in these cells remained unchanged ruling out effects of cell cycle misregulation (Supplemental Fig. 5E). Together these results suggest that USP26 and USP37 promote the BRCA1-dependent loading of PALB2 and RAD51 by counteracting the repressive impact of RAP80-dependent BRCA1 sequestration during HR (Fig. 7).
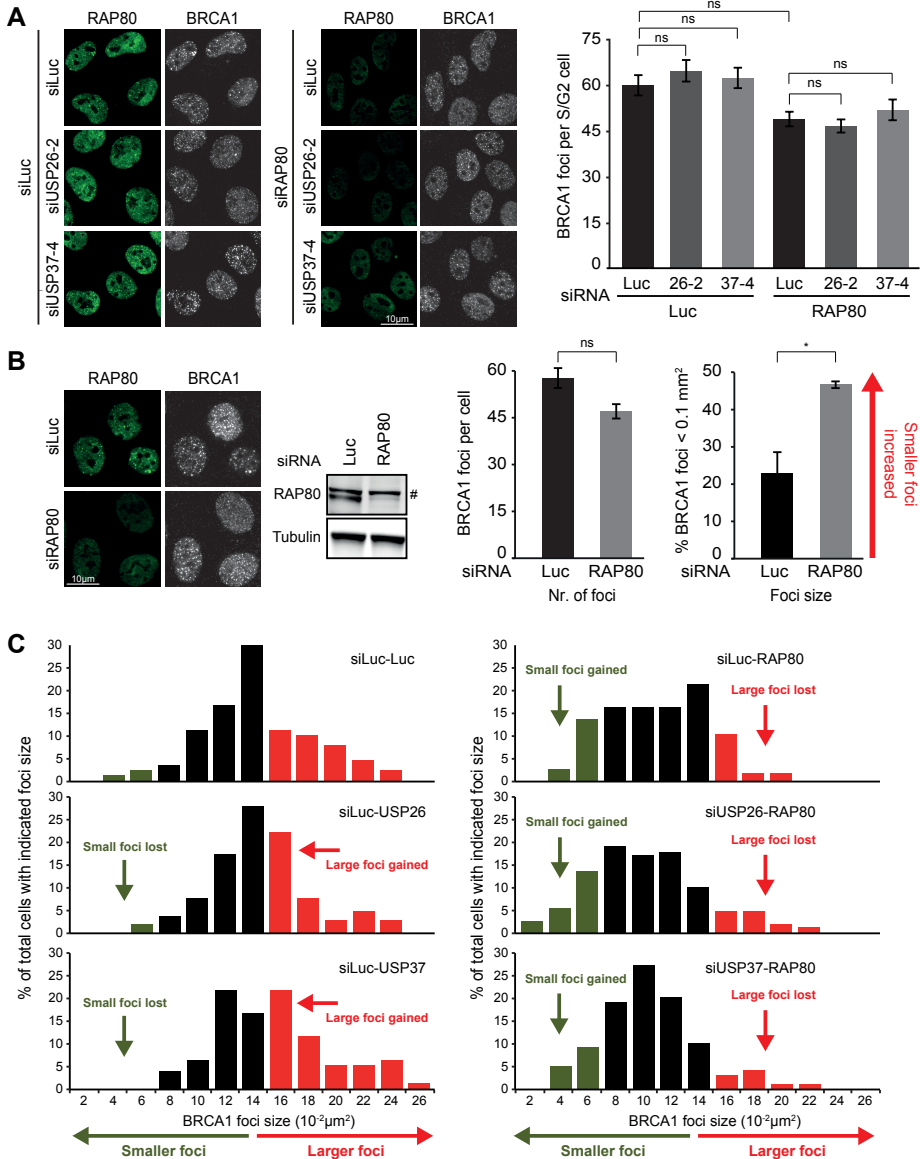
Figure 5. RAP80 depletion restores the formation of small BRCA1 IRIF, indicative of HR centers in USP26 and USP37 knock-down cells. (A) Effect of RAP80 depletion on RAP80 (green) and BRCA1 (white) IRIF formation (left and middle-right panel), endogenous RAP80 expression on Western blot (middle-left panel) and BRCA1 IRIF size (right panel). (B) Effect of DUB and RAP80 depletion on RAP80 (green) and BRCA1 (white) IRIF formation. (C) Histograms of BRCA1 foci size in cells treated with the indicated siRNAs. Green indicates small foci of typical HR size, while red indicates larger foci of the size observed for signalling factors. Quantified data are represented as mean ± S.D. (n=2). *, P<0.05, **, P<0.01, ***, P<0.001 (student's t test).

3
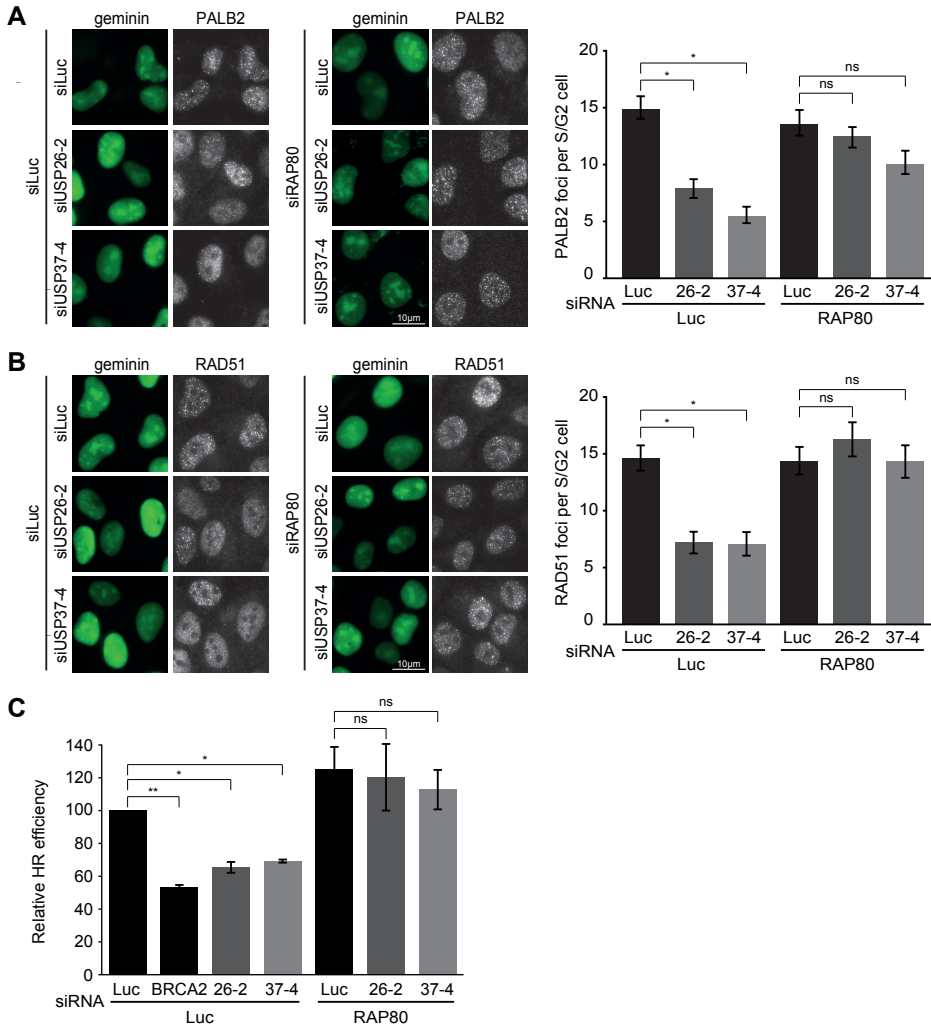
Figure 6. HR defects caused by the loss of USP26 and USP37 are reversed upon concomitant RAP80 removal. (A) Effect of DUB and RAP80 depletion on PALB2 (white) foci formation in mAG-geminin expressing (green) S/G2 cells. (B) As in A, but stained for RAD51 (white). (C) Effect of the indicated siRNAs on HR efficiency measured using the DR-GFP reporter. Quantified data are represented as mean ± S.E.M. (n=2). *, P<0.05, **, P<0.01, ***, P<0.001 (student's t test).

DISCUSSION

DSBs elicit a signalling cascade that is driven by the ubiquitin E3 ligases RNF8 and RNF168. These ligases promote progressive chromatin ubiquitylation, eventually leading to the ubiquitin-dependent assembly of BRCA1, RAD18 and 53BP1 onto damaged chromosomes [7-9, 13-16]. However, while a clear picture of the factors that orchestrate the RNF8/RNF168 signalling pathway has emerged, we are only starting to understand how it is linked to DSBs repair [12, 30, 38, 40, 49-53].

In this study, we identify USP26 and USP37 as novel DUBs that reverse RNF168-mediated ubiquitylation (Fig. 1-2, Supplemental Fig. 1-2), a process known to repress HR by sequestering the BRCA1-Abraxas-RAP80-MERIT40 complex through its ubiquitin-binding subunit RAP80 [38, 40]. By removing RNF168-induced ubiquitin conjugates distal from DSBs, USP26 and USP37 prevent the RAP80-dependent assembly of this BRCA1-containing complex, allowing BRCA1 to function in the BRCA1-PALB2-BRCA2-RAD51 complex during HR (Fig. 7). These findings advance our conceptual understanding of the RNF168-dependent response to DSBs, by revealing pathways that differentially regulate the spatial assembly and function of HR complexes at DSBs.

We propose the following model for RNF168-dependent regulation of HR (Fig. 7): RNF168-induced ubiquitin conjugates spread away from DSBs into more distal chromatin regions [20]. The BRCA1-Abraxas-RAP80-MERIT40 complex through RAP80 interactions associates with the RNF168-induced ubiquitin conjugates in these regions, thereby sequestering BRCA1 from the ssDNA compartment and inhibiting HR [38, 40]. In line with this model, we demonstrate that supra-physiological levels of RNF168 triggered extensive ubiquitylation of H2A (Fig. 2E), concomitant with a substantial reduction in HR efficiency (Fig. 4B). We extend these findings by showing that this phenomenon is actively antagonised by USP26 and USP37. Loss of USP26/USP37 function markedly impairs the assembly of PALB2, RAD51 and efficient HR (Fig. 3C, 4A and 6A-C). However, these defects can be rescued

3

3

by the additional loss of RAP80 (Fig. 6A-C). Together, these data suggest that USP26/37 limit the magnitude of the BRCA1-Abraxas-RAP80-MERIT40 complex assembly in DSB-neighbouring chromatin, by actively removing RNF168-mediated H2A ubiquitylation (Fig. 2E and Supplemental Fig. 3). Indeed, depletion of either DUB resulted in an increase in the size of BRCA1 foci, indicative of more extensive spreading of the BRCA1-Abraxas-RAP80-MERIT40 complex from the DSB site, which could be rescued by additional loss of RAP80 (Fig. 5A,B and Supplemental Fig. 5D). This scenario explains how these DUBs limit the repressive impact of RAP80 on HR. An alternative, yet not mutually exclusive scenario, would be in line with recent findings showing that DSB-induced H2A/H2AX ubiquitylation needs to be reversed in the core of IRIF for DNA end-resection to occur [39]. Given that USP26 and USP37 are able to reverse RNF8/168-mediated ubiquitylation and promote HR, these enzymes would be ideal candidates to facilitate such events.
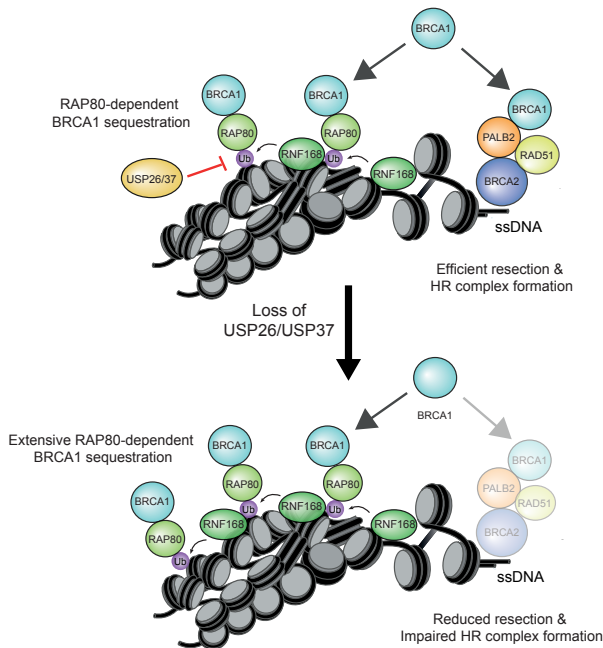
Figure 7. Molecular model for the role of USP26 and USP37 in HR. BRCA1 is sequestered from HR sites through RAP80, which is functionally antagonised by USP26- and USP37-dependent de-ubiquitylation of RNF168-modified chromatin (see discussion for details). Loss of USP26 or USP37 leads to more extensive RNF168-dependent sequestration of BRCA1, thereby preventing BRCA1 to form a complex with PALB2-BRCA2-RAD51 in HR. Additionally, the more extensive spreading of RAP80 upon USP26 or USP37 depletion reduces DNA end-resection, which also impairs HR.

Several other DUBs that affect H2A ubiquitination have been identified as important players in the DDR. For instance, the activity of tumour suppressor BAP1, which de-ubiquitylates H2A at K119, appeared to be critical for efficient HR [42, 54]. However, whether the BAP1-dependent removal of this histone modification is important during HR remains unclear. Similar to USP26 and USP37, two other DUBs, USP3 and USP44, were shown to reverse RNF168-induced chromatin ubiquitylation, thereby controlling the accumulation of BRCA1 and 53BP1 at sites of DNA damage [21, 25, 55]. Future work has to reveal whether these DUBs, similarly to USP26 and USP37, operate to control DSB repair, in particular HR. Unravelling the interplay between different DUBs during HR may uncover how ubiquitin-dependent control of this important DNA damage repair process is orchestrated.

Notably, both USP26 and USP29 are retrogenes of USP37, which likely explains why these DUBs display certain functional similarities. Although USP26 is often considered as testis-specific, we were able to detect USP26 expression in different cell types (U2OS and HEK293, Fig. 3A and Supplemental Fig. 4A), showing that this classification is incorrect. In agreement, it has been shown by extensive proteomic analysis that USP26 is expressed in various human cell-lines and organs [56, 57]. Moreover, knockdown of USP26, similar to that of USP37, confers defects in the signalling and repair of DSBs in human cells, illustrating non-redundant roles for both DUBs in the DSB response.

A striking conclusion from our study is that non-physiological expression of USP26 and USP37 impairs HR. Therefore, it seems likely that the expression of USP26 and USP37 needs to be tightly controlled. Failure to do so might not only correlate with enhanced genomic instability, but also with increased malignant transformation rates. Indeed, a plethora of cancer cell lines appear to have either lost (USP26=1457/USP37=446; COSMIC) or amplified (USP26=309/USP37=359; COSMIC) the expression of these DUBs. In conclusion, we report distinct ubiquitin-dependent pathways that orchestrate the assembly and function of HR complexes at DSBs and identify the factors responsible for these events.

3

MATERIALS AND METHODS

Cell culture

U2OS, HEK293 and VH10-SV40-immortalised cells were grown in DMEM (Gibco) containing 10% FCS (Bodinco BV). U2OS cells containing an inducible shRNA against endogenous RNF8 and stably expressing FLAG-RNF8, U2OS 2–6-3 cells containing 200 copies of a LacO-containing cassette (~4 Mbp) and U2OS 2-6-3 cells stably expressing an inducible version of FokI-mCherry-LacR fused to the estrogen receptor (ER) and harbouring a destabilisation domain (DD) were previously described [7, 15, 43, 58]. The ViraPower system (Life Science) was used to produce lentivirus using mAG- or mCherry-geminin expression vectors [59]. U2OS cells stably expressing mAG- or mCherry-geminin were made by standard lentiviral transduction, followed by FACS sorting, in order to select homogeneously fluorescent cells.

Plasmids

A collection of cDNAs encoding FLAG-tagged DUBs, originally generated in Wade Harper's laboratory [60], was obtained from Addgene. An IRES-Puro cassette was amplified by PCR and inserted as an EcoRV-EcoRV fragment into the HpaI site of EGFP-C1 (Addgene). The USP26 and USP37 cDNAs were inserted in EGFP-C1-IRES-Puro. Overlap PCR was used to introduce the inactivation mutations C304S into GFP-USP26 and C350S into GFP-USP37. Wild-type and catalytic inactive versions of USP26 and USP37 were also inserted into mCherry-C1. A BsrGI-BstZ17I fragment encompassing amino acids 1-641 of USP26 was inserted into the BsrGI-SmaI site of EGFP-C1 to generate GFP-USP26 lacking the putative C-terminal UIM. Likewise, a BsrGI-SacI fragment encompassing amino acids 1-643 of USP37 was inserted into the BsrGI-SacI site of EGFP-C1 to generate GFP-USP37 lacking the C-terminal UIM domains. Additional plasmids used are listed in the Supplemental Table.

Transfections and RNAi interference

siRNA and plasmid transfections were performed using Lipofectamine

RNAiMAX (Invitrogen), Lipofectamine 2000 (Invitrogen) and JetPEI (Polyplus Transfection) according to the manufacturer's instructions. Cells were transfected twice with siRNAs (40 nM) within 24 h and examined further 48 h after the second transfection, unless stated otherwise. siRNA sequences are listed in the Supplemental Table.

Generation of DSBs

IR was delivered by a YXlon X-ray generator (YXlon International, 200 KV, 10 mA, dose rate 2 Gy/min).

Cell survival assay

VH10-SV40 or U2OS cells were transfected with siRNAs, trypsinised, seeded at low density and exposed to IR. 7 days later cells were washed with 0.9% NaCl and stained with methylene blue. Colonies of more than 10 cells were scored.

FokI assays

U2OS 2-6-3 cells expressing inducible FokI-mCherry-LacR [43] were treated with 300 nM 4-OHT and 1 μM Shield-I for 5 hrs. Subsequently, cells were fixed with formaldehyde and immunostained with the indicated antibodies.

UV-A laser micro-irradiation

U2OS cells were grown on 18 mm coverslips and sensitised with 10 μM 5′-bromo-2-deoxyuridine (BrdU) for 24 hours as described [18, 44]. For micro-irradiation, the cells were placed in a Chamlide TC-A live-cell imaging chamber that was mounted on the stage of a Leica DM IRBE wide-field microscope stand (Leica, Wetzlar, Germany) integrated with a pulsed nitrogen laser (Micropoint Ablation Laser System; Photonic Instruments, Inc., Belfast, Ireland). The pulsed nitrogen laser (16 Hz, 364 nm) was directly coupled to the epifluorescence path of the microscope and focused through a Leica 40x HCX PLAN APO 1.25-0.75 oil-immersion objective. The growth medium was replaced by CO_2-independent Leibovitz's L15 medium supplemented with 10% FCS and penicillin-streptomycin and cells

3

3

were kept at 37°C. The laser output power was set to 78 to generate strictly localised sub-nuclear DNA damage. Following micro-irradiation, cells were incubated for the indicated time-points at 37°C in Leibovitz's L15 and subsequently fixed with 4% formaldehyde before immunostaining. Typically, an average of 50 cells was micro-irradiated (2 iterations per pixel) within 10–15 minutes using Andor IQ software.

Multiphoton laser micro-irradiation

U2OS cells were grown on 18 mm coverslips. Subsequently, they were placed in a Chamlide CMB magnetic chamber and the growth medium was replaced by CO_2-independent Leibovitz's L15 medium supplemented with 10% FCS and penicillin-streptomycin. Laser micro-irradiation was carried out on a Leica SP5 confocal microscope equipped with an environmental chamber set to 37°C. DSB-containing tracks (1.5 μm width) were generated with a Mira mode-locked titanium-sapphire (Ti:Sapphire) laser (l = 800 nm, pulse length = 200 fs, repetition rate = 76 MHz, output power = 80 mW) using a UV-transmitting 63× 1.4 NA oil immersion objective (HCX PL APO; Leica). Confocal images were recorded before and after laser irradiation at 5 or 10 seconds time intervals over a period of 5 - 10 minutes.

Microscopy analysis

Images of fixed cells were acquired on a Zeiss AxioImager D2 widefield fluorescence microscope equipped with 40x, 63x and 100x PLAN APO (1.4 NA) oil-immersion objectives (Zeiss) and an HXP 120 metal-halide lamp used for excitation. Fluorescent probes were detected using previously described filters [61]. Images were recorded using ZEN 2012 software and analysed using ImageJ. The average reflects the quantification of 50-150 cells from 3 independent experiments.

IRIF analysis

PALB2, RAD51, BRCA1 and RAP80 (except in Supplemental Fig. 2B) IRIF were analyzed in U2OS cells 6hr after 10Gy, RPA and CtIP IRIF were assayed 4hr after 10Gy, whereas conjugated ubiquitin (FK2), γH2AX, MDC1, FLAG-RNF8, RNF168, BRCA1 and RAP80 (at Supplemental Fig.

2B) and 53BP1 IRIF were examined 1hr after 2Gy, unless stated otherwise. IRIF were evaluated in ImageJ, using a custom-built macro that enabled automatic and objective analysis of the foci. Full details of this macro will be published elsewhere. In brief, cell nuclei were detected by thresholding the (median-filtered) DAPI signal, after which touching nuclei were separated by a watershed operation. The foci signal was background-subtracted using a Difference of Gaussians filter. For every nucleus, foci were identified as regions of adjacent pixels satisfying the following criteria: (i) the grey value exceeds the nuclear background signal by a set number of times (typically 2-4x) the median background standard deviation of all nuclei in the image, and is higher than a user-defined absolute minimum value; (ii) the area is larger than a defined area (typically 2 pixels). These parameters were optimised for every experiment by manually comparing the detected foci with the original signal.

Immunofluorescent labelling

Immunofluoresecent labelling was carried out as described previously [18, 19]. Briefly, cells were grown on glass coverslips and treated as indicated in the figure legends. Subsequently, cells were washed with PBS, then fixed with 2% formaldehyde for 20 minutes and permeabilised with 0.25% Triton X-100 in PBS for 5 minutes. Cells were rinsed with phosphate-buffered saline (PBS) and then treated with 100 mM glycine in PBS for 10 minutes to block unreacted aldehyde groups. Finally, cells were equilibrated in PBS containing 0.5% BSA and 0.05% Tween 20, and incubated with primary antibodies. Detection was done using goat anti-mouse or goat anti-rabbit IgG coupled to Alexa 488, 555 or 647 (Invitrogen Molecular Probes). Samples were incubated with 0.1 µg/ml DAPI and mounted in Polymount. Primary antibodies and secondary antibodies are listed in the Supplemental Table.

Western blotting

Cell extracts were generated by boiling cell pellets in Laemmli buffer, separated by SDS-PAGE and transferred to PVDF membranes (Millipore). Membranes were probed with the antibodies listed in Supplemental Table 1

followed by protein detection using the Odyssey infrared imaging scanning system (LI-COR Biosciences).

HR and NHEJ assay

HEK293 and U2OS cells containing a stably integrated copy of either the DR-GFP of EJ5-GFP reporter were used to measure the repair of I-SceI-induced DSBs by HR or NHEJ, respectively [48, 62]. Briefly, 48 h after siRNA transfection, cells were transfected with the I-SceI expression vector pCBASce and an mCherry expression vector. [62] 48 or 72 h later the fraction of GFP-positive cells among the mCherry-positive cells was determined by FACS on a LSRII flow cytometer (BD Bioscience) using FACSDiva software version 5.0.3. Quantifications were performed using Flowing Software (www.flowingsoftware.com).

Cell cycle profiling

For cell cycle analysis cells were fixed in 70% ethanol, followed by DNA staining with 50 μg/ml propidium iodide in the presence of RNase A (0.1 mg/ml). Cell sorting was performed on a LSRII flow cytometer (BD Bioscience) using FACSDiva software (version 5.0.3; BD). Quantifications were performed using Flowing Software.

RT-qPCR-based gene expression analysis

RNA isolation, reverse transcription (RT)-based cDNA synthesis and quantitative (q)PCR were carried out as previously described [61]. The primers used are listed in the Supplemental Table.

ACKNOWLEDGEMENTS

3
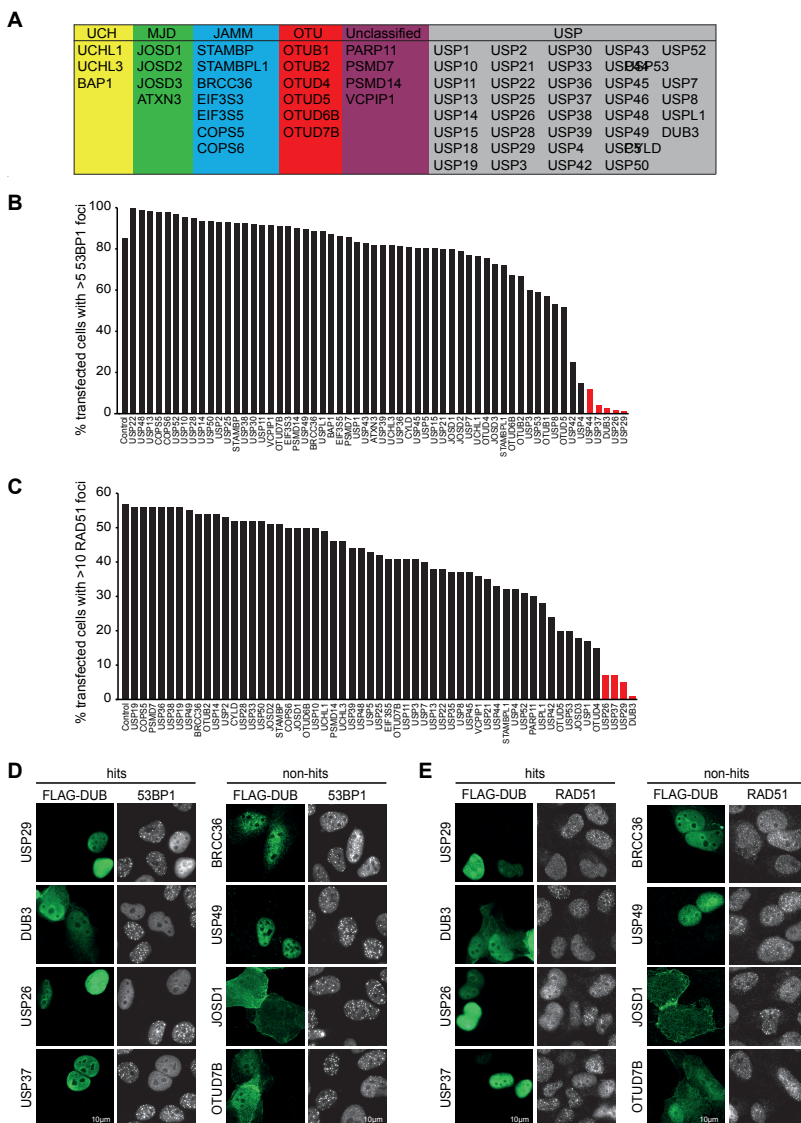
Supplementary Figure 1. A DUB over-expression screen reveals novel DSB response regulators. (A) List of FLAG-tagged DUBs expressed in U2OS cells. Enzymes are colour-coded to signify the different DUB families. In yellow Ubiquitin C-terminal Hydrolases (UCH), in green Machado-Josephin Domain-DUBs (MJD), in blue JAMM metalloproteases (JAMM), in red OTUbain domain-DUBs (OTU), in purple unclassified DUBs and in grey Ubiquitin Specific Proteases (USP). (B) Quantification of 53BP1 IRIF formation upon over-expression of the indicated DUBs. Red bars signify hits, i.e. population of cells with >5 53BP1 IRIFs is lower than 15% of total transfected cells. (C) Quantification of RAD51 IRIF formation upon over-expression of the indicated DUBs. Red bars signify hits, i.e. population of cells with >10 RAD51 IRIFs is lower than 15% of total transfected cells. (D) Examples of the impact of the over-expression of the indicated (non-) hits/DUBs (green) on 53BP1 IRIF formation (white). (E) Examples of the impact of the over-expression of the indicated (non-) hits/DUBs (green) on RAD51 IRIF formation (white).

3
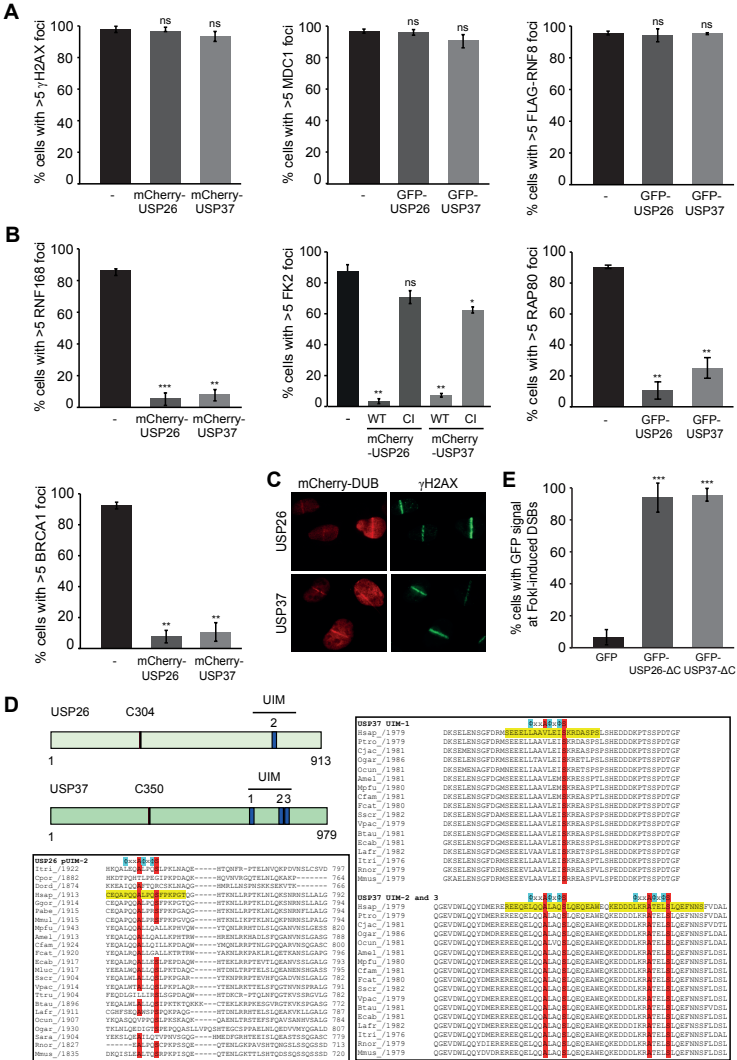
Supplemental Figure 2. USP26 and USP37 accumulate at DSBs and regulate chromatin ubiquitylation. (A) Quantification of the impact of the expression of GFP- or mCherry-tagged DUBs (green or red) on γH2AX, MDC1, FLAG-RNF8 IRIF formation. (B) As in A, but RNF168, FK2, RAP80 and BRCA1 IRIF formation was quantified. (C) Recruitment of mCherry-tagged DUBs (red) to laser-induced DNA damage, marked by γH2AX (green). (D) Schematic representation of the catalytic cysteine residues and UIMs of USP26 and USP37. In yellow: alignment between UIMs 1 - 3 of USP37 and UIM2 of USP26 in different species. Note that USP26 lost two UIMs during evolution. In red: conserved residues important for interaction with ubiquitin. UIM consensus sequence: ΦxxAΦxΦS. In light blue: Φ=hydrophobic residues (A, F, G, I, L, P, V). (E) Quantification of the localisation of GFP-DUBs lacking their C-termini (ΔC) at FokI-induced DSBs in cells containing a LacO array. The ΔC mutants lack functional UIMs. All IRIF data obtained 1hr after treatment with 2Gy. Quantified data are represented as mean ± S.D. (n=3). *, P<0.05, **, P<0.01, ***, P<0.001 (student's t test).
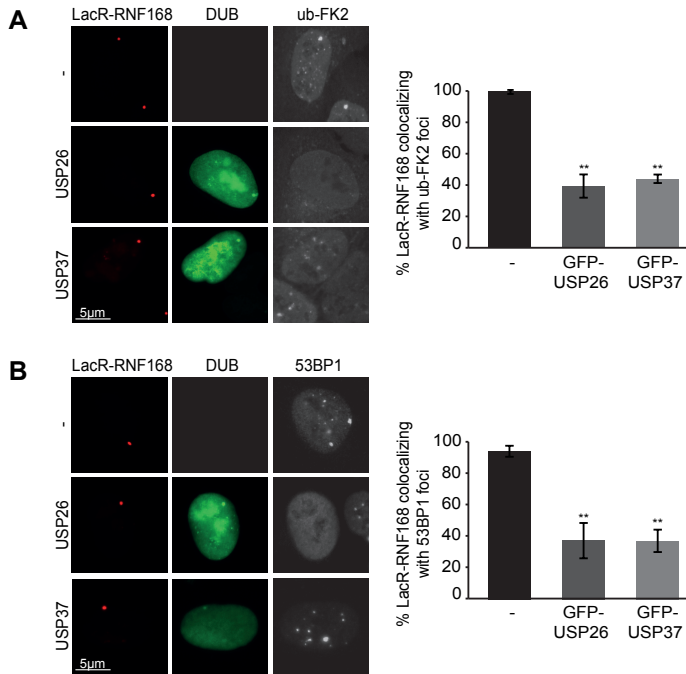
Supplemental Figure 3. USP26 or USP37 can remove RNF168-induced ubiquitylation.
(A) Effect of GFP-DUB over-expression on conjugated ubiquitin (FK2) (white) upon tethering of mCherry-LacR-RNF168 in cells containing a LacO array. (B) As in (A) only stained for 53BP1 (white). Quantified data are represented as mean ± S.D. (n=3). *, $P<0.05$, **, $P<0.01$, ***, $P<0.001$ (student's t test).

3
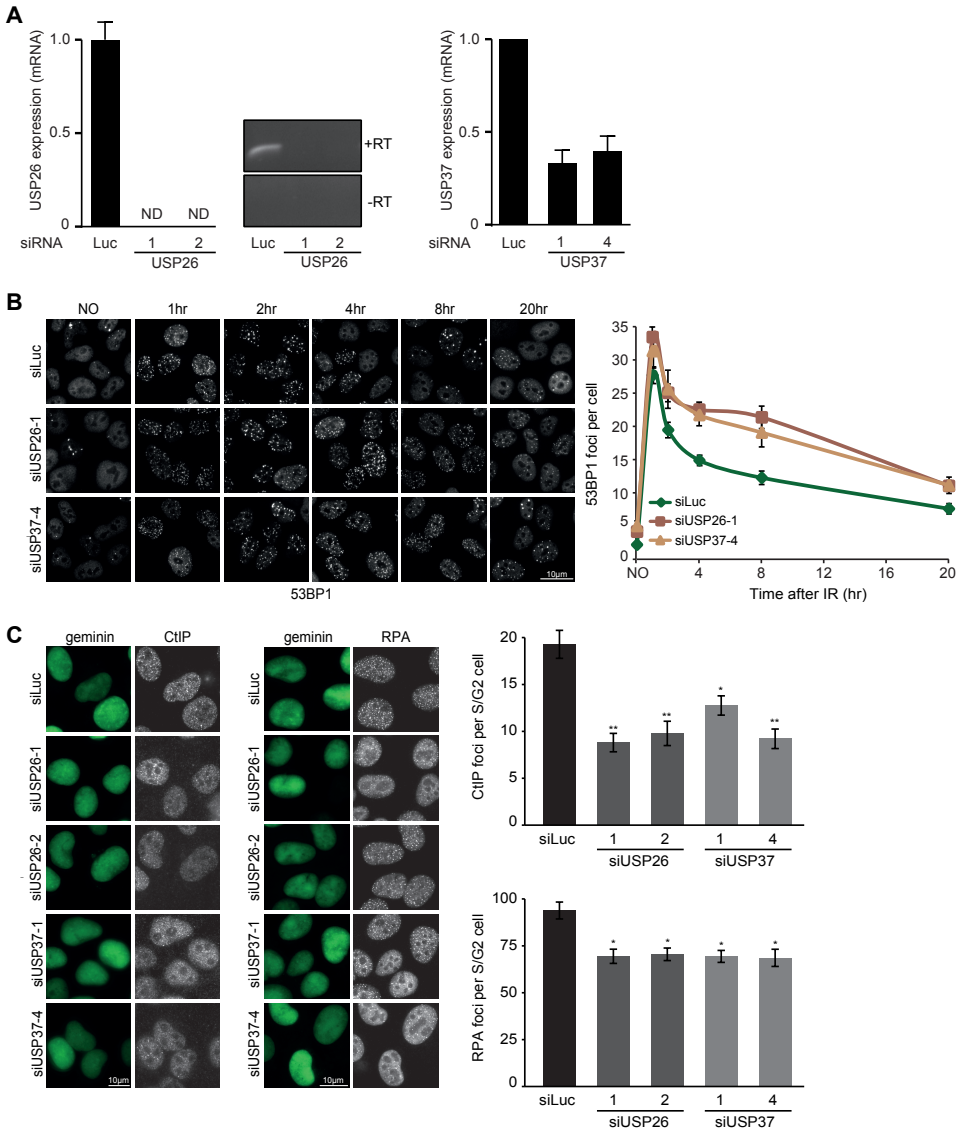
Supplemental Figure 4. USP26 or USP37 depletion impairs the DSB response. (A) Relative USP26 mRNA expression in U2OS cells treated with the indicated siRNAs. The USP26 transcript was not detectable (ND) by reverse transcriptase (RT)-qPCR in cells treated with siRNAs against USP26 (left panel). Representative agarose gel showing USP26 PCR product amplified from total RNA without (-RT) or with (+RT) reverse transcriptase reaction (middle panel). Relative USP37 mRNA expression in U2OS cells treated with the indicated siRNAs (right panel). (B) Effect of DUB depletion on 53BP1 IRIF formation in time after 2 Gy of IR. (C) Effect of DUB depletion on CtIP and RPA IRIF formation 4hr after 10Gy of IR. Quantified data are represented as mean ± S.D. (n=3). *, $P<0.05$, **, $P<0.01$, ***, $P<0.001$ (student's t test).
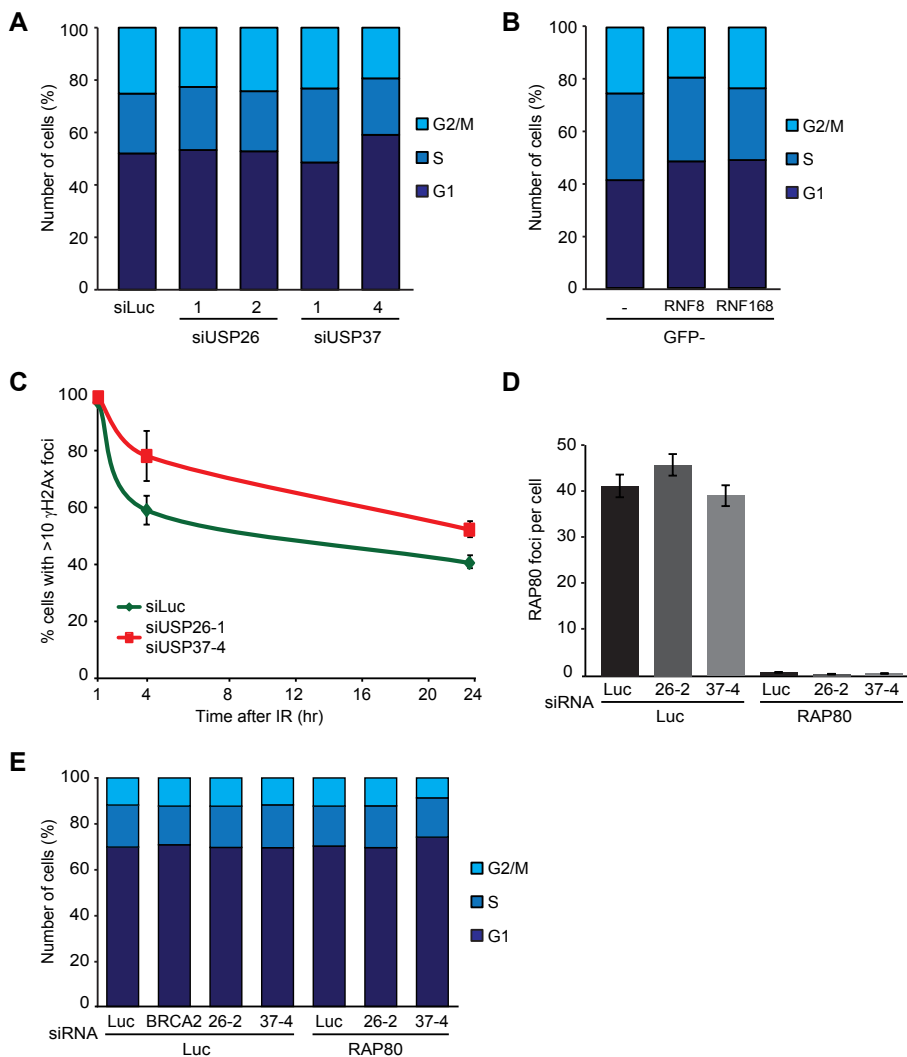
Supplemental Figure 5. USP26 or USP37 depletion does not alter cell-cycle progression.
(A) Cell cycle profiles of cells treated with the indicated siRNAs. (B) Cell cycle profiles of cells over-expressing the indicated GFP fusion proteins. (C) Effect of combined DUB depletion on DSB repair, assayed by clearance of γH2AX foci after 2 Gy of IR. (D) Effect of DUB and RAP80 depletion on RAP80 IRIF formation. (E) Cell cycle profiles of cells treated with the combinations of the indicated siRNAs. Quantified data are represented as mean ± S.D. (n=3), except in (D) where mean ± S.E.M. (n=2).

Supplemental Table

Antibodies					
Target protein	Host	Obtained from	Cat. nr.	IF	WB
53BP1	rabbit	Novus Biologicals	NB100-304	1:2000	
BRCA1	mouse	SantaCruz	sc-6954	1:100	
BRCA1	rabbit	gift Dr. Daniel Durocher			1:1000
BRCC36	rabbit	Abcam	ab62075		1:1000
FLAG	mouse	Sigma	F1804	1:1000	
GFP	rabbit	Abcam	ab290		1:1000
GFP	mouse	Roche	#11814460001		1:2000
γH2AX	mouse	Millipore	JBW301	1:2000	
H2AX	rabbit	Bethyl	A330-082A		1:10000
H2B	rabbit	Millipore	07-371		1:10000
HA	mouse	SantaCruz	sc-7392	1:500	
mCherry	mouse	Abcam	ab125096		1:1000
MDC1	rabbit	Abcam	ab11171	1:1000	
PALB2	rabbit	Bethyl	A301-246A		1:1000
PALB2	rabbit	gift Dr.Bing Xia		1:100	
RAD51	rabbit	SantaCruz	sc-8349	1:100	
RNF168	rabbit	Millipore	ABE367	1:200	1:500
Tubulin	mouse	Sigma	T6199		1:5000
Ubiquitin K48 chains	rabbit	Millipore	APU2/05-1307		1:100
Ubiquitin K63 chains	rabbit	Millipore	APU3/05-1308		1:1000
Ubiquitin-FK2	mouse	EnzoLifeSciences	BML-PW8810-0500	1:100	
RPA	mouse	ThermoScientific	Ab-1 9H8	1:1000	
CtIP	mouse	gift Dr. Richard Baer		1:10	
RAP80	rabbit	Bethyl	A300-764		1:1000
RAP80	rabbit	Bethyl	A300-763A	1:500	
Rabbit-700CW	donkey	Licor			1:20000
Mouse-800CW	donkey	Licor			1:20000

siRNAs		
Target Protein	siRNA name	Sequence (5'-3')
Luciferase	Luc	CGUACGCGGAAUACUUCGA
BRCA2	BRCA2	GAAGAAUGCAGGUUUAAUA
RNF8	RNF8-1	GAGGGCCAAUGGACAAUUA
USP26	USP26-1	CCACAAAGCUGGAGGUAAA
USP26	USP26-2	CCACAAAGUUGAUGAGAAA
USP26	USP26-3	CAGAAGAGCTTGAGTATAA
USP37	USP37-1	CUACAAUACUGGAGGAAUU
USP37	USP37-4	GAAGAUUACCCUAAGGAAA
RAP80	RAP80 (Dharmacon SMARTpool L-006995-00-0005)	GTAAATCCCTGGTCCCATT AAATGAATCTCCCGTCAAG AGAGCAGGCTAGTGAGAAA AGAGGCAGCTCCTTAATAA

qPCR primers		
Target gene	Gene/Primer	Sequence (5'-3')
USP26	USP26-Forward	AGTGTTGTCAGCCATCTTGG
USP26	USP26-Reverse	CCCGCATATCATCGTAAGTG
USP37	USP37-Forward	GCCCAAAACAATCACAGAGC
USP37	USP37-Reverse	TCCCTTTCACGCTCCATATC

Plasmids	
Encoded fusion protein	Described in
GFP-H2A	Luijsterburg *et al. Journal of Cell Biology* **197**: 267-281 (2012)
FokI-LacR-mCherry	Tang *et al. Nature Structural & Molecular Biology* **20**: 317-325 (2013)
mCherry-LacR-RNF168	Luijsterburg *et al. EMBO Journal* **31**: 2511-2527(2012)
mCherry-LacR-RNF8	Luijsterburg *et al. EMBO Journal* **31**: 2511-2527(2012)
mCherry-RNF168	Smeenk *et al. Journal of Cell Science* **126**: 889-903 (2013)
mCherry-RNF8	Smeenk *et al. Journal of Cell Science* **126**: 889-903 (2013)

REFERENCES

1. Jackson, S.P. and J. Bartek, The DNA-damage response in human biology and disease. Nature, 2009. 461(7267): p. 1071-8.

2. Bekker-Jensen, S. and N. Mailand, Assembly and function of DNA double-strand break repair foci in mammalian cells. DNA Repair (Amst), 2010. 9(12): p. 1219-28.

3. Luijsterburg, M.S. and H. van Attikum, Chromatin and the DNA damage response: the cancer connection. Mol Oncol, 2011. 5(4): p. 349-67.

4. Huen, M.S. and J. Chen, Assembly of checkpoint and repair machineries at DNA damage sites. Trends Biochem Sci, 2010. 35(2): p. 101-8.

5. Polo, S.E. and S.P. Jackson, Dynamics of DNA damage response proteins at DNA breaks: a focus on protein modifications. Genes Dev, 2011. 25(5): p. 409-33.

6. Stucki, M., et al., MDC1 directly binds phosphorylated histone H2AX to regulate cellular responses to DNA double-strand breaks. Cell, 2005. 123(7): p. 1213-26.

7. Doil, C., et al., RNF168 binds and amplifies ubiquitin conjugates on damaged chromosomes to allow accumulation of repair proteins. Cell, 2009. 136(3): p. 435-46.

8. Stewart, G.S., et al., The RIDDLE syndrome protein mediates a ubiquitin-dependent signaling cascade at sites of DNA damage. Cell, 2009. 136(3): p. 420-34.

9. Mattiroli, F., et al., RNF168 ubiquitinates K13-15 on H2A/H2AX to drive DNA damage signaling. Cell, 2012. 150(6): p. 1182-95.

10. Pinato, S., et al., RNF168, a new RING finger, MIU-containing protein that modifies chromatin by ubiquitination of histones H2A and H2AX. BMC Mol Biol, 2009. 10: p. 55.

11. Fradet-Turcotte, A., et al., 53BP1 is a reader of the DNA-damage-induced H2A Lys 15 ubiquitin mark. Nature, 2013. 499(7456): p. 50-4.

12. Huang, J., et al., RAD18 transmits DNA damage signalling to elicit homologous recombination repair. Nat Cell Biol, 2009. 11(5): p. 592-603.

13. Huen, M.S., et al., RNF8 transduces the DNA-damage signal via histone ubiquitylation and checkpoint protein assembly. Cell, 2007. 131(5): p. 901-14.

14. Kolas, N.K., et al., Orchestration of the DNA-damage response by the RNF8 ubiquitin ligase. Science, 2007. 318(5856): p. 1637-40.

15. Mailand, N., et al., RNF8 ubiquitylates histones at DNA double-strand breaks and promotes assembly of repair proteins. Cell, 2007. 131(5): p. 887-900.

16. Wang, B. and S.J. Elledge, Ubc13/Rnf8 ubiquitin ligases control foci formation of the Rap80/Abraxas/Brca1/Brcc36 complex in response to DNA damage. Proc Natl Acad Sci U S A, 2007. 104(52): p. 20759-63.

3

17.   Larsen, D.H., et al., The chromatin-remodeling factor CHD4 coordinates signaling and repair after DNA damage. J Cell Biol, 2010. 190(5): p. 731-40.

18.   Luijsterburg, M.S., et al., A new non-catalytic role for ubiquitin ligase RNF8 in unfolding higher-order chromatin structure. EMBO J, 2012. 31(11): p. 2511-27.

19.   Smeenk, G., et al., Poly(ADP-ribosyl)ation links the chromatin remodeler SMARCA5/SNF2H to RNF168-dependent DNA damage signaling. J Cell Sci, 2013. 126(Pt 4): p. 889-903.

20.   Gudjonsson, T., et al., TRIP12 and UBR5 suppress spreading of chromatin ubiquitylation at damaged chromosomes. Cell, 2012. 150(4): p. 697-709.

21.   Mosbech, A., et al., The deubiquitylating enzyme USP44 counteracts the DNA double-strand break response mediated by the RNF8 and RNF168 ubiquitin ligases. J Biol Chem, 2013. 288(23): p. 16579-87.

22.   Nakada, S., et al., Non-canonical inhibition of DNA damage-dependent ubiquitination by OTUB1. Nature, 2010. 466(7309): p. 941-6.

23.   Shao, G., et al., The Rap80-BRCC36 de-ubiquitinating enzyme complex antagonizes RNF8-Ubc13-dependent ubiquitination events at DNA double strand breaks. Proc Natl Acad Sci U S A, 2009. 106(9): p. 3166-71.

24.   Nishi, R., et al., Systematic characterization of deubiquitylating enzymes for roles in maintaining genome integrity. Nat Cell Biol, 2014.

25.   Sharma, N., et al., USP3 counteracts RNF168 via deubiquitinating H2A and gammaH2AX at lysine 13 and 15. Cell Cycle, 2013. 13(1).

26.   Nishi, R., et al., Systematic characterization of deubiquitylating enzymes for roles in maintaining genome integrity. Nat Cell Biol, 2014. 16(10): p. 1016-26, 1-8.

27.   Feng, L. and J. Chen, The E3 ligase RNF8 regulates KU80 removal and NHEJ repair. Nat Struct Mol Biol, 2012. 19(2): p. 201-6.

28.   Huang, T.T. and A.D. D'Andrea, Regulation of DNA repair by ubiquitylation. Nat Rev Mol Cell Biol, 2006. 7(5): p. 323-34.

29.   Noon, A.T., et al., 53BP1-dependent robust localized KAP-1 phosphorylation is essential for heterochromatic DNA double-strand break repair. Nat Cell Biol, 2010. 12(2): p. 177-84.

30.   Zhang, F., et al., MDC1 and RNF8 function in a pathway that directs BRCA1-dependent localization of PALB2 required for homologous recombination. J Cell Sci, 2012. 125(Pt 24): p. 6049-57.

31.   Zhang, F., et al., PALB2 links BRCA1 and BRCA2 in the DNA-damage response. Curr Biol, 2009. 19(6): p. 524-9.

32.   Zhang, F., et al., PALB2 functionally connects the breast cancer susceptibility proteins BRCA1 and BRCA2. Mol Cancer Res, 2009. 7(7): p. 1110-8.

33.   Sy, S.M., M.S. Huen, and J. Chen, PALB2 is an integral component of the BRCA

complex required for homologous recombination repair. Proc Natl Acad Sci U S A, 2009. 106(17): p. 7155-60.

34. Huen, M.S., S.M. Sy, and J. Chen, BRCA1 and its toolbox for the maintenance of genome integrity. Nat Rev Mol Cell Biol, 2010. 11(2): p. 138-48.

35. Kim, H., J. Chen, and X. Yu, Ubiquitin-binding protein RAP80 mediates BRCA1-dependent DNA damage response. Science, 2007. 316(5828): p. 1202-5.

36. Sobhian, B., et al., RAP80 targets BRCA1 to specific ubiquitin structures at DNA damage sites. Science, 2007. 316(5828): p. 1198-202.

37. Wang, B., et al., Abraxas and RAP80 form a BRCA1 protein complex required for the DNA damage response. Science, 2007. 316(5828): p. 1194-8.

38. Hu, Y., et al., RAP80-directed tuning of BRCA1 homologous recombination function at ionizing radiation-induced nuclear foci. Genes Dev, 2011. 25(7): p. 685-700.

39. Kakarougkas, A., et al., Co-operation of BRCA1 and POH1 relieves the barriers posed by 53BP1 and RAP80 to resection. Nucleic Acids Res, 2013. 41(22): p. 10298-311.

40. Coleman, K.A. and R.A. Greenberg, The BRCA1-RAP80 complex regulates DNA repair mechanism utilization by restricting end resection. J Biol Chem, 2011. 286(15): p. 13669-80.

41. Murai, J., et al., The USP1/UAF1 complex promotes double-strand break repair through homologous recombination. Mol Cell Biol, 2011. 31(12): p. 2462-9.

42. Yu, H., et al., Tumor suppressor and deubiquitinase BAP1 promotes DNA double-strand break repair. Proc Natl Acad Sci U S A, 2013.

43. Tang, J., et al., Acetylation limits 53BP1 association with damaged chromatin to promote homologous recombination. Nat Struct Mol Biol, 2013. 20(3): p. 317-25.

44. Acs, K., et al., The AAA-ATPase VCP/p97 promotes 53BP1 recruitment by removing L3MBTL1 from DNA double-strand breaks. Nat Struct Mol Biol, 2011. 18(12): p. 1345-50.

45. Panier, S., et al., Tandem protein interaction modules organize the ubiquitin-dependent response to DNA double-strand breaks. Mol Cell, 2012. 47(3): p. 383-95.

46. Gatti, M., et al., A novel ubiquitin mark at the N-terminal tail of histone H2As targeted by RNF168 ubiquitin ligase. Cell Cycle, 2012. 11(13): p. 2538-44.

47. McCabe, N., et al., Deficiency in the repair of DNA damage by homologous recombination and sensitivity to poly(ADP-ribose) polymerase inhibition. Cancer Res, 2006. 66(16): p. 8109-15.

48. Bennardo, N., et al., Alternative-NHEJ is a mechanistically distinct pathway of mammalian chromosome break repair. PLoS Genet, 2008. 4(6): p. e1000110.

49. Lu, C.S., et al., The RING finger protein RNF8 ubiquitinates Nbs1 to promote DNA double-strand break repair by homologous recombination. J Biol Chem, 2012.

3

287(52): p. 43984-94.

50. Nakada, S., R.M. Yonamine, and K. Matsuo, RNF8 regulates assembly of RAD51 at DNA double-strand breaks in the absence of BRCA1 and 53BP1. Cancer Res, 2012. 72(19): p. 4974-83.

51. Sy, S.M., et al., Critical roles of ring finger protein RNF8 in replication stress responses. J Biol Chem, 2011. 286(25): p. 22355-61.

52. Meerang, M., et al., The ubiquitin-selective segregase VCP/p97 orchestrates the response to DNA double-strand breaks. Nat Cell Biol, 2011. 13(11): p. 1376-82.

53. Munoz, M.C., et al., RING finger nuclear factor RNF168 is important for defects in homologous recombination caused by loss of the breast cancer susceptibility factor BRCA1. J Biol Chem, 2012. 287(48): p. 40618-28.

54. Ismail, I.H., et al., Germline mutations in BAP1 impair its function in DNA double-strand break repair. Cancer Res, 2014. 74(16): p. 4282-94.

55. Nicassio, F., et al., Human USP3 is a chromatin modifier required for S phase progression and genome stability. Curr Biol, 2007. 17(22): p. 1972-7.

56. Kim, M.S., et al., A draft map of the human proteome. Nature, 2014. 509(7502): p. 575-81.

57. Wilhelm, M., et al., Mass-spectrometry-based draft of the human proteome. Nature, 2014. 509(7502): p. 582-7.

58. Shanbhag, N.M., et al., ATM-dependent chromatin changes silence transcription in cis to DNA double-strand breaks. Cell, 2010. 141(6): p. 970-81.

59. Sakaue-Sawano, A., et al., Visualizing spatiotemporal dynamics of multicellular cell-cycle progression. Cell, 2008. 132(3): p. 487-98.

60. Sowa, M.E., et al., Defining the human deubiquitinating enzyme interaction landscape. Cell, 2009. 138(2): p. 389-403.

61. Helfricht, A., et al., Remodeling and spacing factor 1 (RSF1) deposits centromere proteins at DNA double-strand breaks to promote non-homologous end-joining. Cell Cycle, 2013. 12(18): p. 3070-82.

62. Pierce, A.J., et al., XRCC3 promotes homology-directed repair of DNA damage in mammalian cells. Genes Dev, 1999. 13(20): p. 2633-8.

3

4

The RNF168 ubiquitin ligase orchestrates PALB2-mediated homologous recombination

Dimitris Typas*, Martijn S. Luijsterburg*, Wouter W. Wiegant, Marie-Christine Caron, Jean-Yves Masson, Leon H. Mullenders, and Haico van Attikum

* These authors contributed equally to this work

ABSTRACT

The PALB2 tumour suppressor protein is an essential mediator of DNA double-strand break (DSB) repair by homologous recombination (HR). PALB2 interacts with and is recruited to DSBs by BRCA1 and subsequently promotes the assembly of the core HR proteins BRCA2 and RAD51. In this study, we show that the ubiquitin ligase RNF168 is essential for PALB2 accrual in a manner that is different from canonical RNF168-dependent signalling. Instead, we show that PALB2 associates with RNF168-ubiquitylated chromatin in a fashion dependent on its WD40 domain. The latter appears to promote a direct interaction between PALB2 and RNF168, which facilitates the formation of functional HR complexes. Our findings reveal an RNF168-dependent mechanism that contributes to efficient execution of error-free DSB repair by HR.

4

INTRODUCTION

Chromosomal DNA double-strand breaks (DSBs) that arise during replication or in early G2 are removed by the Homologous Recombination (HR) machinery, which utilises the genetic information from the sister chromatid as a template for error-free repair. Following their detection by the MRN complex, DSB-ends are resected by specific nucleases to generate 3' single-stranded DNA (ssDNA) overhangs, which are bound by the ssDNA-binding protein RPA. In order for homology search to begin, RPA needs to be exchanged for the recombinase RAD51. A complex comprising of the PALB2 (Partner And Localiser of BRCA2) protein and BReast CAncer susceptibility proteins 1 and 2 (BRCA1 and BRCA2) is responsible for RAD51 loading on ssDNA. More specifically, once recruited to resected DSB ends, PALB2 physically bridges the interaction between BRCA1 and BRCA2, thereby facilitating the subsequent assembly of the core HR proteins BRCA2 and RAD51 onto broken DNA ends [1-3]. Finally, RAD51 probes for homology and, upon its detection, catalyses strand invasion and DNA transfer during HR.

Further delineating the mechanistic basis for PALB2 recruitment to DSBs, it was recently demonstrated that recombinant PALB2 directly binds DNA in vitro and associates with chromatin in vivo through its evolutionary conserved Chromatin Association Motif (ChAM) [4]. Though the association of PALB2 with resected DNA is primarily mediated by BRCA1, it additionally exploits PALB2 oligomerisation and protein-protein interactions with ubiquitin-binding proteins, such as MRG15 [2, 3, 5].

The choice between the major DSB repair pathways HR and Non-Homologous End-Joining (NHEJ) is regulated throughout the cell cycle by signalling pathways that involve MDC1 and the two E3 ubiquitin ligases RNF8 and RNF168 [6, 7]. These enzymes ubiquitylate chromatin in the vicinity of DSBs and promote the ubiquitin-dependent recruitment of the RAP80-BRCA1 and 53BP1-RIF1 complexes [8, 9]. The assembly of both of these complexes antagonises HR, largely by limiting DNA end-resection. Therefore it has been suggested that RNF8/RNF168-mediated signalling pathways may be generally inhibitory to HR [8, 10-12]. On the other hand, several reports have

implicated that RNF8 promotes HR [13-16], suggesting that the intricate interplay between RNF8/RNF168-induced ubiquitylation and HR is currently not understood in its entirety.

In this study, we show that PALB2 associates with RNF168-, but not RNF8-, ubiquitylated chromatin, indicating that the RNF168-dependent ubiquitylation events that promote PALB2 chromatin assembly are not the canonical ones. Subsequently, we demonstrate that efficient recruitment and retention of PALB2 at DSBs is also dependent on RNF168-induced ubiquitylation, promoting BRCA1-dependent PALB2 accrual and the subsequent formation of functional HR complexes. Finally, we reveal that PALB2 directly interacts with RNF168 via its WD40 domain. These findings define a new RNF168-mediated mechanism that contributes to PALB2 recruitment and efficient HR.

RESULTS AND DISCUSSION

RNF168-mediated ubiquitylation promotes PALB2 recruitment to chromatin

To explore potential links between RNF8/RNF168 and the homologous recombination (HR) machinery, we used a chromatin-tethering approach, exploiting the strong interaction between the LacR protein and the LacO DNA sequence [17, 18]. Human U2OS cells with stably incorporated LacO arrays [19] were transfected with LacR-tagged RNF8 or RNF168 (Fig. 1A), which triggered the accumulation of 53BP1 and ubiquitin (FK2) conjugates (Fig. 1B) at the LacO array, as previously reported [17, 18, 20]. Surprisingly, we found that tethering LacR-RNF168 specifically attracted PALB2 and RAD51 to the array, while LacR-RNF8 or LacR alone failed to do so. The ubiquitin ligase activity of RNF168 was required for these events, since tethering of catalytically inactive RNF168^{C16S} (RNF168ΔRING) significantly reduced PALB2 and RAD51 accrual (Fig. 1C,D). Importantly, immobilising either RNF168 or RNF168ΔRING hardly triggered any accumulation of phosphorylated RPA, suggesting that there is little DNA end-resection at the

array (Supplemental Fig. 1A).

Supporting the ubiquitin-dependent nature of PALB2 accrual, we found that over-expression of the de-ubiquitylating enzymes USP26 or USP37, which we recently showed that reverse RNF168-induced ubiquitylation (Chapter 3), efficiently suppressed accrual of both PALB2 (Supplemental Fig. 1B) and RAD51 (Supplemental Fig. 1C). The RNF8 pathway was recently linked to PALB2 recruitment through the assembly of the BRCA1-RAP80-Abraxas complex [16]. Conversely, several other studies found RAP80 and Abraxas to strongly inhibit HR, likely by sequestering BRCA1 away from resected DNA where it loads PALB2 for HR [10, 11, 21]. In line with the latter studies, knock-down of RAP80 did not affect PALB2 recruitment after RNF168 tethering, while BRCA1 recruitment was moderately reduced (Fig. 1E) and RAP80 accrual was undetectable (Supplemental Fig. 1D). We conclude that forced chromatin binding of RNF168 triggers PALB2 and RAD51 loading onto chromatin in a ubiquitin-dependent manner that does not require canonical signalling through the BRCA1-Abraxas-RAP80-MERIT40 complex.

4

4
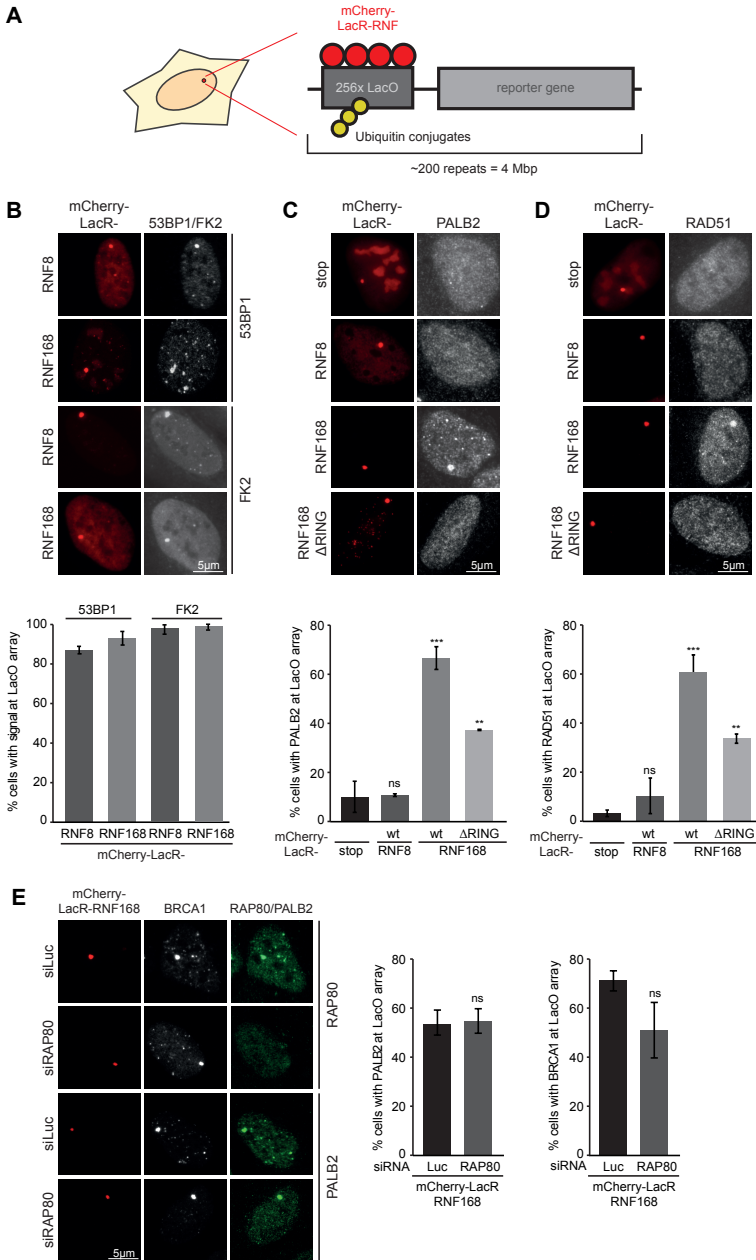
Figure 1. RNF168-dependent chromatin recruitment of PALB2. (A) Schematic of the RNF8/ RNF168 tethering system. (B) 53BP1 (white; upper images) and ubiquitin-FK2 accumulation (white; lower images) upon tethering of the indicated mCherry-LacR fusion proteins (red) in cells containing a LacO array. (C) As in B, but stained for PALB2 (white). (D) As in C, but stained for RAD51 (white). (E) As in C, but stained for PALB2 or RAP80 in control (siLuc) or RAP80-depleted cells. 50-100 cells were analysed per experiment. Quantified data are represented as mean ± S.D. (n=3). *, P<0.05, **, P<0.01, ***, P<0.001 (student's t test). See also Supplemental Figure 1.

RNF168-mediated ubiquitylation promotes PALB2 recruitment to DSBs

To examine the functional relevance of our findings in the tethering system, we depleted cells of RNF8 or RNF168 and assessed the assembly of HR factors into ionising radiation-induced foci (IRIF) that contain DSBs. In order to specifically monitor recruitment in S and G2 cells, we engineered U2OS cells stably expressing the mAG-tagged cell cycle marker geminin and validated this cell-line by flow cytometry (Supplemental Fig. 2A). RNF8 or RNF168 loss largely abolished the accrual of PALB2 in mAG-geminin-positive cells (Fig. 2A). Comparable results were obtained in cyclin B1-positive G2 cells (Supplemental Fig. 2B). Importantly, BRCA1 depletion completely abolished PALB2 recruitment [2, 3], while knock-down of RAP80 had no appreciable impact (Fig. 2A and Supplemental Fig. 1E). These results suggest that RNF8/RNF168 contribute to the BRCA1-dependent loading of PALB2 at DSBs independently of RAP80, in agreement with our tethering results (Fig. 1E). Depletion of RNF8 or RNF168 also impaired efficient RAD51 assembly in cycling cells, following either IR-inflicted DNA damage (Fig. 2B) or laser micro-irradiation (Supplemental Fig. 2C) consistent with the role of PALB2 in loading RAD51. We confirmed these findings in an siRNA-independent manner by using RNF168-deficient RIDDLE cells, which displayed markedly reduced RAD51 recruitment after IR compared to RNF168-complemented RIDDLE cells [7] (Fig. 2B).

To directly measure HR efficiency, we utilised the flow cytometry-based DR-GFP reporter gene [22]. As expected, BRCA2 loss impaired the ability to repair a DSB induced in the gfp reporter gene demonstrating that the reporter accurately reflects HR (Fig. 2C). Depletion of either RNF8 or RNF168, with independent siRNAs, also caused a notable reduction in HR efficiency (Fig. 2C) without any impact on cell cycle distribution (Supplemental Fig. 2D). These findings suggest that RNF168-mediated ubiquitylation promotes HR by modulating BRCA1-dependent PALB2 recruitment and the subsequent formation of a functional HR complex. The fact that RNF8 is dispensable for PALB2 recruitment in the tethering system (Fig. 1A,C), but necessary for IR-induced PALB2 recruitment, is consistent with the strict requirement for RNF8 in the IR-induced recruitment of RNF168 [6, 7].

RNF168-mediated ubiquitylation confines PALB2 recruitment to DSB proximal sites

Chromatin marked by γH2AX is occupied by signalling factors, such as ATM, MDC1 and 53BP1, which spread within megabase-sized DSB-flanking domains. In contrast, HR factors such as RPA, BRCA2 and RAD51 accumulate in micro-domains delineated by the presence of single-stranded DNA (ssDNA), generated by nucleolytic processing of the broken ends [23, 24]. Given the interplay between RNF168 and PALB2 during HR (Fig. 2A), we sought to determine their spatial organization at DSBs by measuring IRIF size. As previously reported [23], we observed a notable difference in the distribution of signalling proteins compared to HR factors. RNF168, similar to the signalling factors γH2AX, MDC1, BRCA1, RAP80 and 53BP1, formed larger foci, indicative of spreading more distally from DSBs, whereas PALB2 and the HR factors RPA and RAD51 formed smaller foci, indicative of binding to regions more proximally to DSBs (Fig. 2D). Thus, even though PALB2 recruitment is facilitated by RNF168, its recruitment is likely confined to the ssDNA compartment proximal to DSBs. RNF168 spreads beyond this compartment into regions more distal to the break, most likely to promote accrual of the BRCA1-Abraxas-RAP80-MERIT40 complex [25-27]. The fact that PALB2 foci are much smaller than those of BRCA1 and RAP80 implies that the BRCA1-Abraxas-RAP80-MERIT40 complex does not trigger PALB2 assembly in regions more distal from the break, which is in agreement with its antagonistic effect on HR [10, 11]. Thus, while BRCA1 assembly at regions distal to the break depends on RAP80, its recruitment to the ssDNA compartment does not require this protein. Together our results suggest that RNF168, in concert with BRCA1 [2, 3], facilitates PALB2 loading and subsequent HR complex formation in DSB-associated micro-domains demarcated by the presence of ssDNA.
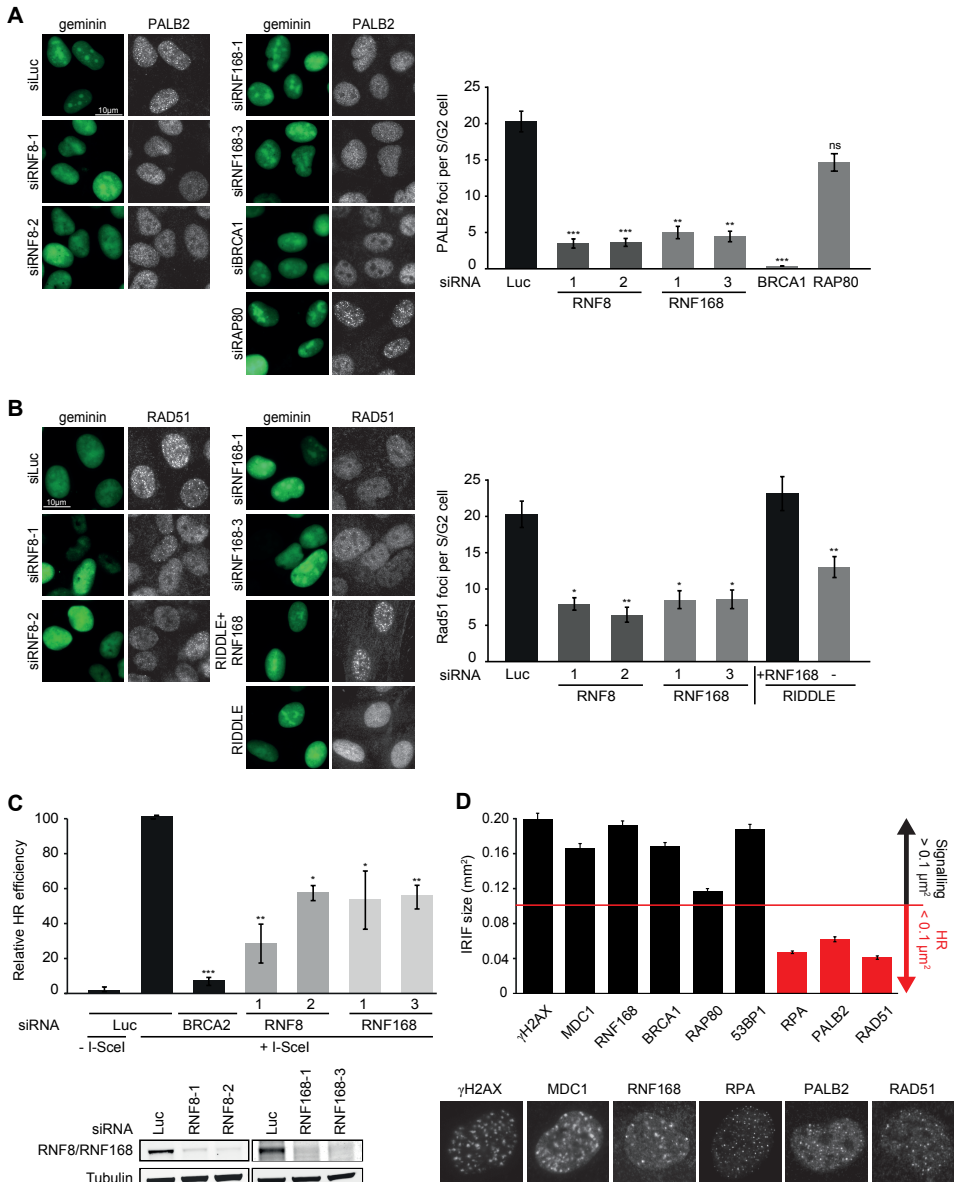
Figure 2. RNF168-dependent recruitment of HR factors PALB2 and RAD51 to DSBs. (A) Effect of the indicated siRNAs on PALB2 (white) IRIF formation in mAG-geminin-expressing (green) S/G2 cells. (B) RAD51 (white) IRIF formation in mAG-geminin-expressing (green) S/G2 cells transfected with the indicated siRNAs and RNF168-deficient RIDDLE S/G2 cells complemented with either an empty vector or wild-type RNF168. (C) Effect of the indicated siRNAs on HR efficiency measured using the DR-GFP reporter. Western blot analysis of RNF8 and RNF168 expression in cells treated with the indicated siRNAs. (D) IRIF foci size (in µm2) of various signalling and HR proteins. Quantified data are represented as mean ± S.D. (n=3), except in D where n=2. *, P<0.05, **, P<0.01, ***, P<0.001 (student's t test). See also Supplementary Figure 2.

PALB2 associates with ubiquitylated chromatin through its WD40 domain

The RNF168-dependent recruitment of PALB2 at DSBs can be either indirect, through association with a ubiquitin-binding partner, or direct, by recognition of ubiquitin chains. PALB2 indeed interacts with the ubiquitylated H2B-binding protein MRG15, which promotes its recruitment to DSBs [28, 29]. However, the tethering of RNF168 to chromatin, which triggered massive ubiquitylation and robust accrual of PALB2, failed to efficiently recruit HA-tagged MRG15 (Supplemental Fig. 3A). This was not due to expressing a nonfunctional fusion protein, as MRG15-HA was efficiently recruited into IRIF (Supplemental Fig. 3B) [5]. Moreover, the recruitment of PALB2 after IR (Fig. 2A) and upon tethering of RNF168 to chromatin did not require RAP80 (Fig. 1E). Thus, the RNF168-dependent binding of PALB2 to chromatin does not involve these known ubiquitin-binding proteins.

By means of in silico analysis, it was predicted that the C-terminal WD40 domain of PALB2 may bind ubiquitin [30], a property that is common amongst a wide range of WD40 domains [31]. To test if PALB2 indeed associates with ubiquitin through its WD40 domain, we generated YFP-tagged wild-type PALB2 or PALB2 lacking its WD40 domain (ΔWD40). Both PALB2 fusion proteins were expressed at comparable levels and localised to the nucleus similarly to endogenous PALB2. Similar to endogenous PALB2, YFP-PALB2^{WT} was recruited to chromatin following tethering of RNF168 (Fig. 3A,B). However, YFP-PALB2^{ΔWD40} failed to associate with RNF168-induced ubiquitin conjugates, suggesting that PALB2's association with ubiquitylated chromatin is WD40 dependent (Fig. 3A,B). Subsequently we assessed the recruitment of YFP-tagged PALB2 variants to sites of DNA damage. YFP-PALB2^{ΔWD40} did not accumulate as readily as YFP-PALB2^{WT} at laser-induced DNA damage (Fig. 3C), as well as at bona fide DSBs, induced at the LacO array by the LacR-tagged FokI nuclease (Fig. 3D,E). In order to exclude possible side effects caused by overexpressing PALB2 (Supplemental Fig. 3C) [32], we complemented PALB2-deficient FANCN cells with the aforementioned constructs. YFP-PALB2^{WT} localised at sites of IR-induced DNA damage in cycling cells more efficiently than its ΔWD40 counterpart (Fig. 3F). Together,

these findings support the notion that the WD40 domain of PALB2 facilitates its association with RNF168-induced ubiquitin conjugates at DSBs.

To confirm that PALB2 can recognise ubiquitin in a WD40-dependent manner, we tested its ability to associate with ubiquitin in an in vitro binding assay. Recombinant GST-ubiquitin efficiently pulled down YFP-PALB2^{WT} and endogenous RNF168, a known ubiquitin-binding factor, from cell extracts. In contrast, GST alone or GST-ubiquitin^{I44A} failed to do so, showing that these interactions require the hydrophobic patch of ubiquitin (I44)[33]. Strikingly, YFP-PALB2$^{\Delta WD40}$ did not interact with GST-ubiquitin (Fig. 3G). In order to verify if the WD40 domain of PALB2 directly binds ubiquitin or rather it interacts with a ubiquitin-binding protein, we performed in vitro interaction experiments. Neither purified GST-WD40^{PALB2} nor any of the other four GST-PALB2 fragments could interact with recombinant mono-ubiquitin (Supplemental Fig. 3D). Similar negative results were obtained when assaying if GST-WD40^{PALB2} could bind poly-ubiquitin chains of various linkages (Supplemental Fig. 3E). Therefore, our results indicate that the WD40 domain of PALB2 supports its association with DSB-induced ubiquitin conjugates but it does not directly bind such ubiquitylated substrates. Furthermore, our findings support a scenario in which PALB2 via its WD40 domain associates with a protein binding RNF168-induced ubiquitylation. Since BRCA1 is essential for PALB2 assembly [2, 3], the WD40-dependent recognition of RNF168-modified chromatin is most likely part of a BRCA1-dependent loading mechanism for PALB2.

4
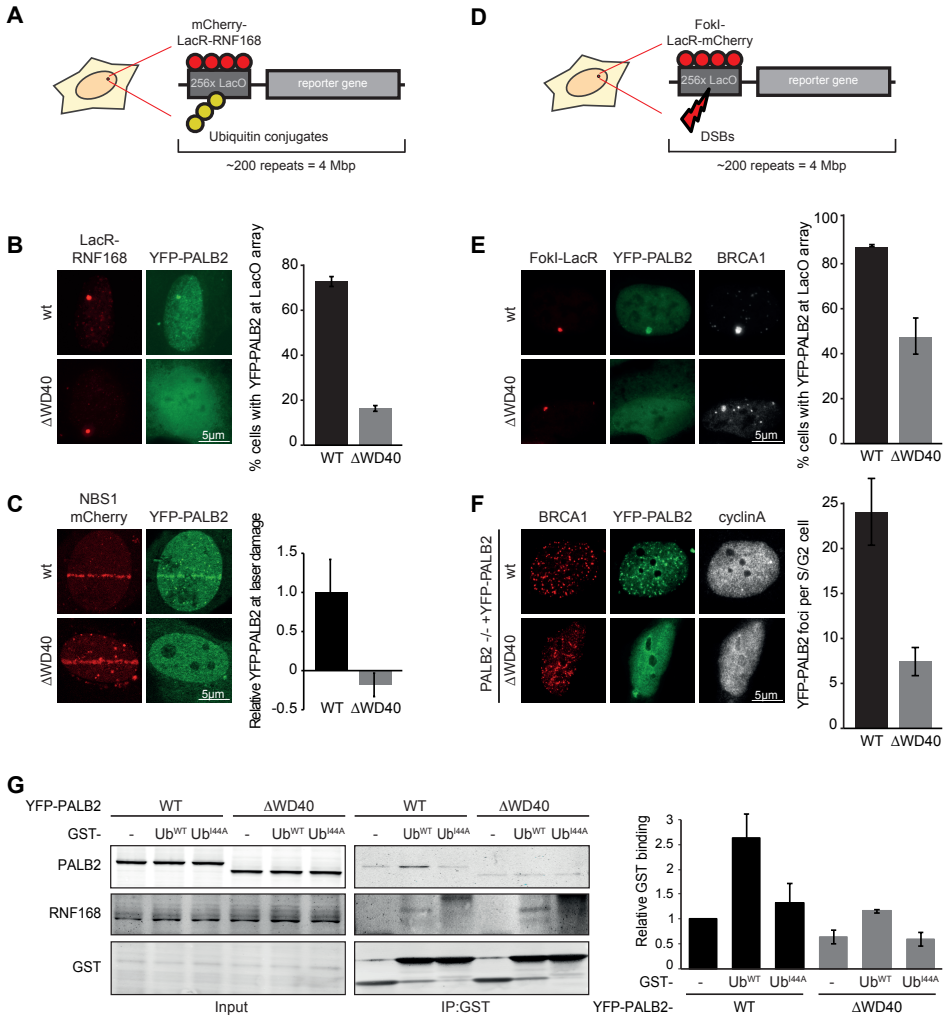
Figure 3. RNF168-dependent recruitment of PALB2 is regulated by an indirect interaction between ubiquitin and its WD40 domain. (A) Schematic of the RNF8/RNF168-tethering system. (B) YFP-PALB2 (green) accumulation upon tethering of mCherry-LacR-RNF168 (red) in cells containing a LacO array. (C) Recruitment of the indicated YFP fusion proteins (green) to mCherry-NBS1-marked DNA damage sites (red) after micro-irradiation. (D) Schematic of the system used to induce multiple DSBs upon tethering of the FokI endonuclease. (E) Recruitment of the indicated YFP fusion proteins (green) to BRCA1-marked (white) DSBs induced by FokI-mCherry-LacR at a LacO array (red). (F) IRIF formation of the indicated YFP fusion proteins (green) in complemented PALB2-deficient cells (EUFA1341). Cells in S/G2 are marked by cyclin A (white) while BRCA1 (red) is used as a DNA damage marker. (G) GST-binding assay to assess the binding of YFP-PALB2-WT and YFP-PALB2-ΔWD40 to the indicated GST-ubiquitin (GST-Ub) fusion proteins or GST alone. Relative binding to GST was determined by normalising the PALB2/GST ratios of each IP sample to that of YFP-PALB2WT/GST alone, which was set to 1. Quantified data are represented as mean ± S.D. (n=2). See also Supplementary Figure 3.

PALB2 interacts with RNF168 via its WD40 domain

Given the fact that residual PALB2 and RAD51 accumulation lingers when catalytically inactive RNF168 is immobilised at chromatin (Fig. 1C, D), and knowing that RNF168 can itself bind the ubiquitylated substrates it catalyses through its MIU domains [6, 7, 20], we sought to examine whether PALB2 and RNF168 directly interact. Therefore, we immunoprecipitated GFP-tagged RNF8 or RNF168 and noticed that endogenous PALB2 was specifically detected upon RNF168-IP (Fig. 4A). Performing the reciprocal experiment we obtained similar results, namely endogenous RNF168 was co-purified along YFP-PALB2 (Fig. 4B). Aiming to verify that this interaction is mediated by the WD40 domain of PALB2, we immunoprecipitated either wild-type or ΔWD40 YFP-PALB2 and checked if it associates with RNF168. While RNF168 readily bound YFP-PALB2^{WT}, this association was all but lost with YFP-PALB2$^{\Delta WD40}$ (Fig. 4C), indicating that the WD40 domain is crucial for the RNF168-PALB2 interaction.

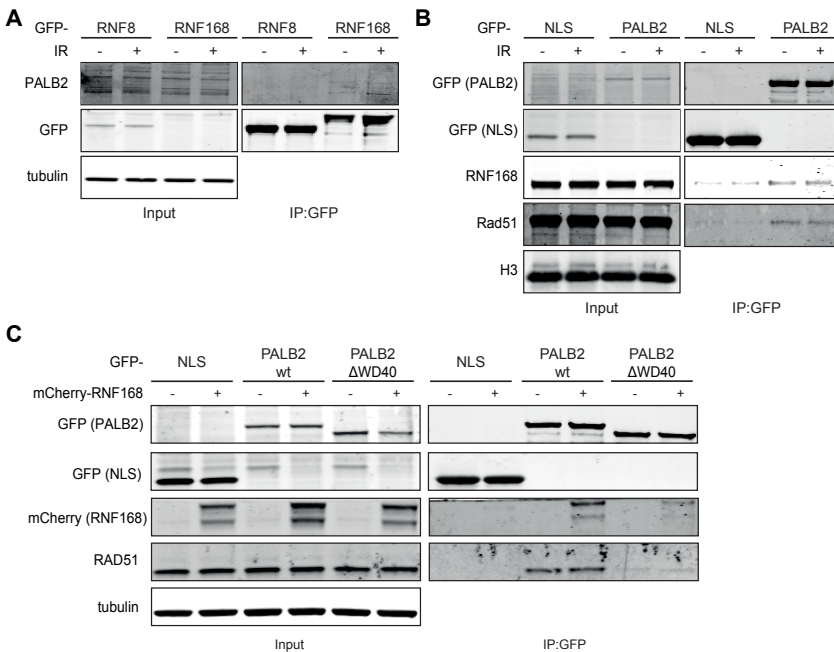**4**

Figure 4. RNF168 and PALB2 interact via the WD40 domain of PALB2. (A) GFP-immunoprecipitation of indicated GFP-fusion proteins. Blots were probed for PALB2 (endogenous), GFP and tubulin (loading control). (B) As in A but stained for GFP, RNF168 (endogenous), RAD51 and histone H3 (loading control). (C) As in B but probed for GFP, mCherry (RNF168), RAD51 and tubulin (loading control).

A trimodular recruitment mechanism for PALB2

We propose the following model for RNF168-dependent regulation of HR: RNF168 decorates chromatin substrates with ubiquitin following its binding to RNF8-modified chromatin proximally to DSBs. Although it may be expected that resected DNA is devoid of histones, recent studies have shown that resection can actually occur in a nucleosomal context [34, 35]. Subsequently, the ubiquitin moieties in the ssDNA compartment attract PALB2 through its WD40 domain, which, in turn, facilitates BRCA2 and RAD51 assembly and promotes efficient HR. This model integrates three WD40-dependent features of PALB2: its accumulation at RNF168-modified chromatin (Fig. 3B), its association with ubiquitin in vitro (Fig. 3G) and its accrual at IR- and FokI-induced DSBs (Fig. 3C-F). We propose that these events contribute to a trimodular mechanism for PALB2 recruitment in which 1) BRCA1 promotes PALB2 assembly through a protein-protein interaction involving its N-terminus [2, 3], 2) the more centrally located chromatin-association motif (ChAM) in PALB2 stabilises and promotes its binding to damaged chromatin (in the ssDNA compartment), and 3) the C-terminal WD40 domain of PALB2 further facilitates its accrual and retention by associating with RNF168-ubiquitylated chromatin. We propose that integrating these independent recruitment signals leads to the efficient and specific accrual of PALB2 to HR sites. Such a recruitment mechanism is not uncommon in the DDR. For instance, the assembly of 53BP1 at damaged chromatin requires the simultaneous presence of two distinct marks on histones H4 and H2A [36, 37]. These findings advance our conceptual understanding of the RNF168-dependent response to DSBs by revealing a new mechanism that contributes to the assembly and function of HR complexes at DSBs.

MATERIALS AND METHODS

Cell culture

U2OS, HEK293, RIDDLE (RNF168-deficient), EUFA1341 (FANCN/PALB2-deficient) and VH10-SV40-immortalised cells were grown in DMEM (Gibco) containing 10% FCS (Bodinco BV). U2OS 2–6-3 cells containing 200 copies of a LacO-containing cassette (~4 Mbp) and U2OS 2-6-3 cells stably expressing an inducible version of FokI-mCherry-LacR fused to the estrogen receptor (ER) and harbouring a destabilisation domain (DD) were previously described [6, 9, 38, 39]. The ViraPower system (Life Science) was used to produce lentivirus using mAG- or mCherry-geminin expression vectors. U2OS and RIDDLE cells stably expressing mAG- or mCherry-geminin were generated by lentiviral infection [40]. U2OS cells were FACS sorted to select fluorescence-positive cells.

4

Plasmids

The WD40 domain of PALB2 was removed by inserting a fragment spanning the first 2874 nucleotides of wild-type PALB2 into YFP-C1. Additional plasmids used are listed in the Supplemental Table.

Transfections

siRNA and plasmid transfections were performed using Lipofectamine RNAiMAX (Invitrogen), Lipofectamine 2000 (Invitrogen) and JetPEI (Polyplus Transfection) according to the manufacturer's instructions. Cells were transfected twice with siRNAs (40 nM) within 24 h and examined further 48 h after the second transfection, unless stated otherwise. siRNA sequences are listed in the Supplemental Table.

Generation of DSBs

IR was delivered by a YXlon X-ray generator (YXlon International, 200 KV, 10 mA, dose rate 2 Gy/min).

FokI assays

U2OS 2-6-3 cells expressing inducible FokI-mCherry-LacR [39] were treated with 300 nM 4-OHT and 1 µM Shield-I for 5 hrs. Subsequently, cells were fixed with formaldehyde and immunostained with the indicated antibodies.

Laser-assisted DSB induction

U2OS cells were irradiated with a pulsed nitrogen laser (Micropoint Ablation Laser System; Photonic Instruments, Inc., Belfast, Ireland; 16 Hz, 364 nm) [17, 18] or a Mira mode-locked titanium-sapphire (Ti:Sapphire) laser (I = 800 nm, pulse length = 200 fs, repetition rate = 76 MHz, output power = 80 mW) as described previously [41].

Microscopy analysis

Images of fixed cells were acquired on a Zeiss AxioImager D2 widefield fluorescence microscope equipped with 40x, 63x and 100x PLAN APO (1.4 NA) oil-immersion objectives (Zeiss) and an HXP 120 metal-halide lamp used for excitation. Fluorescent probes were detected using previously described filters [42]. Images were recorded using ZEN 2012 software and analysed using ImageJ. The average reflects the quantification of 50-150 cells from 3 independent experiments.

IRIF analysis

PALB2, RAD51 and MRG15-HA IRIF were analysed in U2OS cells 6hr after 10Gy, whereas γH2AX, MDC1, conjugated ubiquitin (FK2), RNF168, RAP80, BRCA1 and 53BP1 IRIF were examined 1hr after 2Gy, unless stated otherwise. IRIF were evaluated in ImageJ, using a custom-built macro that enabled automatic and objective analysis of the foci. Full details of this macro will be published elsewhere. In brief, cell nuclei were detected by thresholding the (median-filtered) DAPI signal, after which touching nuclei were separated by a watershed operation. The foci signal was background-subtracted using a Difference of Gaussians filter. For every nucleus, foci were identified as regions of adjacent pixels satisfying the following criteria: (i) the grey value exceeds the nuclear background signal by a set number of times (typically 2-4x) the median background standard deviation of all nuclei in the image, and is higher than a user-defined absolute minimum value; (ii)

the area is larger than a defined area (typically 2 pixels). These parameters were optimized for every experiment by manually comparing the detected foci with the original signal.

Immunofluorescent labeling

Immunofluoresecent labeling was carried out as described previously [17, 41]. Briefly, cells were grown on glass coverslips and treated as indicated in the figure legends. Subsequently, cells were washed with PBS, then fixed with 2% formaldehyde for 20 minutes and permeabilized with 0.25% Triton X-100 in PBS for 5 minutes. Cells were rinsed with phosphate-buffered saline (PBS) and then treated with 100 mM glycine in PBS for 10 minutes to block unreacted aldehyde groups. Finally, cells were equilibrated in PBS containing 0.5% BSA and 0.05% Tween 20, and incubated with primary antibodies. Detection was done using goat anti-mouse or goat anti-rabbit IgG coupled to Alexa 488, 555 or 647 (Invitrogen Molecular Probes). Samples were incubated with 0.1 µg/ml DAPI and mounted in Polymount. Primary antibodies and secondary antibodies are listed in the Supplemental Table.

GST-binding assay

HEK293 cells were transfected with the indicated YFP-tagged PALB2 constructs after which ubiquitin-binding assays were performed as described [33]. Shortly, HEK293 cells were transfected with the indicated YFP-tagged PALB2 constructs, lysed for 10 min on ice in lysis buffer (50 mM HEPES, 150 mM NaCl, 1 mM EDTA, 1 mM EGTA, 10% glycerol, 1% Triton-X-100, 25 mM NaF, 10 µM ZnCl2, pH 7.5) containing protease inhibitors. Cell lysates were collected, centrifuged for 15 min (13,000g) to remove the insoluble fraction and incubated with GST, GST–ubiquitin[WT] or GST–ubiquitin[I44A] (UBPBio, Aurora, USA) coupled to Glutathione sepharose 4B (Amersham Biosciences, Freiburg, Germany) for 4 h at +4 °C. After incubation, the sepharose matrix was washed three times with lysis buffer. Bound proteins were eluted with 10mM reduced glutathione and analysed by immunoblotting.

Western blotting

Cell extracts were generated by boiling cell pellets in Laemmli buffer,

separated by SDS-PAGE and transferred to PVDF membranes (Millipore). Membranes were probed with the antibodies listed in the Expanded view followed by protein detection using the Odyssey infrared imaging scanning system (LI-COR Biosciences).

HR assay

HEK293 and U2OS cells containing a stably integrated copy of the DR-GFP reporter were used to measure the repair of I-SceI-induced DSBs by HR as described [22]. Briefly, 48 h after siRNA transfection, cells were transfected with the I-SceI expression vector pCBASce and an mCherry expression vector. 48 or 72 h later the fraction of GFP-positive cells among the mCherry-positive cells was determined by FACS on a LSRII flow cytometer (BD Bioscience) using FACSDiva software version 5.0.3. Quantifications were performed using Flowing Software (www.flowingsoftware.com).

Cell cycle profiling

For cell cycle analysis cells were fixed in 70% ethanol, followed by DNA staining with 50 μg/ml propidium iodide in the presence of RNase A (0.1 mg/ml). Cell sorting was performed on a LSRII flow cytometer (BD Bioscience) using FACSDiva software (version 5.0.3; BD). Quantifications were performed using Flowing Software.

Supplemental Figure 1. PALB2 accumulates at RNF168-induced ubiquitylated substrates. (A) Phosphorylated RPA accumulation (white) upon tethering of the indicated mCherry-LacR fusion proteins (red) in cells containing a LacO array. (B) Effect of the overexpression of the GFP-tagged deubiquitylating enzymes USP26 and USP37 (green) in the accumulation of PALB2 (white) upon tethering of mCherry-LacR-RNF168 (red) in cells containing a LacO array. (C) As in B but stained for RAD51 (white). (D) As in C, but stained for RAP80 (green) in control (siLuc) or RAP80-depleted cells. (E) Effect of the indicated siRNAs in the formation of BRCA1 (white; left) and RAP80 (white; right) IRIF in S/G2 cells. 50-100 cells were analysed per experiment. Quantified data are represented as mean ± S.D. (n=3). *, P<0.05, **, P<0.01, ***, P<0.001 (student's t test).
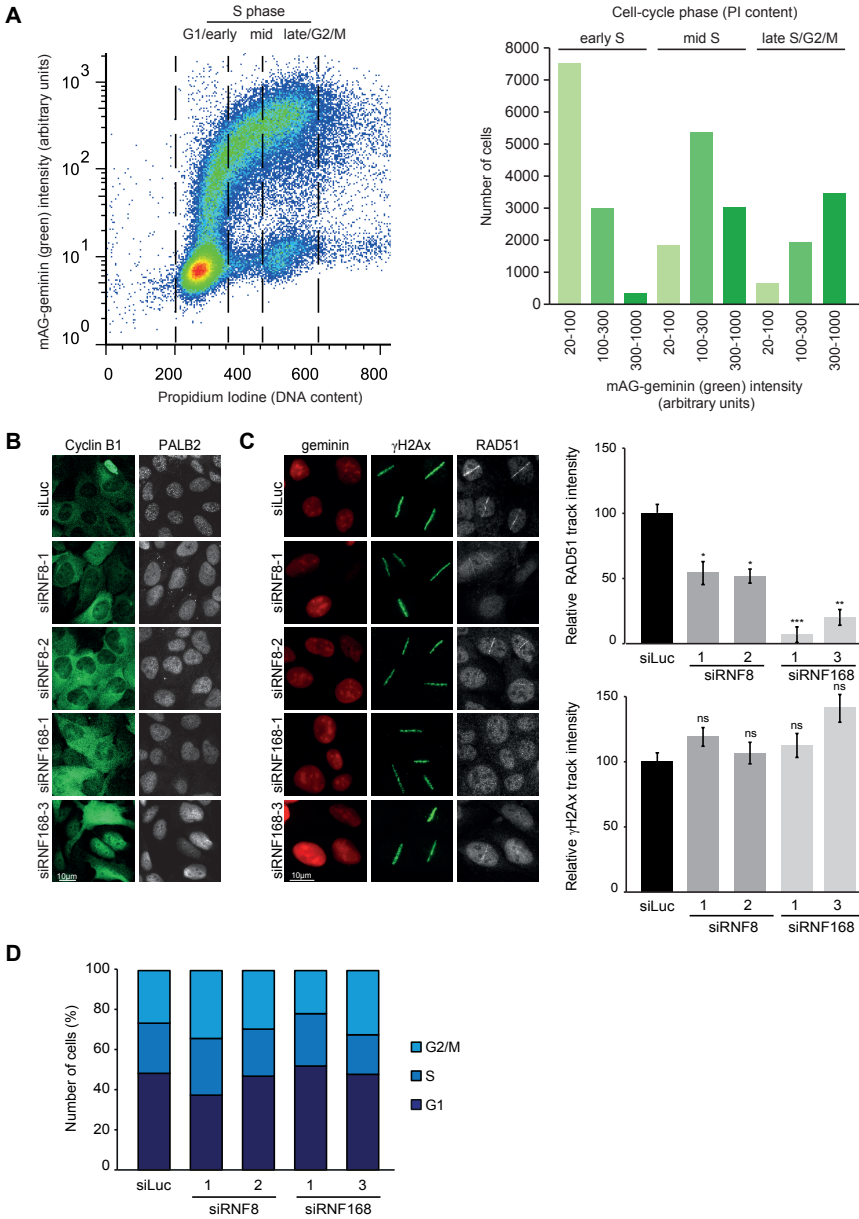
Supplemental Figure 2. RNF8/RNF168 depletion impairs HR in mAG-geminin U2OS cells.
(A) Validation of the mAG-geminin U2OS cell line by FACS; plot of propidium iodine staining, indicative of DNA content (x-ayis), and mAG-geminin expression (y-axis). Quantification of FACS results (right panel). (B) Effect of the indicated siRNAs on PALB2 (white) IRIF formation in cyclin B1-expressing (green) S/G2 cells. (C) Impact of the indicated siRNAs on RAD51 recruitment (white) to γH2AX-marked DSB tracks (green) generated after UV-A laser micro-irradiation in mCherry-geminin-expressing (red) S/G2 cells. (D) Cell cycle profiles of cells treated with the indicated siRNAs. Quantified data are represented as mean ± S.D. (n=3). *, P<0.05, **, P<0.01, ***, P<0.001 (student's t test).
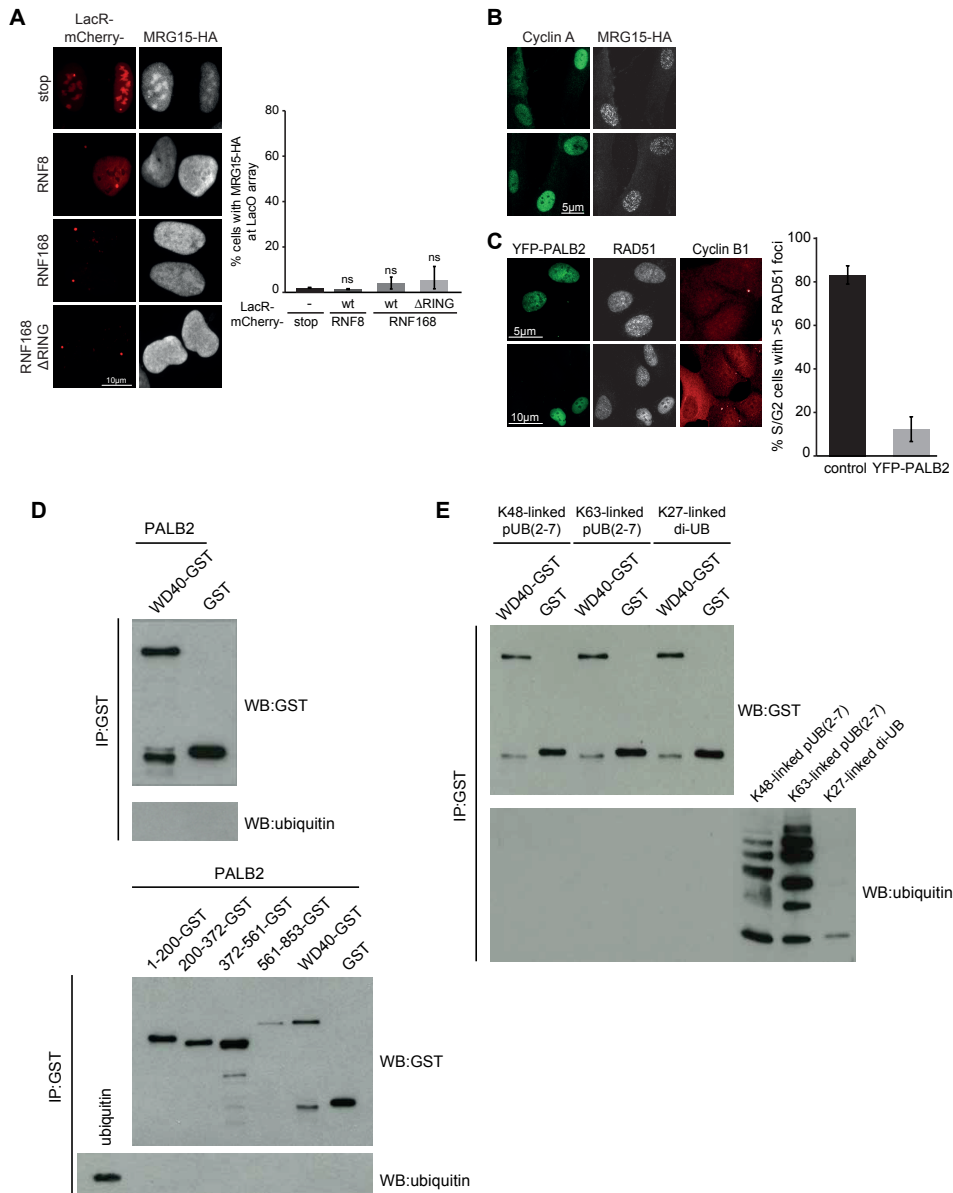
Supplemental Figure 3. PALB2 accrual at RNF168-ubiquitylated chromatin is not mediated by MRG15 or direct ubiquitin binding. (A) MRG15-HA (white) accumulation upon tethering of the indicated mCherry-LacR fusion proteins (red) in cells containing a LacO array. (B) MRG15-HA (white) IRIF formation in cyclin A-expressing (green) S/G2 cells. (C) Impact of the overexpression of YFP-PALB2 (green) in the formation of RAD51 IRIF (white) in cyclin B1-expressing (red) S/G2 cells. (D) GST-immunoprecipitation based in vitro interaction studies of the indicated GST fusion proteins and recombinant mono-ubiquitin. Blots were probed for GST and ubiquitin. (E) As in (D) only incubated with recombinant polyubiquitin chains of K48, K63 or K27 linkage. Quantified data are represented as mean ± S.D. (n=3). *, P<0.05, **, P<0.01, ***, P<0.001 (student's t test).

REFERENCES

1. Sy, S.M., M.S. Huen, and J. Chen, PALB2 is an integral component of the BRCA complex required for homologous recombination repair. Proc Natl Acad Sci U S A, 2009. 106(17): p. 7155-60.

2. Zhang, F., et al., PALB2 functionally connects the breast cancer susceptibility proteins BRCA1 and BRCA2. Mol Cancer Res, 2009. 7(7): p. 1110-8.

3. Zhang, F., et al., PALB2 links BRCA1 and BRCA2 in the DNA-damage response. Curr Biol, 2009. 19(6): p. 524-9.

4. Bleuyard, J.Y., et al., ChAM, a novel motif that mediates PALB2 intrinsic chromatin binding and facilitates DNA repair. EMBO Rep, 2012. 13(2): p. 135-41.

5. Sy, S.M., M.S. Huen, and J. Chen, MRG15 is a novel PALB2-interacting factor involved in homologous recombination. J Biol Chem, 2009. 284(32): p. 21127-31.

6. Doil, C., et al., RNF168 binds and amplifies ubiquitin conjugates on damaged chromosomes to allow accumulation of repair proteins. Cell, 2009. 136(3): p. 435-46.

7. Stewart, G.S., et al., The RIDDLE syndrome protein mediates a ubiquitin-dependent signaling cascade at sites of DNA damage. Cell, 2009. 136(3): p. 420-34.

8. Escribano-Diaz, C., et al., A cell cycle-dependent regulatory circuit composed of 53BP1-RIF1 and BRCA1-CtIP controls DNA repair pathway choice. Mol Cell, 2013. 49(5): p. 872-83.

9. Mailand, N., et al., RNF8 ubiquitylates histones at DNA double-strand breaks and promotes assembly of repair proteins. Cell, 2007. 131(5): p. 887-900.

10. Hu, Y., et al., RAP80-directed tuning of BRCA1 homologous recombination function at ionizing radiation-induced nuclear foci. Genes Dev, 2011. 25(7): p. 685-700.

11. Coleman, K.A. and R.A. Greenberg, The BRCA1-RAP80 complex regulates DNA repair mechanism utilization by restricting end resection. J Biol Chem, 2011. 286(15): p. 13669-80.

12. Munoz, M.C., et al., RING finger nuclear factor RNF168 is important for defects in homologous recombination caused by loss of the breast cancer susceptibility factor BRCA1. J Biol Chem, 2012. 287(48): p. 40618-28.

13. Meerang, M., et al., The ubiquitin-selective segregase VCP/p97 orchestrates the response to DNA double-strand breaks. Nat Cell Biol, 2011. 13(11): p. 1376-82.

14. Huang, J., et al., RAD18 transmits DNA damage signalling to elicit homologous recombination repair. Nat Cell Biol, 2009. 11(5): p. 592-603.

15. Lu, C.S., et al., The RING finger protein RNF8 ubiquitinates Nbs1 to promote DNA double-strand break repair by homologous recombination. J Biol Chem, 2012.

287(52): p. 43984-94.

16.   Zhang, F., et al., MDC1 and RNF8 function in a pathway that directs BRCA1-dependent localization of PALB2 required for homologous recombination. J Cell Sci, 2012. 125(Pt 24): p. 6049-57.

17.   Luijsterburg, M.S., et al., A new non-catalytic role for ubiquitin ligase RNF8 in unfolding higher-order chromatin structure. EMBO J, 2012. 31(11): p. 2511-27.

18.   Acs, K., et al., The AAA-ATPase VCP/p97 promotes 53BP1 recruitment by removing L3MBTL1 from DNA double-strand breaks. Nat Struct Mol Biol, 2011. 18(12): p. 1345-50.

19.   Janicki, S.M., et al., From silencing to gene expression: real-time analysis in single cells. Cell, 2004. 116(5): p. 683-98.

20.   Panier, S., et al., Tandem protein interaction modules organize the ubiquitin-dependent response to DNA double-strand breaks. Mol Cell, 2012. 47(3): p. 383-95.

21.   Kakarougkas, A., et al., Co-operation of BRCA1 and POH1 relieves the barriers posed by 53BP1 and RAP80 to resection. Nucleic Acids Res, 2013. 41(22): p. 10298-311.

22.   Pierce, A.J., et al., XRCC3 promotes homology-directed repair of DNA damage in mammalian cells. Genes Dev, 1999. 13(20): p. 2633-8.

23.   Bekker-Jensen, S., et al., Spatial organization of the mammalian genome surveillance machinery in response to DNA strand breaks. J Cell Biol, 2006. 173(2): p. 195-206.

24.   Iacovoni, J.S., et al., High-resolution profiling of gammaH2AX around DNA double strand breaks in the mammalian genome. EMBO J, 2010. 29(8): p. 1446-57.

25.   Feng, L., J. Huang, and J. Chen, MERIT40 facilitates BRCA1 localization and DNA damage repair. Genes Dev, 2009. 23(6): p. 719-28.

26.   Shao, G., et al., MERIT40 controls BRCA1-Rap80 complex integrity and recruitment to DNA double-strand breaks. Genes Dev, 2009. 23(6): p. 740-54.

27.   Wang, B., et al., NBA1, a new player in the Brca1 A complex, is required for DNA damage resistance and checkpoint control. Genes Dev, 2009. 23(6): p. 729-39.

28.   Hayakawa, T., et al., MRG15 binds directly to PALB2 and stimulates homology-directed repair of chromosomal breaks. J Cell Sci, 2010. 123(Pt 7): p. 1124-30.

29.   Wu, J., et al., Chfr and RNF8 synergistically regulate ATM activation. Nat Struct Mol Biol, 2011. 18(7): p. 761-8.

30.   Keren-Kaplan, T., et al., Structure-based in silico identification of ubiquitin-binding domains provides insights into the ALIX-V:ubiquitin complex and retrovirus budding. EMBO J, 2013. 32(4): p. 538-51.

31.   Pashkova, N., et al., WD40 repeat propellers define a ubiquitin-binding domain that regulates turnover of F box proteins. Mol Cell, 2010. 40(3): p. 433-43.

4

32. Buisson, R. and J.Y. Masson, PALB2 self-interaction controls homologous recombination. Nucleic Acids Res, 2012. 40(20): p. 10312-23.

33. Hoeller, D., et al., Regulation of ubiquitin-binding proteins by monoubiquitination. Nat Cell Biol, 2006. 8(2): p. 163-9.

34. Costelloe, T., et al., The yeast Fun30 and human SMARCAD1 chromatin remodellers promote DNA end resection. Nature, 2012. 489(7417): p. 581-4.

35. Tsukuda, T., et al., Chromatin remodelling at a DNA double-strand break site in Saccharomyces cerevisiae. Nature, 2005. 438(7066): p. 379-83.

36. Tuzon, C.T., et al., Concerted activities of distinct H4K20 methyltransferases at DNA double-strand breaks regulate 53BP1 nucleation and NHEJ-directed repair. Cell Rep, 2014. 8(2): p. 430-8.

37. Fradet-Turcotte, A., et al., 53BP1 is a reader of the DNA-damage-induced H2A Lys 15 ubiquitin mark. Nature, 2013. 499(7456): p. 50-4.

38. Shanbhag, N.M., et al., ATM-dependent chromatin changes silence transcription in cis to DNA double-strand breaks. Cell, 2010. 141(6): p. 970-81.

39. Tang, J., et al., Acetylation limits 53BP1 association with damaged chromatin to promote homologous recombination. Nat Struct Mol Biol, 2013. 20(3): p. 317-25.

40. Sakaue-Sawano, A., et al., Visualizing spatiotemporal dynamics of multicellular cell-cycle progression. Cell, 2008. 132(3): p. 487-98.

41. Smeenk, G., et al., Poly(ADP-ribosyl)ation links the chromatin remodeler SMARCA5/SNF2H to RNF168-dependent DNA damage signaling. J Cell Sci, 2013. 126(Pt 4): p. 889-903.

42. Helfricht, A., et al., Remodeling and spacing factor 1 (RSF1) deposits centromere proteins at DNA double-strand breaks to promote non-homologous end-joining. Cell Cycle, 2013. 12(18): p. 3070-82.

4

5

The E3 ubiquitin ligase ARIH1 protects against genotoxic stress by initiating a 4EHP-mediated mRNA translation arrest

Louise von Stechow*, Dimitris Typas*, Jordi Carreras Puigvert, Laurens Oort, Ramakrishnaiah Siddappa, Alex Pines, Harry Vrieling, Bob van de Water, Leon H. Mullenders and Erik H.J. Danen

* These authors contributed equally to this work

ABSTRACT

DNA damage response signalling is crucial for the protection of the genome in all organisms and presents avenues to combat chemo- or radio-therapy resistance of cancer cells. In an RNAi screen for (de)ubiquitylases and sumoylases modulating the apoptotic response of embryonic stem (ES) cells to DNA damage, we identified the E3 ubiquitin ligase/ ISGylase, Ariadne homologue 1 (ARIH1). ARIH1 depletion sensitised ES and cancer cells to genotoxic compounds, irrespective of their p53- or caspase-3 status. Expression of wild-type, but not ubiquitylase-defective, ARIH1 constructs reversed the ARIH1-loss-induced sensitisation. ARIH1 protein abundance increased after DNA damage through attenuation of proteasomal degradation that required ATM signalling. ARIH1 associated with 4EHP and in turn, this competitive inhibitor of the translation initiation factor eIF4E, underwent increased non-degradative ubiquitylation upon DNA damage. Genotoxic stress led to an enrichment of ARIH1 in perinuclear, ribosome-containing regions and triggered 4EHP association with the mRNA 5' cap as well as mRNA translation arrest, in an ARIH1-dependent manner. Finally, restoration of DNA damage-induced translation arrest in ARIH1-depleted cells, by means of an eiF2 inhibitor, was sufficient to reinstate resistance to genotoxic stress. These findings establish ARIH1 as a potent mediator of DNA-damage-induced translation arrest that protects stem and cancer cells against genotoxic stress.

INTRODUCTION

DNA damage leads to acute toxicity, accumulation of mutations and subsequent chromosomal instability, potentially resulting in malignant transformation [1, 2]. To counteract these deleterious effects of DNA damage the cell is equipped with a highly complex signalling response termed the DNA damage response (DDR). The DDR activates effector components involved in protective pathways, including DNA damage repair, cell cycle arrest, transcription regulation, chromatin remodelling and cell death (1). The several complexes that collectively constitute the DDR are crucial for the protection of the genome in all organisms. Moreover, understanding DDR signalling in the context of chemical or ionising radiation-induced DNA damage is important to design improved strategies to combat therapy resistance. In tandem with phosphorylation-mediated signalling, which is largely executed by the PI3KI like kinases ATM, ATR and DNA-PK, the checkpoint kinases Chk1 and Chk2, and members of the MAPK family [3, 4], protein modifications by ubiquitin and ubiquitin-like moieties are crucial at all levels of the DDR [5].

The ubiquitylation machinery can form various, differentially interpreted tags, including both degradative (K48-, K11-linked chains) and non-degradative (mono-ubiquitylation, K63-linked chains) signals [6]. In parallel, a growing family of UBiquitin-Like (UBL) proteins such as SUMO, Nedd8 and ISG15 has been identified. Covalent attachment of these UBLs on downstream targets mostly provides non-degradative signals. The ubiquitylation, sumoylation, and ISGylation systems have been shown to share several common enzymes [7-9]. Ubiquitin mediated signalling is vital to many cellular processes, including the response to DNA damage. Recognition and processing of double strand breaks (DSBs) and intrastrand crosslinks, polymerase switching during translesion synthesis (TLS), nucleotide excision repair, and p53 stability are all regulated by ubiquitylation [5, 10, 11]. More recently, ISGylation was also implicated in the DDR, as ATM-mediated deactivation of the ISG system was demonstrated to serve as a mechanism enhancing ubiquitylation-mediated

5

protein turnover after DNA damage [12].

Ubiquitin and ubiquitin-like modifications occur through three enzymatic steps, commencing with an E1 activating enzyme, which forms a thioester bond to the ubiquitin protein. Subsequently, the charged ubiquitin monomer is relayed to an E2 enzyme that conjugates the ubiquitin molecule to its target protein with the aid of an E3 ubiquitin ligase [13]. While there are only a few E1 and E2 enzymes, a large number of E3 ubiquitin ligases dictates substrate specificity and ensures substrate diversity of the ubiquitin system (13). There are two E3 ubiquitin ligase families. In RING ubiquitylases, the ligase functions as an adaptor between the E2 enzyme and the substrate, facilitating transfer of the ubiquitin moiety to the target protein. In HECT ubiquitylases, the ubiquitin is first conferred to a conserved residue within the HECT domain and then added to the substrate protein [14]. Recently, it was established that ubiquitin ligases of the Parkin family, including Parkin and the human homologue of Ariadne1 (ARIH1; HHARI) resemble hybrids between HECT and RING domain ubiquitin ligases [15].

In response to DNA damage, ongoing transcription and translation have to be adjusted to allow execution of stress-specific programs, save energy, accomplish DNA repair and avoid the transcription and subsequent translation of potentially mutated genetic material [16]. Genotoxic stress has been shown to induce a block in protein synthesis [17-19]. Eukaryotic mRNAs are mostly recruited to the ribosome through their 5' 7-methylguanosine cap [20]. The rate-limiting step of eukaryotic cap-dependent translation initiation is the binding of the eIF4F complex to the mRNA 5' cap structure. eIF4F is composed of the cap-binding protein eIF4E, the RNA helicase eIF4A and the scaffold protein eIF4G [21, 22]. Recruitment of additional eIF proteins and the 40S ribosomal subunit completes the pre-initiation complex that scans the mRNA for the AUG codon and drives mRNA translation initiation (20-22). If eIF4E is substituted by its structural analog 4EHP at the mRNA 5' cap, the formation of the pre-initiation complex is abolished [20]. Thus, 4EHP constitutes a negative regulator of translation initiation.

Here, we describe the identification of the Parkin family E3 ubiquitin ligase, ARIH1 in an RNAi screen for modulators of chemosensitivity. We show that

ARIH1 levels and cellular localisation are regulated in response to DNA damage. In turn, ARIH1 protects stem- and cancer cells against genotoxic compounds and γ-irradiation (IR) by promoting and fine-tuning a 4EHP-mediated mRNA translation arrest.

RESULTS

Identification of CP response modulators by an RNAi screen for ubiquitylation-family enzymes

We performed an siRNA-based screen using the Dharmacon ubiquitylation SMARTpool library and custom made SMARTpool libraries targeting all known cellular deubiquitylases (DUBs), sumoylases, and desumoylases (Table S1). Mouse embryonic stem (ES) cells that display a robust apoptotic response to genotoxic compounds including CP (Fig S1A, B), were treated with 10mM CP or vehicle and cell viability was monitored after 24h. 50 identified SMARTpools met our selection criteria [no significant effect under control conditions; modulation of viability in presence of CP with Z-score +/- 1.5 and p-value > 0.05] (Fig 1A; Table S2). As controls, we included siRNA SMARTpools targeting either Kif11, expected to already induce cell killing under control conditions due to mitotic spindle defects, or p53, expected to protect ES cells against CP-induced killing. In all experimental plates, siKif11 resulted in ~90% reduction in viability under both control and CP-treated conditions whereas sip53 protected against CP-induced loss of viability (Fig S1C). As a quality measurement, Z'-factors were calculated based on siLamin (negative control) and sip53. The average of calculated Z'-factors was 0.45, indicating a good signal to noise ratio and reproducibility of the screens (Fig S1D). To exclude off-target effects, the 50 identified SMARTpools entered a deconvolution screen, where 28/50 hits were confirmed with at least 2/4 independent sequences reproducing the effect of the SMARTpool (Fig 1B,C, Table S3).

The 28 confirmed hits included siRNAs targeting six DUBs, one E1 ubiquitin-activating enzyme, Ube1x, one E2 ubiquitin-conjugating enzyme, UBE2D3,

as well as 12 siRNAs targeting E3 ubiquitin ligases (Fig 1D). Moreover, we identified seven siRNAs targeting proteins with no described ubiquitylation-related function that were included in the ThermoFischer "ubiquitylation library" based on the presence of predicted domains associated with ubiquitylase function, such as RING, SOCS, or SPRY (see discussion). The knockdown of the E1 ubiquitin enzyme Ube1x (Uba), which has recently been shown to be a crucial E1 enzyme in the DDR following ionising radiation and replication stress [23], resulted in a particularly strong reduction of viability (Fig 1C).

Enrichment of p53-modyfiers and DNA repair regulators

A large proportion of the identified hits have been previously shown to control the levels or activity of the transcription factor p53, which acts as a master regulator of the outcome of the DDR in various cell types, including ES cells (Fig 1E) [1, 2, 24]. Three of the identified DUBs, USP7 (HAUSP), USP4, and USP5 can directly or indirectly influence p53 protein levels [10, 25-27]. In addition, the E3 ligases Rfwd3, Pirh2 and TOPORS were previously implicated in regulation of p53 stability [10, 28, 29] (Fig 1E; Table S3). Besides p53 regulators, we identified several other ubiquitin ligases involved in DDR-related processes, like post-replication repair (SHPRH [30]), translesion synthesis (Pirh2 [31]), DSB repair (BRCA1 [32]), and the RPA-mediated repair of single strand breaks (Rfwd3 [33]), further confirming the validity of the targets identified in our screen.
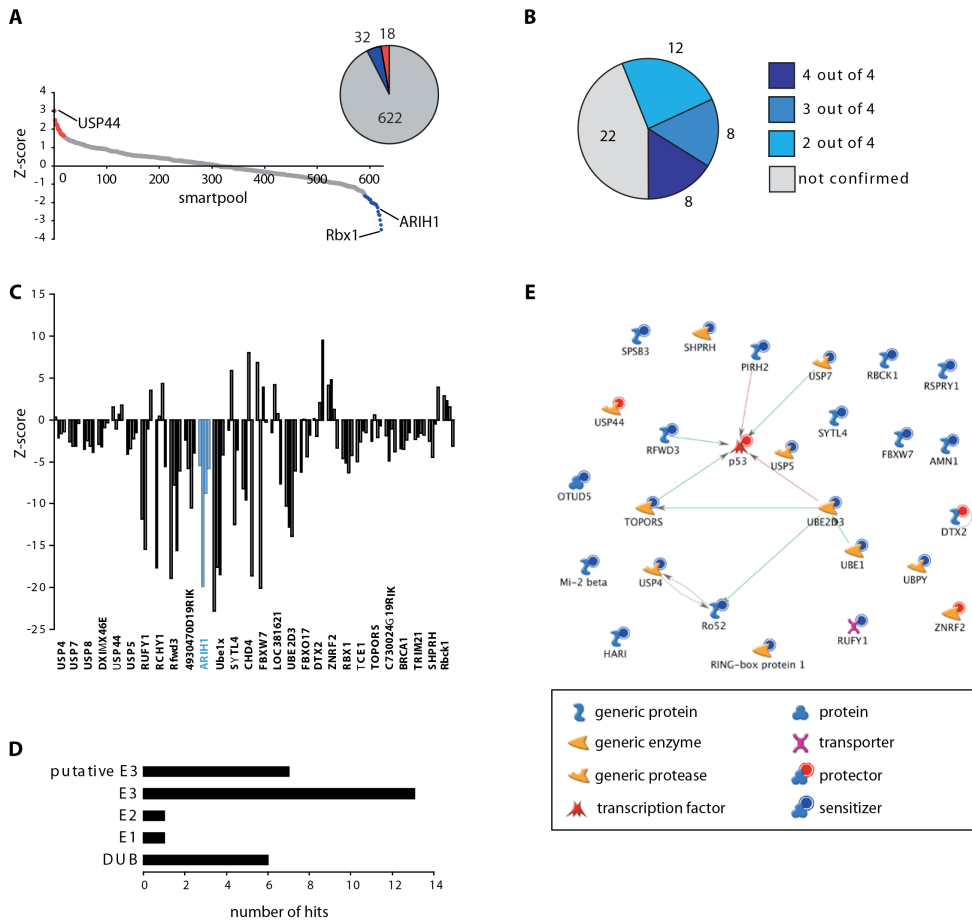
Figure 1. Identification of modulators of the CP response by an RNAi screen for ubiquitylation / sumoylation enzymes. (A) Hits identified in primary screens; protecting siRNA SMARTpools in red, sensitising siRNA SMARTpools in blue. (B) Results of deconvolution screen for 50 SMARTpools identified in primary screen. (C) Z-scores obtained for 28 confirmed hits in deconvolution screen. ARIH1 results indicated in blue. (D) Distribution of hits over different gene families as indicated. (E) Metacore-predicted network derived from screen hits; interactions with p53 are indicated. Red circles, protecting siRNAs; blue circles, sensitising siRNAs.

Silencing ARIH1 sensitises to genotoxic stress

One of the strongest obtained hits was the Parkin family ubiquitin ligase Ariadne Homologue 1 (ARIH1) [34]. The ARIH1 SMARTpool, as well as all four of the individual sequences tested in the deconvolution experiments, significantly sensitised ES cells to CP-induced loss of viability (Fig 1A,C; Table

S3). In order to examine if ARIH1 was involved in the response to specific types of stress, the effect of ARIH1 knockdown in ES cells was examined after treatment with various genotoxic and non-genotoxic compounds. All compounds were used at equitoxic doses causing ~50% loss-of-viability after 24h treatment (Fig 2A). ARIH1 depletion, using the SMARTpool or individual siRNAs, did not affect ES cell viability under control conditions (Fig 2B,C). Similar to its effect on CP-sensitivity, silencing ARIH1 using the SMARTpool or individual siRNAs significantly sensitised ES cells to all tested genotoxic drugs, including the topoisomerase inhibitor etoposide, the DNA intercalator doxorubicin, and the DNA crosslinking compound mitomycin C (Fig 2B,C). In contrast, ARIH1 loss did not sensitise ES cells to non-genotoxic agents such as the oxidative stressor diethyl maleate (DEM), the ER stressor thapsigargin (THAPS), or the microtubule poison Vincristine (VINC) (Fig 2C). Decreased viability, as measured in the ATPlite assay, correlated with an increased subG1/G0 fraction in ARIH1-depleted ES cells that could be detected after treatment with a lower dose of CP, pointing to increased cell death (Fig 2D).

In order to validate these findings in human cancer cells, we examined the effect of silencing ARIH1 in U2OS, p53 wild-type human sarcoma cells. We introduced lentiviral shRNAs targeting ARIH1 and, following bulk puromycin selection, identified two short hairpins providing ~90% reduction in ARIH1 protein levels (Fig 2E). Basal cell survival was somewhat reduced when compared to a lentiviral control cell line (Fig 2F). Nevertheless, analogous to the effect observed in ES cells, both ARIH1-depleted cell lines showed a significantly increased loss of viability in response to treatment with 10 or 25mM CP for 48h (Fig 2F). In further agreement with these findings, clonogenic survival in a colony-formation assay of ARIH1-depleted U2OS cells was also markedly more impaired by 24 hour pretreatment with a dose range of CP as compared to control cells (Fig 2G).
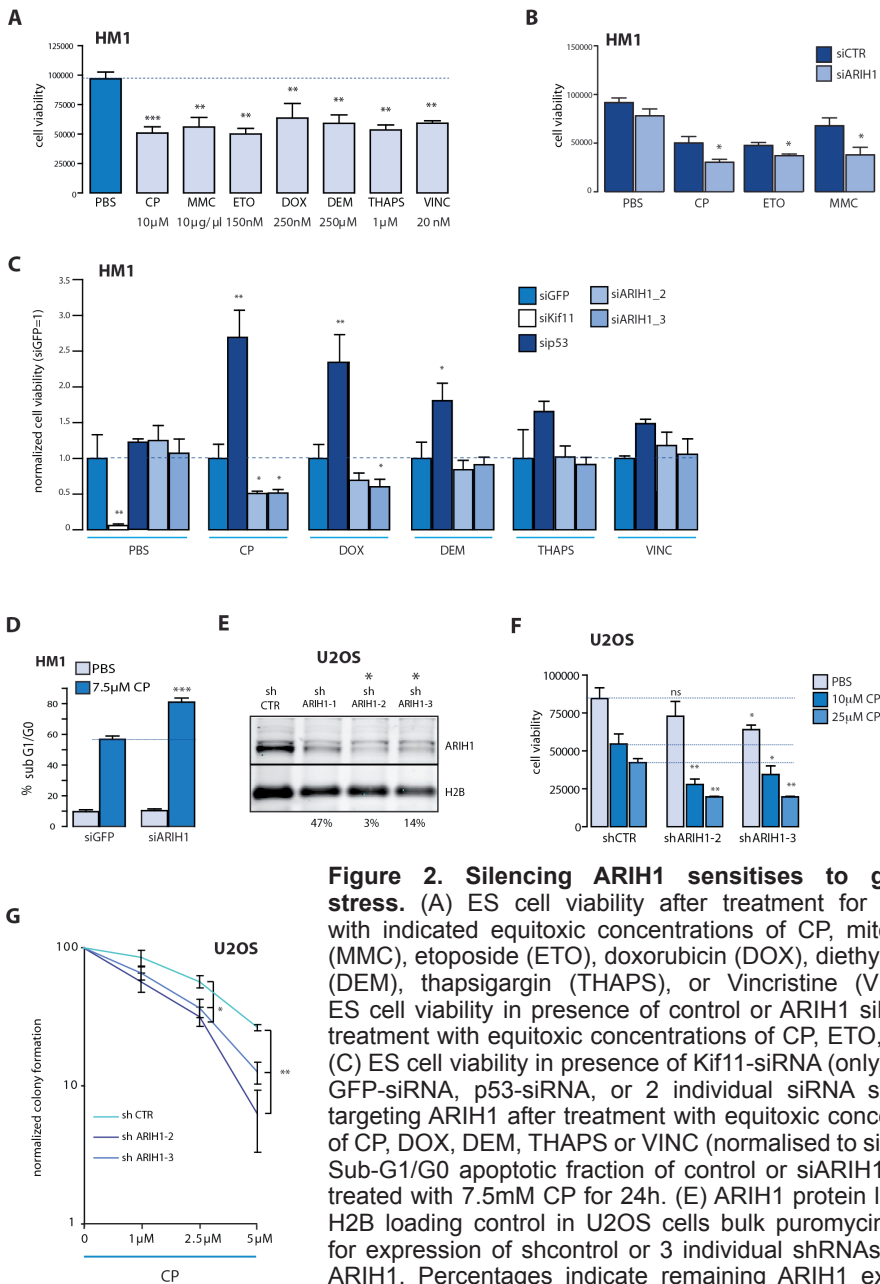
Figure 2. Silencing ARIH1 sensitises to genotoxic stress. (A) ES cell viability after treatment for 24 hours with indicated equitoxic concentrations of CP, mitomycin C (MMC), etoposide (ETO), doxorubicin (DOX), diethylmaleathe (DEM), thapsigargin (THAPS), or Vincristine (VINC). (B) ES cell viability in presence of control or ARIH1 siRNA after treatment with equitoxic concentrations of CP, ETO, or MMC. (C) ES cell viability in presence of Kif11-siRNA (only for PBS), GFP-siRNA, p53-siRNA, or 2 individual siRNA sequences targeting ARIH1 after treatment with equitoxic concentrations of CP, DOX, DEM, THAPS or VINC (normalised to siGFP). (D) Sub-G1/G0 apoptotic fraction of control or siARIH1 ES cells treated with 7.5mM CP for 24h. (E) ARIH1 protein levels and H2B loading control in U2OS cells bulk puromycin-selected for expression of shcontrol or 3 individual shRNAs targeting ARIH1. Percentages indicate remaining ARIH1 expression. Asterisks indicate shARIH1 #2 and #3 used in all further experiments. (F) U2OS cell viability in shcontrol or 2 individual shARIH1 cell lines after treatment with vehicle (PBS) or 10 or 25mM CP for 48h. (G) Colony formation capacity in shcontrol or shARIH1-2 and -3 U2OS cell lines after 24h treatment with CP at indicated concentrations. *p<0.05; **p<0.01, ***p<0.001 (students t-test).

Genotoxic stress-induced ARIH1 accumulation represents a p53- and caspase-3-independent adaptive response

In contrast to reported functions for many of the other identified hits (Fig 1E, Table S3), ARIH1 did not control basal or genotoxic stress-induced p53 stability in ES or U2OS cells (Fig 3A,B). In further disagreement with a role for p53 in the enhanced sensitivity to genotoxic stress observed in ARIH1-depleted cells, silencing ARIH1 effectively sensitised the p53-deficient non-small-cell lung cancer cell line H1299 [35] to CP (Fig 3C,D). Transient knockdown of ARIH1 also sensitised the caspase-3 deficient human breast cancer cell line MCF7, indicating that the effect of ARIH1 was not restricted to caspase 3-mediated apoptosis (Fig 3E). Although less prominent, the same effect was observed using 2 independent MCF7 shARIH1 lines (Fig 3F,G). DNA damage can trigger a p53-dependent or independent cell cycle arrest [36]. In MCF7, ARIH1 loss did not alter the basal cell-cycle distribution or the CP-induced increase of S/G2 populations (Fig 3H,I). Likewise, ARIH1 knockdown did not affect the basal cell-cycle distribution or the CP-induced G2/S arrest in ES cells (Fig 3J,K). Together, these data indicate that ARIH1-depleted cells display normal cell-cycle arrest in response to genotoxic stress, while cell survival upon DNA damage is compromised in the absence of ARIH1, with this increased sensitivity being independent of p53 or caspase-3-mediated apoptosis.
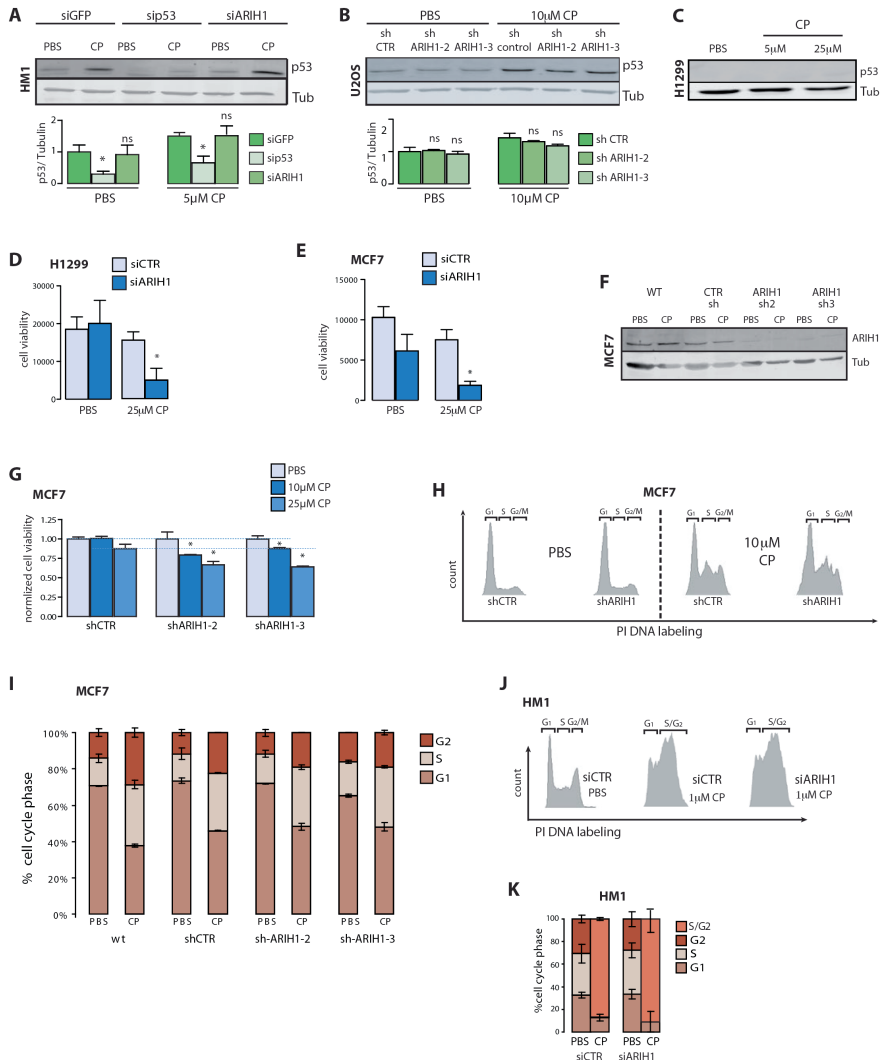
Figure 3. Silencing ARIH1 enhances cell death in response to genotoxic stress in a p53 and caspase-3 independent manner. (A) p53 and tubulin control protein levels in ES cells in presence of indicated siRNAs treated with PBS control or 5mM CP for 8h (n=4). (B) p53 and tubulin control protein levels in U2OS cells in the presence of the indicated shRNAs treated with PBS control or 10mM CP for 16h (n=3). (C) p53 and tubulin control protein levels in p53-deficient H1299 cells treated with indicated concentrations of CP for 24h. Note absence of p53. (D) H1299 cell viability under control or siARIH1 conditions after treatment with vehicle control PBS or 25mM CP for 24h. (E) MCF7 cell viability under control or siARIH1 conditions after treatment with PBS or 25mM CP for 48h. (F) ARIH1 and tubulin control protein levels in MCF7 cells in the presence of the indicated shRNAs (G) Cell viability for shcontrol and two shARIH1 MCF7 cell lines treated for 48h with PBS, 10 or 25mM CP. (H) FACS analysis for cell cycle content in shcontrol and shARIH1 MCF7 cell lines treated for 24h with PBS or 10µM CP. (I) Quantification of cell cycle profiles in wt, shcontrol and shARIH1-2 and -3 MCF7 cell lines after treatment with PBS or 10mM CP for 24h. (J) FACS profiles for HM1 cell cycle content under control, siGFP, or siARIH1 conditions after treatment with vehicle control or 1µM CP. (K) Cell cycle distribution derived from profiles in J (n=3). *p<0.05.

Subsequently, we tested if DNA damage affected the abundance of ARIH1. ARIH1 protein levels were boosted following CP treatment in U2OS cells (Fig 4A). This could not be explained by elevated mRNA levels, indicating that genotoxic stress triggered either increased synthesis or enhanced stability of the ARIH1 protein (Fig 4B). Treatment with the proteasome inhibitor MG132 led to increased basal ARIH1 levels, with CP treatment not causing further ARIH1 accumulation under these conditions (Fig 4C). KU-5593, an inhibitor of ATM, a central kinase within the DDR signalling network, blocked CP-induced ARIH1 accumulation, suggesting that DNA-damage caused ATM-mediated attenuation of proteasomal degradation of ARIH1 (Fig 4C). We then sought to address whether regulation of ARIH1 abundance might occur through suppression of self-ubiquitylation. Although ARIH1 indeed appeared to be ubiquitylated, this modification was not regulated by CP and was unaffected by ATM inhibition (Fig S2A). Moreover, a ubiquitylation-deficient ARIH1 mutant (C208A) displayed a markedly similar ubiquitylation pattern (Fig S2A) (24). Notably, by MS analysis of GFP-ARIH1 immuno-precipitations we identified K144 as a ubiquitylated site in ARIH1, yet this was not modulated by CP treatment (Fig S2B). We also identified multiple ARIH1-interacting components of the ubiquitylation machinery (i.e. ubiquitin itself, the E1 enzyme UBA1, and the E2 enzyme UBE2L3 known to interact with ARIH1). Such interactions, as well as a potential product (K48 poly-ubiquitin chains), were moderately increased upon CP treatment (Fig S2B).

CP treatment induces 4EHP ubiquitylation

In response to DNA damage, ongoing cellular activities are suppressed while stress programs and DNA repair processes are activated. One aspect of the DNA damage response is the acute inhibition of protein synthesis through alterations of the cap-dependent translation initiation complex [37]. This can be achieved in several ways, including cap-recruitment of 4EHP (eIF4E2), a competitive inhibitor of the canonical cap-binding translation initiation factor, eIF4E [20]. In contrast to eIF4E, 4EHP cannot bind the structural component eIF4G that is required for ribosome accrual and subsequent mRNA translation. Although ARIH1 can act as an E3 ubiquitin ligase for 4EHP [38], there is also evidence that ARIH1 can ISGylate 4EHP, thus enhancing its

affinity for the mRNA cap structure and its ability to replace eIF4E [39]. Co-immunoprecipitations in U2OS cells showed that the increased abundance of ARIH1 in CP-treated cells was accompanied by increased association of ARIH1 with 4EHP and this 4EHP-associated ARIH1 was lost in shARIH1 cells (Fig 4D,E).

Furthemore, we analysed CP-induced posttranslational modification of wild-type 4EHP and a [K121/130/134/222R]-mutant (4KR) that cannot be ISGylated [39]. Immunoprecipitation of wild -ype 4EHP showed bands of higher molecular weight appearing upon CP treatment (Fig 4F). Identical bands were also observed for the 4KR-4EHP mutant arguing against a CP-induced 4EHP-ISGylation. Moreover, such species were detected by a ubiquitin antibody, whereas Western blotting for co-expressed HA-ISG15 did not detect these species, despite the fact that free ISG15 was readily detected in the FLAG immunoprecipitations. The most prominent modification corresponded to mono-ubiquitylated 4EHP (28+7 kDa) although the ubiquitin Western blot indicated that 4EHP di-ubiquitylation may also occur.

5

ARIH1 ubiquitylation function mediates adaptation to genotoxic stress

Results thus far suggested that 4EHP is ubiquitylated, not ISGylated, after genotoxic stress. We tested whether the ISGylation or ubiquitylation function of ARIH1 was required for its protective role in genotoxic stress. Therefore, we silenced endogenous ARIH1 using an siRNA targeting the 3' UTR in U2OS cells expressing either exogenous wild-type ARIH1 or a C208A mutant that fails to associate with the E2 enzyme UbcH7, rendering it defective in ubiquitylation (whereas interaction with UbcH8 and hence, ISGylase activity remains intact) [40]. In agreement with earlier findings, ARIH1-silenced cells were more sensitive to CP treatment although the effect of the transient siRNA was less prominent than stable shRNA-mediated silencing (see Fig 2G). More importantly, expression of wild-type- but not ubiquitylation-deficient (C208A) ARIH1, restored colony formation capacity under genotoxic stress in cells depleted for endogenous ARIH1 (Fig 4G). Put together, these data indicate that 4EHP ubiquitylation constitutes the predominant modification induced by genotoxic stress, with the ubiquitylase function of ARIH1 being crucial for its protective role in the genotoxic stress response.
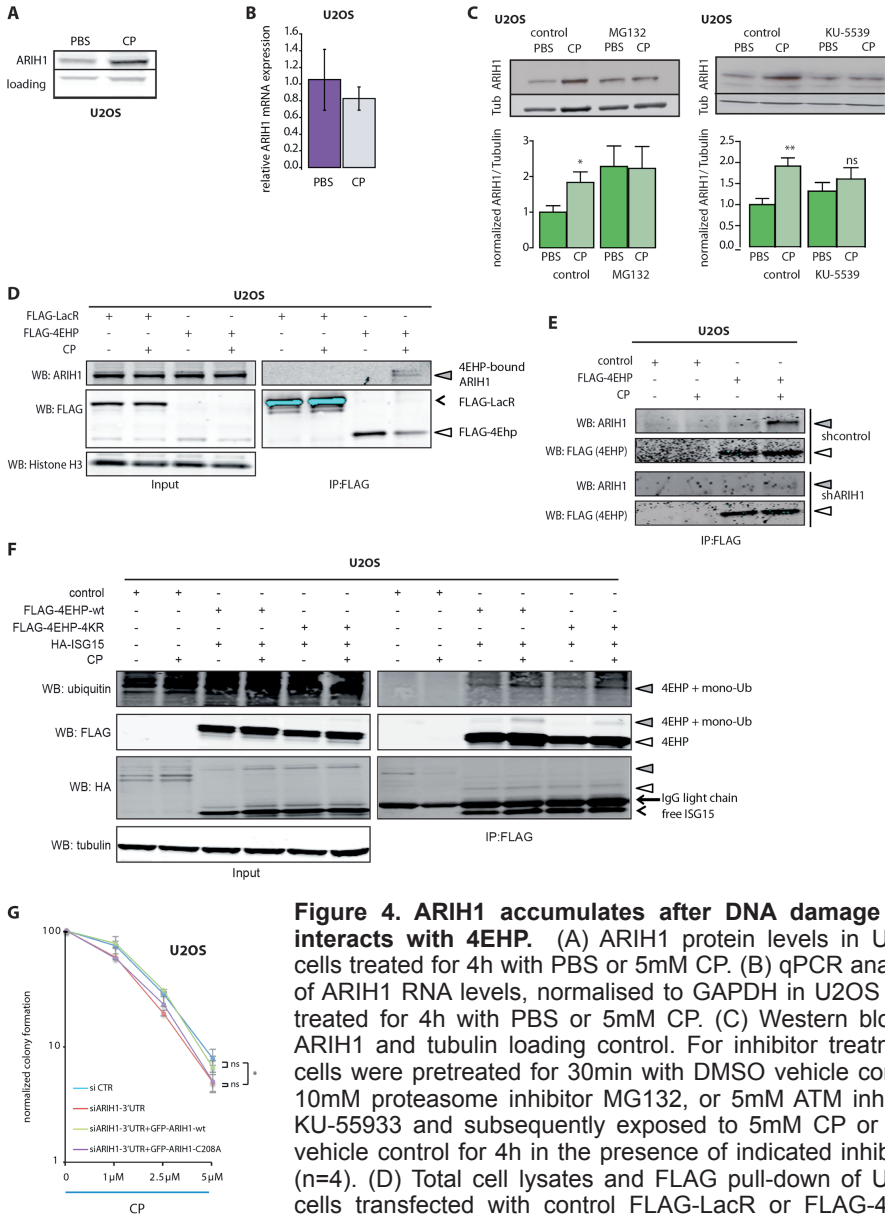
Figure 4. ARIH1 accumulates after DNA damage and interacts with 4EHP. (A) ARIH1 protein levels in U2OS cells treated for 4h with PBS or 5mM CP. (B) qPCR analysis of ARIH1 RNA levels, normalised to GAPDH in U2OS cells treated for 4h with PBS or 5mM CP. (C) Western blot for ARIH1 and tubulin loading control. For inhibitor treatment, cells were pretreated for 30min with DMSO vehicle control, 10mM proteasome inhibitor MG132, or 5mM ATM inhibitor KU-55933 and subsequently exposed to 5mM CP or PBS vehicle control for 4h in the presence of indicated inhibitors (n=4). (D) Total cell lysates and FLAG pull-down of U2OS cells transfected with control FLAG-LacR or FLAG-4EHP with vehicle control or 5µM CP for 4h. Blots were probed for FLAG, ARIH1 and Histone H3 (loading control). (E) FLAG pull-down of U2OS cells in the presence of the indicated shRNAs, subsequently transfected with control (empty) or FLAG-4EHP cDNAs, and treated with vehicle control or 5µM CP for 4h. Blots were probed for 4EHP (FLAG) and ARIH1. Open and shaded arrowheads as explained in D. (F) Total cell lysates and FLAG pull-down of U2OS cells transfected with FLAG-4EHP (wt or 4KR) in combination with HA-ISG15 and treated with vehicle control or 5µM CP for 4h. Blots were probed for FLAG, HA, ubiquitin and tubulin (loading control) (G) Colony formation capacity after 24h treatment with CP at indicated concentrations in control U2OS cells or U2OS cells stably expressing GFP-tagged wild-type or C208A mutant ARIH1, in absence or presence of siRNA targeting luciferase (control) or the ARIH1 3'UTR. * p<0.05.

CP-treatment induces 4EHP cap-binding and translation arrest in an ARIH1-dependent manner

ARIH1-dependent ISGylation has been reported to regulate 4EHP association with the mRNA 5' cap but ARIH1-mediated ubiquitylation of 4EHP, although described, is not known to affect this process. In order to clarify whether ARIH1 supported 4EHP translocation to the mRNA cap upon CP treatment, we utilised 5' 7-methylguanosine cap-pulldown assays. Indeed, 4EHP binding to the mRNA cap was induced in response to CP in U2OS, MCF7, as well as ES cells (Fig 5A-D). Importantly, this response was dependent on ARIH1 as the CP-induced 4EHP:cap association was abrogated in U2OS, MCF7, and ES cells upon ARIH1 depletion (Fig 5A-D). Subsequently, to test if the 4EHP:cap association represents an ARIH1-regulated pathway that is involved in protection against CP, 4EHP itself was silenced. In line with such a protective function, ES cells and U2OS cells were sensitised to genotoxic compounds following 4EHP silencing, while viability of H1299 in presence of CP and control conditions was compromised (Fig 5E-H).

These findings hint that the ability of ARIH1 to protect against genotoxic stress-induced cell death involves 4EHP-mediated translation inhibition at the mRNA 5' cap. To address whether ARIH1 localised at sites of mRNA translation upon genotoxic stress, we performed immunostainings to assess subcellular distribution of ARIH1. Whereas in untreated U2OS cells ARIH1 resided in the nucleus and diffusely throughout the cytoplasm, treatment with CP or IR caused ARIH1 accumulation at both the nucleus and speckled structures in perinuclear regions, which markedly resemble ribosomes (Fig 5H). In agreement with a genotoxic stress-induced transittion of ARIH1 to ribosomes, and a role in 4EHP-mediated translation arrest, eIF4G2, a ribosomal marker, co-localised to such ARIH1-containing perinuclear regions upon either CP treament or IR (Fig 5I,J).

5
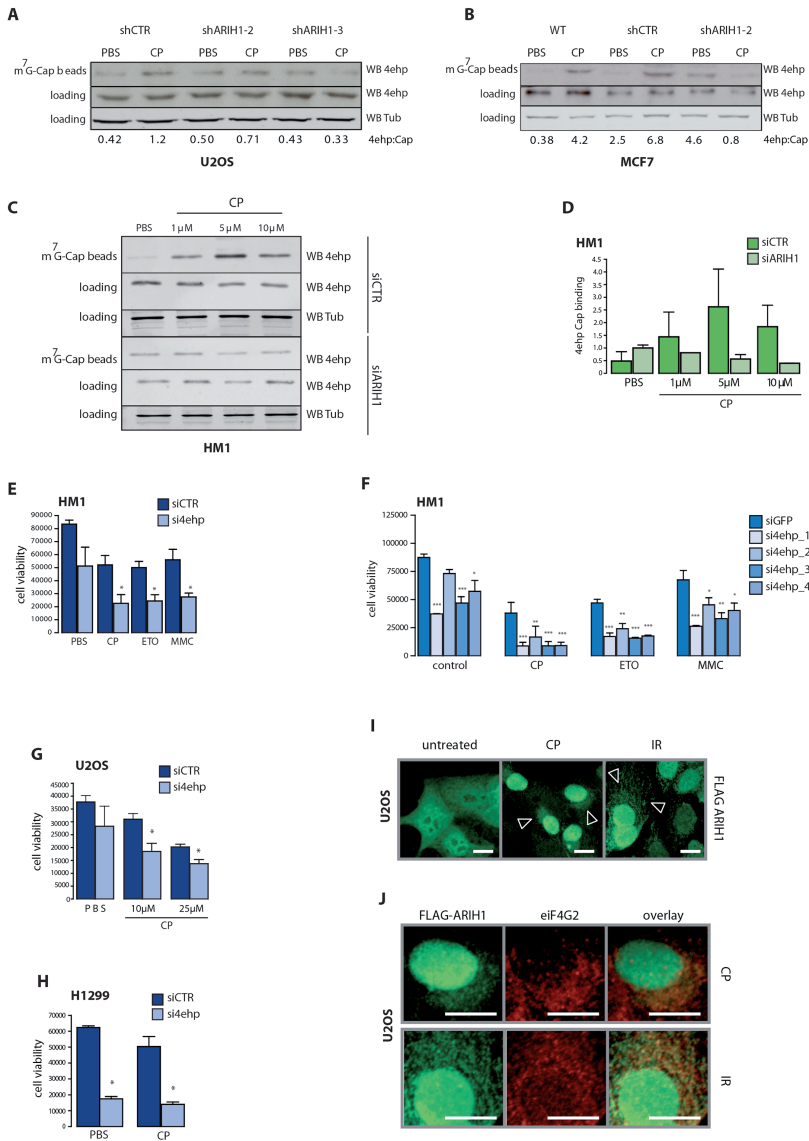
Figure 5. ARIH1 mediates DNA damage-induced cap binding of 4EHP. (A-C) m7G-cap pulldown from control and ARIH1-silenced U2OS (A), MCF7 (B) or HM1 ES cells (C) treated with vehicle control or indicated concentrations of CP. Blots were probed for 4EHP and tubulin (loading control). Numbers at the bottom of A and B indicate cap-associated 4EHP levels relative to total 4EHP. (D) Quantification of m7G-cap-bound 4EHP in ES cells treated with indicated siRNAs (n=2). (E) ES cell viability in the presence of the indicated siRNAs after treatment with PBS, 10mM CP, 150nm ETO, 10mg/ml MMC for 24h. (F) ES cell viability in the presence of the indicated siRNAs after treatment with vector, 10mM CP, 150nm ETO or 10mg/mL MMC. (G) As in (F) but for U2OS after treatment with PBS, 10 or 25µM CP. (H) As in (F) for H1299 cells after treatment with PBS or 25µM CP. (I) FLAG-ARIH1 localisation before or after treatment with 5µM CP for 4h or 4h after treatment with 2Gy IR. Arrowheads indicate regions of perinuclear accumulation. (J) Higher magnification of perinuclear staining for FLAG-ARIH1 (green), ribosomal marker eiF4G2 (red) staining after CP treatment or IR. *p<0.05; **p<0.01.

To directly address whether ARIH1 was important for inducing a DNA damage-induced translation arrest, Click-iT® metabolic labelling was used to quantify newly synthesised proteins. CP treatment caused a significant translation arrest in U2OS cells with a 30% reduction of protein synthesis at 2h post-treatment and maintenance of a 25% reduction at 4 and 8h post-treatment (Fig 6A). In line with a critical role for ARIH1 in mediating this arrest, two independent shARIH1 lines did not show this CP-induced translation arrest. Notably, a 60% reduction in translation caused by cyclohexamide in wild-type U2OS remained intact in ARIH1-silenced cells (Fig 6A,B).

Finally, we investigated if the ARIH1-mediated translation arrest was critical for the role of ARIH1 in adaptation to genotoxic stress. For this, we made use of salubrinal, an inhibitor of eIF2a dephosphorylation that renders the eIF2 initiation factor inactive and inhibits mRNA translation under stressed conditions. Co-treatment with salubrinal restored the CP-induced translation arrest in ARIH1-depleted cells (Fig 6B). Indeed, such an alternatively triggered translation arrest significantly restored viability of CP-treated ARIH1-silenced U2OS, ES and MCF7 cells (Fig 6C-E).

Altogether, these findings support a model in which DNA damage induces an increase in ARIH1 protein levels and an association of ARIH1 with 4EHP. In turn, this causes 4EHP recruitment to the mRNA cap where it is known to compete with eIF4E. The resulting mRNA translation arrest represents an adaptive response to genotoxic stress: ARIH1 depletion sensitises cells to genotoxic stress while reestablishing the translation arrest at the level of eIF2 with salubrinal alleviates this effect (Fig 6F).

5
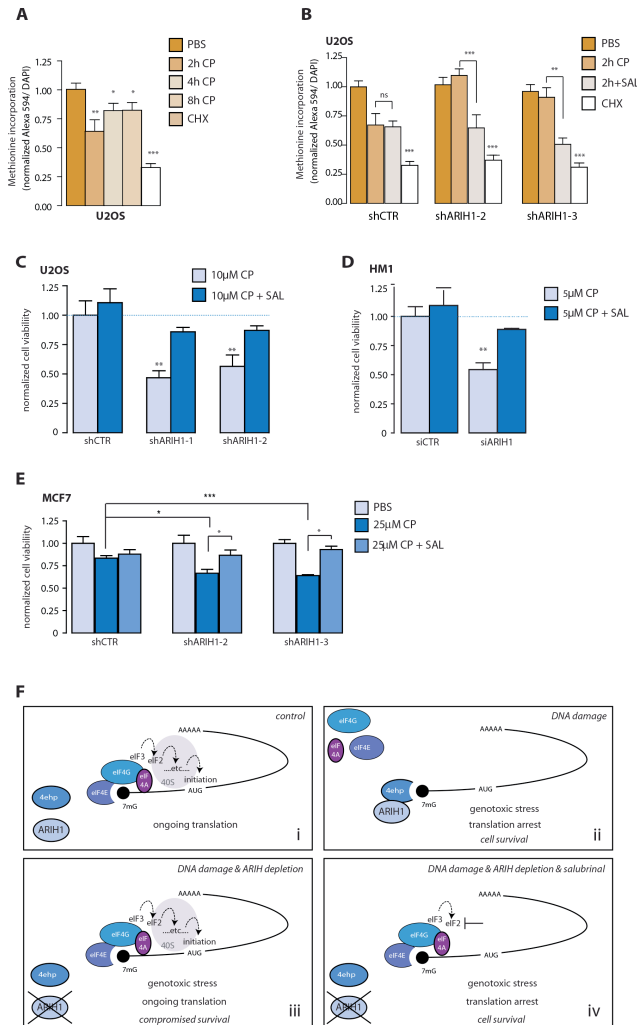
Figure 6. ARIH1 mediates CP-induced mRNA translation arrest. (A) Methionine incorporation in U2OS cells after treatment with 15mM CP for 2h, 4h or 8h or 2mg/ml cyclohexamide (CHX) for 1h. Alexa546 signal (reflecting newly synthesised protein) / number of nuclei (DAPI), normalised to PBS condition is shown. (B) As in (A) but in the presence of the indicated shRNAs and after treatment with 2mg/ml CHX for 1h, 15μM CP for 2h, or co-treatment with 15μM CP and 2.5mM salubrinal (SAL) for 2h. Alexa546 signal / number of nuclei, normalised to PBS condition is shown. (C-E) Cell survival in cells treated with the indicated siRNAs or shRNAs after treatment with indicated concentrations of CP (hr treatment) in absence or presence of 2.5mM SAL. C, U2OS 48; D, ES cells 24h; E, MCF7 48h. (F) Model for the role of ARIH1 in regulating sensitivity to genotoxic stress. i) Under non-stressed conditions, eIF4E binds the mRNA m7G-cap, a pre-initiation complex is formed scanning the mRNA until the AUG codon is found. ii) Upon genotoxic stress, ARIH1 associates with 4EHP, resulting in recruitment of 4EHP to the 5' cap where it replaces eIF4E, resulting in a cytoprotective translation arrest. iii) In the absence of ARIH1, 4EHP is not recruited to the mRNA 5' cap, DNA damage-induced translation arrest does not occur, and cell survival is compromised. iv) Restoration of translation arrest in ARIH1-depleted cells by preventing formation of a pre-initiation complex through inhibition of eIF2 also restores cell survival.

DISCUSSION

Ubiquitylation plays a vital role in the DDR signal transduction cascade. Our RNAi screen targeting the cellular ubiquitylation and sumoylation machinery helped us identify several genes that modulate the response to the chemotherapeutic drug CP. Some of the identified DUBs and E3 ubiquitin ligases have been previously implicated in p53 regulation or DNA repair processes [5, 10]. In addition, through our screen we picked up genes associated with cell cycle control or developmental processes. These include Fbxw7, a tumour suppressor that marks several proto-oncogenes, such as Myc, Jun, cyclin E, and Notch for degradation; and Dtx2, an E3 ligase also proposed to control the Notch signalling pathway [41-43]. Which of these functions explains the role of these ubiquitin ligases in the response to genotoxic stress is not known. Moreover, while two of the individual siRNAs mimicked the SMARTpool for these genes, the deconvolution screen also revealed one individual siRNA for these genes to have the opposite effect. This indicates that either of those outcomes is likely an off-target effect and further experiments are required to determine the role of these genes in the response to genotoxic stress. We also identified another F-box protein, Fbx017, where the SMARTpool and 3/4 individual siRNAs caused sensitisation, thus bestowing more confidence in a potential role of this gene in adaptation to genotoxic stress. However, no mechanism of action has been described for Fbx017 yet.

Another group of identified hits has been associated with intracellular transport processes, including the DUB USP8, which regulates endosomal sorting of membrane receptors and RUFY and SYTL4, which are involved in Rab-mediated vesicular transport [44-46].Notably, some of the hits from the "ubiquitylation SMARTpool library" do not have established (de)ubiquitylase function. These include i) the Zinc finger-containing chromatin remodeling factor CHD4 that lacks domains associated with (de)ubiquitylase activity [47]; ii) the Rab-interacting proteins RUFY and SYTL4 that have a FYVE-Zinc finger domain, which is structurally similar to the RING domain [45,

5

46]; and iii) TCE1 and Rspry1, containing a SPRY domain that is found in members of the TRIM-family of ubiquitin ligases [48]. In addition, Rspry1 contains a RING domain and TCE1 also harbors a SOCS box domain, which mediates interactions with the Elongin BC complex, an adapter module in E3 ubiquitin ligase complexes [49].

The Parkin family ubiquitin ligase, ARIH1 has not been previously implicated in DDR signalling. Our findings reveal that ARIH1 protects pluripotent stem cells, as well as various cancer cells, from the toxic effects of genotoxic chemical agents that cause DSBs. The cytoprotective role of ARIH1 is also observed in cancer cells lacking a functional p53 or caspase-3 response. Hence, ARIH1 is not required specifically for dampening p53-induced, caspase-3-mediated apoptosis. Instead, we find that ARIH1 mediates an mRNA translation arrest in response to DNA damage by binding to 4EHP and stimulating its recruitment to the mRNA 5' cap.

The temporary arrest of mRNA translation is an important event in the response to cellular stress and alterations in this regulatory hub have been suggested to be important for resistance of cancer cells to therapy [19, 50]. A well-described mechanism for translation repression is the enhanced interaction of the cap-binding protein eIF4E with its negative regulator eIF4-BP1. Under normal conditions this interaction is suppressed by mTOR-mediated phosphorylation of eIF4-BP1 [51]. Alternative eIF4E-dependent and independent mechanisms for translation repression have also been described [20]. For instance, impaired Met t-RNA recruitment, through eif2a Ser51 phosphorylation, represents a canonical response to accumulation of improperly folded proteins in the endoplasmic reticulum; the so-called unfolded protein response [52]. Yet another way to arrest mRNA translation is through enhanced mRNA 5' cap-binding of eIF4E2, also known as 4EHP [53]. Our findings implicate this latter mechanism in the DNA damage-induced protein synthesis arrest and provide evidence that it is regulated through ARIH1.

4EHP is an eIF4E homologue that has low affinity for binding the cap structures of most mRNAs [54]. The protein has been implicated in the regulation of translation of a specific subset of mRNAs in Drosophila involved in embryonic

patterning [55, 56]. ARIH1 can ISGylate 4EHP, thus leading to increased mRNA 5' cap affinity, but it is not known under which conditions ARIH1-mediated ISGylation of 4EHP is induced [39]. Here, we demonstrate that in response to DSB-inducing genotoxic stress, ARIH1 protein accumulates and interacts with 4EHP, leading to increased recruitment of 4EHP to the mRNA 5' cap. Our findings using a non-ISGylatable 4EHP mutant and 4EHP:ISG15 co-immunoprecipitations, indicate that ubiquitylation, not ISGylation is the predominant DNA damage-induced 4EHP modification. Moreover, we show that ubiquitylation capacity is required for the ARIH1-mediated adaptive response to genotoxic stress.

The accumulation of ARIH1 depends on activity of ATM, a key kinase in the DDR, and most likely involves inhibition of proteasomal degradation. Despite a putative ATM target motif (S-Q) in the ARIH1 protein at Serine 514, phosphorylation of this site has not been detected by us or by other groups in the presence or absence of genotoxic stress (unpublished data; [3, 57, 58]; http://www.phosphosite.org). Although this may be an outcome of technical limitations of MS used in these studies (for example a very short tryptic fragment), it points to an indirect mechanism by which ATM signalling leads to increased ARIH1 expression after genotoxic stress. One possible mechanism would involve attenuation of ARIH1 self-ubiquitylation following genotoxic stress. However, our results do not suggest auto-ubiquitylation, or its regulation by genotoxic stress or ATM, as the relevant mechanism. It is worth mentioning that our MS analysis indicates that ARIH1 is primarily part of a complex of ubiquitylation-related enzymes. The detailed composition of this complex and its regulation in response to genotoxic stress will be the topic of further study.

Translation arrest is effectuated by 4EHP due to its capacity to act as a competitive inhibitor for eIF4E. Unlike eIF4E, 4EHP cannot interact with the scaffolding protein eIF4G, which is required for formation of the pre-initiation complex. In line with this, 4EHP cannot complement eIF4E in gene knockout experiments in yeast [59]. Our following findings indicate that ARIH1-mediated recruitment of 4EHP to the mRNA 5' cap underlies the cytoprotective role of ARIH1: i) DNA damage-induced recruitment of

5

4EHP to the mRNA 5' cap is ARIH1-dependent, ii) DNA damage-induced translation arrest is ARIH1-dependent, and iii) RNAi targeting ARIH1 or 4EHP sensitises ES or cancer cells to DNA damage. In H1299 cells, 4EHP depletion also compromises viability under control conditions, which may be related to endogenous genotoxic stress. Our data do not support the notion that a genotoxic stress-induced mRNA translation arrest is lost in cancer cells, as was described for other eIF4E dependent routes, such as 4EBP-1 phosphorylation [19]. U2OS cells do attenuate protein synthesis following genotoxic stress and depletion of ARIH1 leads to sensitisation of all cancer cell lines tested thus far. Intriguingly, while inhibition of eIF4E cap binding can sensitise cancer cells to different chemotherapeutics [19, 50], we show that inhibition of the competitive process involving ARIH1 and 4EHP has the same effect. Clearly, ongoing mRNA 5' cap-mediated translation, as well as the ability to temporarily halt translation in response to DNA damage is required for (cancer) cells to escape genotoxic stress-induced death. Our immunofluorescence experiments indicate that upon genotoxic stress, ARIH1 is increasingly concentrated in nuclei and perinuclear regions where ribosomes cluster, placing ARIH1 at the correct location to control this process.

As mentioned above, an alternative route to attenuate protein synthesis is through eiF2a Ser51 phosphorylation, a modification typically triggered by accumulation of misfolded proteins in the ER [52]. This response can be enhanced by salubrinal, an inhibitor of the phosphatase complex that dephosphorylates eIF2a [60]. Interestingly, treatment with salubrinal restores the CP-induced translation arrest and the subsequent cellular survival in ARIH1-depleted cells. This shows that alternative means for restricting protein synthesis can compensate for the inability to do so through enhanced 4EHP:cap binding. Moreover, it provides further evidence in favour of a model showing that the ability of ARIH1 to couple DSB-induced genotoxic stress to attenuation of mRNA translation underlies its cytoprotective role.

MATERIAL AND METHODS

Cell culture, plasmids and other reagents

HM1 mouse ES cells derived from OLA/129 genetic background (provided by Dr. Klaus Willecke, University of Bonn GE) were maintained under feeder free conditions in GMEM medium containing 5×10^5U mouse recombinant leukemia inhibitory factor (LIF; PAA). All other cell lines were purchased from ATCC. MCF7 human breast cancer cells and H1299 human non-small cell lung cancer cells were maintained in RPMI medium. U2OS human sarcoma cells were kept in DMEM. All media contained 10% FBS and 25U/ml penicillin, and 25µg/ml streptomycin. All cell lines, including stable shRNA expressing derivatives, were confirmed to be mycoplasma-free using the Mycosensor kit from Stratagene.

Wild-type (#17342) and non-ISGylatable [K121/130/134/222R]-mutant (4KR) (#17353) FLAG-tagged versions of 4EHP, as well as HA-tagged ISG15 (#12444) were provided by Dr. Dong-Er Zhang, Scripps Research Institute, La Jolla CA - through Addgene [39]. By means of site-directed mutagenesis, a point mutation (C208A) was introduced into wild-type ARIH1 cDNA, yielding an ubiquitylation-deficient ARIH1 mutant [40]. Wild-type and C208A ARIH1 cDNAs were cloned into entry vector pENTR4-GFP-C1 (#w392-1) provided by Dr. E. Campeau, University of Massachusetts Medical School, Worcester, MA - through Addgene [61]. Subsequently, they were recombined into pLenti6.3 V5-DEST (Invitrogen) using Gateway® recombination. Destination vectors containing such GFP-tagged ARIH1 versions were used for either direct overexpression in mammalian cells or lentiviral production.

Genotoxicants included the DNA cross-linkers cisplatin (CP; Cis-PtCl$_2$(NH$_3$)$_2$) (provided by the Pharmacy unit of University Hospital, Leiden NL) and mitomycin C (Sigma), as well as the inhibitors of topoisomerase II-mediated DNA unwinding, doxorubicin (Sigma) and etoposide (Sigma). Oxidative stressor diethyl maleate (DEM), microtubule-poison Vincristine, and ER-stressor Thapsigargin were also obtained from Sigma. The pan-caspase inhibitor z-Val-Ala-DL-Asp-fluoromethylketone (z-VAD-fmk) was purchased from Bachem, the eif2a dephosphorylation inhibitor salubrinal was from

5

Calbiochem. ATM inhibitor KU-5593 and proteasome inhibitor MG132 were acquired from Tocris Biosciences. Antibodies against p53 and phospho-p53(Ser15) were purchased from Novacostra and Cell signalling, respectively. Antibodies against tubulin and FLAG were obtained from Sigma. Antibodies against mouse or human 4EHP and eIF4G2 were from Cell Signalling. ARIH1 antibody was from Novus Biologicals. Monoclonal antibody against ubiquitin was purchased from Enzo-Biosciences (FK2 clone).

RNAi experiments

siRNAs were purchased from ThermoFisher Scientific. For primary screens, the Dharmacon siGENOME SMARTpool siRNA Library- Mouse Ubiquitin Conjugation Subsets 1 (G-015610), 2 (G-015620) and 3 (G-015630) were used. For Deubiquitylation and SUMOylation-screens customised siGENOME SMARTpool siRNA libraries were used (Table S1). For deconvolution confirmation screens, customised libraries containing 4 individual siRNAs targeting each selected mRNA were used. GFP, Lamin A/C, and RISC free control siRNAs were used according to MIARE guidelines. Kif11 siRNA was used as transfection efficiency control.

The siRNA screens were performed on a Biomek FX (Beckman Coulter) liquid handling system. 50nM siRNA was transfected in 96 well plates using Dharmafect1 transfection reagent (ThermoFisher Scientific). The medium was refreshed every 24h and cells were exposed to indicated compounds or vehicle controls 64h post-transfection for 24h. Primary screens were done in duplicate and deconvolution screens were done in quadruplicate. As readout, a cell viability assay using ATPlite 1Step kit (Perkin Elmer) was performed according to the manufacturer's instructions followed by luminescence measurement using a plate reader.

For stable gene silencing, cells were transduced using lentiviral TRC shRNA vectors at MOI 1 (LentiExpressTM; Sigma-Aldrich; Dr. Rob Hoeben and Mr Martijn Rabelink, University Hospital, Leiden NL) according to the manufacturer's procedures and bulk selected in medium containing 2.5μg/ml puromycin. Control vector expressed shRNA targeting TurboGFP. shRNAs targeting ARIH1 were CCAGATGAATACAAGGTCATC

(shARIH1#1), CTACCTTGAACGAGATATTTC (shARIH1#2), CTGTTAAATGTAAGTGGTTAC (shARIH1#3). For ARIH1 gene silencing in combination with ectopic expression of GFP-ARIH1 constructs, an siRNA targeting the 3'UTR (GCACACAGCUGUAGGCAUUUU) of ARIH1 was used (ThermoFisher Scientific).

RNAi screen data analysis

As a quality control Z'-factors were determined for each plate, using Lamin A/C as a negative control and p53 as a positive control. To rank the results, Z-scores were calculated using as a reference i) the mean of all test samples in the primary screen and ii) the mean of the negative control samples in the secondary deconvolution screen (in order to prevent bias due to pre-enrichment of hits) [62]. Hit determination was done using Z-scores with a cut off value of 1.5 below or above the reference and p-value lower than 0.05. Enrichment of canonical pathways and formation of p53/ ubiquitylation signalling network was performed using MetaCore™ data-mining software.

Apoptosis and cell cycle analysis

ES cells were exposed to vehicle or CP for 8h for cell cycle analysis or 24h for apoptosis analysis. MCF7 cells were exposed for 24h for cell cycle analysis. Floating and attached cells were pooled and fixed in 80% ethanol overnight. Cells were stained using PBS EDTA containing 7.5mM propidium iodine and 40mg/ml RNAseA and measured by flow cytometry (FACSCanto II; Becton Dickinson). The amount of cells in the different cell cycle fractions or in sub G0/G1 for apoptotic cells was calculated using BD FACSDiva software. Alternatively, apoptosis was determined using live imaging of Annexin V labelling, as described previously [63].

Clonogenic survival assay

U2OS cells (250 cells/plate) expressing different shRNAs were seeded in triplicate in 9cm plates. The following day, cells were treated for 24h with a dose range of CP or IR. After a recovery period of 10 days, surviving cells were fixed, stained and colonies were counted to assay each cell-line's clonogenic potential.

Western blot analysis

Extracts were prepared in Tris/Sucrose/EDTA buffer containing protein inhibitor cocktail and separated by SDS-PAGE on polyacrylamide gels, transferred to PVDF membranes, and membranes were blocked using 5% BSA. Following incubation with primary and secondary antibodies signal was detected using a Typhoon™ 9400 from GE Healthcare.

Immunofluorescence

U2OS cells were seeded on glass coverslips and allowed to grow for two days. Subsequently, they were treated with CP and fixed using 2% formaldehyde for 20min at the indicated time-points. After washing extensively and rehydrating in PBS, post-fixation extraction took place by incubating with 0.25% Triton-X for 5min. Cells were extensively washed with PBS to remove any detergent and then blocked in 5% BSA. Finally, coverslips were immunostained with mouse anti FLAG and rabbit anti eiF4G2 antibodies and appropriate secondary fluorescent antibodies.

Cap binding assay

HM1 ES cells, U2OS, and MCF7 breast cancer cells were seeded in 6-well plates at a density of 0.5 million cells/ well. Cells were treated with different concentrations of CP for 4h (U2OS, MCF7) or 8h (ES) and proteins were harvested in lysis buffer containing 1mM phenylmethylsulfonyl fluoride (Cell Signalling). Cap binding proteins were precipitated using 7-methyl-GTP-Sepharose 4B beads (Amersham) as described previously [64]. Precipitated proteins were separated on 12% SDS-PAGE gels and analysed by immunoblotting for 4EHP (EIF4E2).

Metabolic labelling for detection of translational changes after CP treatment

Click-iT® metabolic labelling reagents for proteins was purchased from Invitrogen and used according to manufacturer's instructions. In short, U2OS cells were seeded to 80% confluence in 96 well mclear plates and subsequently treated with 15mM CP for 2-8h or with 2mg/ml cyclohexamide

(CHX) for 1h, or for 2h with a combination of 15mM CP and 2.5mM salubrinal. During the last hour of treatment DMEM was replaced with methionine-free medium. Subsequently, cells were incubated with azide-labeled methionine analogue for 1h and fixed for 15min in 4% formaldehyde and stained according to manufacturer's protocol. DAPI was used as counterstain and images were acquired using a BD-pathway imaging system. Image analysis was performed using BD Attovision software.

FLAG-Co-Immunoprecipitation

U2OS cells, expressing different shRNAs, were transiently transfected with FLAG-tagged wild-type 4EHP or [K121/130/134/222R]-mutant (4KR) 4EHP cDNAs or FLAG-LacR control plasmid in absence or presence of pCAGGS-5HA-mISG15 cDNA in OptiMEM (Invitrogen), using JetPEI (Polyplus Transfection). The following day, medium was refreshed and 48h post transfection cells were lysed in FLAG-lysis buffer (50mM Tris-HCl pH 7.4, 150mM NaCl, 1mM EDTA, 0.5% NP-40, 0.5% Triton-X, 1mM PMSF, supplemented with complete protease inhibitor cocktail (Roche)). After 30 min incubation on ice, lysates were diluted 5 times with FLAG-dilution buffer (50mM Tris-HCl pH 7.4, 150mM NaCl, 1mM EDTA, 1mM PMSF, supplemented with complete protease inhibitor cocktail) and incubated with prewashed M2-FLAG magnetic beads (Sigma) for 3h. Subsequently, beads were washed 3 times for 5min with FLAG-dilution buffer and lysed in Laemmli-SDS-sample buffer. FLAG-ARIH1 co-immunoprecipitation from lysates from SILAC-labeled cells followed by Mass Spectrometry (MS) was performed as described above, with the exception of eluting FLAG-bound proteins by competition with the 3xFLAG peptide instead of boiling in sample buffer. Following elution, samples were trypsinised over-night, desalted, freeze-dried and finally used for MS analysis.

qPCR

RNA was extracted using RNeasy Plus Mini Kit from Qiagen. cDNA was made from 50ng total RNA with RevertAid H minus First strand cDNA synthesis kit (Fermentas) and real-time qPCR was subsequently performed in triplicate using SYBR green PCR (Applied Biosystems) on a 7900HT fast real-time PCR

system (Applied Biosystems). The following qPCR primer sets were used: GAPDH forward (fw) AGCCACATCGCTCAGACACC; GAPDH reverse (rev) ACCCGTTGACTCCGACCTT; ARIH1 fw TCATGCCTCTACCCAAGCCTT; ARIH1 rev ACCAAACCCACAGCAACACA. Data were collected and analysed using SDS2.3 software (Applied Biosystems). Relative mRNA levels after correction for GAPDH control mRNA were expressed using $2^{\wedge}(-\Delta\Delta Ct)$ method.

ACKNOWLEDGEMENTS

A

B

C

5

D

$$Z' \text{-factor} = 1 - \frac{3 \times (s_p + s_n)}{|m_p - m_n|} = 0.45$$
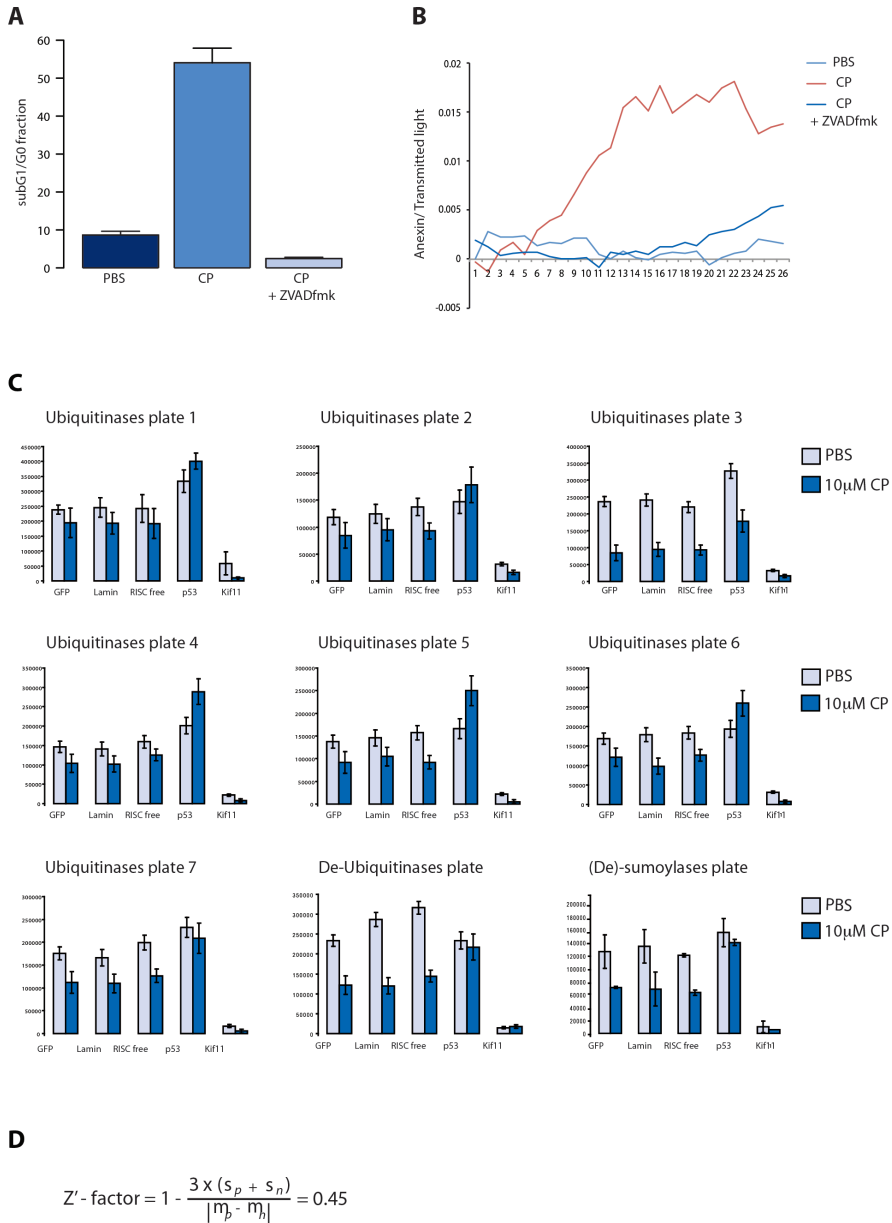
Figure S1. Caspase-dependent apoptosis in ES cells treated with CP and quality of ubiquitination/sumoylation screen. (A) Induction of SubG1/G0 apoptotic fraction in HM1 ES cells treated with 7.5µM CP for 24h and prevention by co-treatment with 100µM pan-Caspase inhibitor ZVADfmk. (B) Real time imaging of fluorescently labeled Annexin V binding (Puigvert et al., 2010) shows accumulation of apoptotic ES cells during treatment with 7.5µM CP and prevention by 100µM ZVADfmk. Ratio [AnexinV signal: total cell area] is shown. (C) ATPlite readout for indicated set of control siRNAs in each Smartpool library plate. Bars show average and standard deviation of two control and two 10µM CP-treated plates. (D) Average Z´-factor calculated for siLamin and sip53.

A
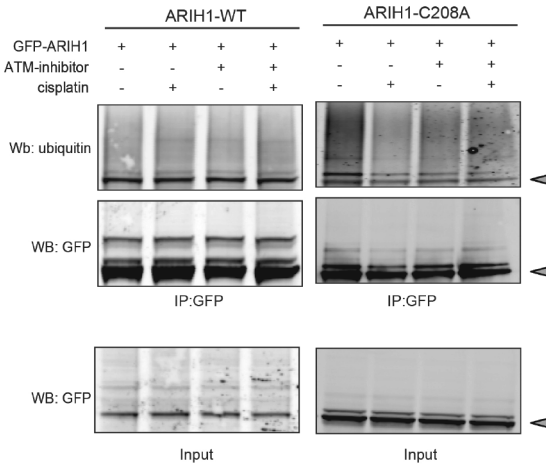
B

IP ARIH1

Protein	Protein name	cPt/untreated
Protein ariadne-1 homolog [Experiment 1]	ARIH1	2,104997264
Ubiquitin-conjugating enzyme E2 L3	UBE2L3/UBCH7 [E2]	1,55649291
Ubiquitin-like modifier-activating enzyme 1	UBA1 [E1]	1,072259573
ubiquitin C;UBC protein;ubiquitin B precursor;ubiquitin and ribosomal protein S27a precursor	Ubiquitin	1,132490006
E3 ubiquitin-protein ligase ARIH1 [Experiment 2]	ARIH1	2,1992039
Ubiquitin-60S ribosomal protein L40;Ubiquitin;60S ribosomal protein L40;Ubiquitin-40S ribosomal protein S27a;Ubiquitin;40S ribosomal protein S27a;Polyubiquitin-B;Ubiquitin;Polyubiquitin-C;Ubiquitin	ubiquitin	1,4406
E3 ubiquitin-protein ligase ARIH1	phospho-ARIH1 Y258	1,0771
Ubiquitin-60S ribosomal protein L40;Ubiquitin;60S ribosomal protein L40;Ubiquitin-40S ribosomal protein S27a;Ubiquitin;40S ribosomal protein S27a;Polyubiquitin-B;Ubiquitin;Polyubiquitin-C;Ubiquitin	K48-ubiquitin	1,5635
E3 ubiquitin-protein ligase ARIH1	ub-ARIH1 K144	0,89212

Figure S2. ARIH1 is part of a ubiquitination complex and CP and ATM inhibitor do not affect ubiquitination of WT or C208A ARIH1. (A) Western blot using antibodies against GFP or ubiquitin on total lysates and GFP-immunoprecipitations from GFP-ARIH1(WT)- and GFP-ARIH(C208A)-expressing U2OS cells treated with vehicle control or treated for 4 hours with 5µM CP with or without pre-treatment for 1hr with 5µM ATM inhibitor KU-55933. Grey arrowheads indicate ARIH1. (B) MS analysis of native FLAG-immunoprecipitations from SILAC-labelled FLAG-ARIH1 U2OS cells. SILAC ratios of peptides detected after 4 hours treatment with 5µM CP and control conditions are shown.

Table S1

Deubiquitinases custom library

Gene Symbol	Gene Id	Accession Number
MJD	110616	NM_029705
E030022H21RIK	217218	NM_001098837
DUB-1A	381944	NM_201409
DUB2	13532	NM_010089
BAP1	104416	NM_027088
C130067A03RIK	320713	NM_177239
TNFAIP3	21929	NM_009397
1810057B09RIK	223527	NM_175009
HIST2H2BE	319190	NM_178214
DXIMX46E	54644	NM_138604
C6.1A	210766	NM_145956
CYLD	74256	NM_173369
FBXO7	69754	NM_153195
FBXO8	50753	NM_015791
E130307M08RIK	68047	NM_026530
1300006C06RIK	74158	NM_028792
1110007C05RIK	66124	NM_025368
OTUB1	107260	NM_134150
4930586I02RIK	68149	NM_026580
4933428L19RIK	71198	XM_991213
D8ERTD69E	73945	NM_001081164
2600013N14RIK	72201	NM_152812
USP1	230484	NM_146144
USP2	53376	NM_198091
USP3	235441	NM_144937
USP4	22258	NM_011678
USP5	22225	NM_013700
USP7	252870	NM_001003918
USP8	84092	NM_019729
USP9X	22284	NM_009481
USP9Y	107868	NM_148943
USP10	22224	NM_009462
USP11	236733	NM_145628
USP12	22217	NM_011669
USP13	72607	NM_001013024
USP14	59025	NM_001038589
USP15	14479	NM_027604
USP16	74112	NM_024258
Usp17	436004	NM_001033494
USP18	24110	NM_011909
USP19	71472	NM_027804
USP20	74270	NM_028846
USP21	30941	NM_013919
USP22	216825	NM_001004143
Usp24	329908	XM_915524
USP25	30940	NM_013918
USP26	83563	NM_031388
USP28	235323	NM_175482
USP29	57775	NM_021323
USP30	100756	NM_001033202
6330567E21RIK	76179	XM_992065
USP32	237898	NM_001029934

5

Table S1. Custom siRNA libraries for Deubiquitinases and (De)-Sumoylases. Indicated are gene symbols, Entrez IDs and Accession numbers.

USP33	170822	NM_001076676
LOC244144	244144	XM_886523
Usp36	72344	XM_916680
4932415L06RIK	319651	NM_176972
USP38	74841	NM_027554
USP39	28035	NM_138592
USP40	227334	NM_001033291
Usp42	76800	NM_029749
USP43	216835	NM_173754
E430004F17	327799	NM_183199
4930550B20RIK	77593	NM_152825
2410018I08RIK	69727	NM_177561
USP47	74996	NM_133758
USP48	170707	NM_130879
C330046L10RIK	224836	NM_198421
4930511O11RIK	75083	NM_029163
LOC635253	635253	NM_001137547
USP52	103135	NM_133992
AA939927	99526	NM_133857
USP54	78787	NM_030180
UBR1	22222	NM_009461
UCHL1	22223	NM_011670
UCHL3	50933	NM_016723
UCHL5	56207	NM_019562
UFD1L	22230	NM_011672
UBE4B	63958	NM_022022
COPS5	26754	NM_013715
PLP2	18824	NM_019755

5

SUMOylation custom library

Gene Symbol	Gene Id	Accession Number
UBLE1B	50995	NM_016682
Ube2i	22196	NM_011665
MDM2	17246	NM_010786
D11BWG0280E	52915	NM_028601
BC065120	328365	NM_183208
PIAS1	56469	NM_019663
MIZ1	17344	NM_008602
PIAS3	229615	NM_018812
PIAS4	59004	NM_021501
RANBP2	19386	NM_011240
CBX4	12418	NM_007625
2510027N19RIK	67711	NM_026330
TOPORS	106021	NM_134097
RNF110	22658	NM_009545
SENP1	223870	NM_144851
SENP2	75826	NM_029457
SENP3	80886	NM_030702
SENP5	320213	NM_177103
SENP6	215351	NM_146003
2810413I22RIK	66315	NM_001003973
SENP8	71599	NM_027838

Table S1 (continued). Custom siRNA libraries for Deubiquitinases and (De)-Sumoylases.
Indicated are gene symbols, Entrez IDs and Accession numbers.

Table S2.

gene symbol	Z-score	p-value
RBX1	-3.49229	0.000239
FBXO6A	-2.96913	0.001493
SYTL4	-2.69639	0.003505
RCHY1	-2.68571	0.003619
RNF166	-2.67699	0.003714
Rfwd3	-2.51751	0.005909
UBE1X	-2.28613	0.011123
TCE1	-2.25446	0.012084
ARIH1	-2.16801	0.015079
FBXW7	-2.11149	0.017365
TOPORS	-2.11004	0.017428
BARD1	-2.05953	0.019722
C730024G19RIK	-2.05522	0.019929
LOC380928	-2.0437	0.020492
LOC381621	-2.02454	0.021458
USP8	-2.02454	0.021458
UBE2D3	-2.02396	0.021487
CHD4	-1.93042	0.026778
BRCA1	-1.85984	0.031454
PHF15	-1.85	0.032157
TRIM21	-1.80426	0.035595
SHPRH	-1.75546	0.03959
MKRN2	-1.73969	0.040957
USP4	-1.73969	0.040957
A530081L18RIK	-1.70491	0.044106
DXIMX46E	-1.70491	0.044106
FBXW5	-1.68291	0.046196
USP5	-1.45575	0.07273
USP7	-1.37068	0.085238
Usp42	1.637496	0.050763
FBXO17	1.650206	0.04945
ASB3	1.656369	0.048824
1110002E23RIK	1.708269	0.043793
LOC668173	1.728961	0.041908
6330567E21RIK	1.728961	0.041908
Trim61	1.750478	0.040018
FBXO34L	1.804707	0.03556
MGRN1	1.934613	0.026519
4933428L19RIK	1.934613	0.026519
DTX2	1.986825	0.023471
AL033326	2.010687	0.022179
USP54	2.078665	0.018824
ZNRF2	2.153452	0.015642
LNX2	2.196345	0.014034
CUL4A	2.21634	0.013334
RNF110	2.29063	0.010992
USP22	2.29063	0.010992
CUL1	2.479363	0.006581
CDC34	2.994131	0.001376
E430004F17	3.097247	0.000977

5

Table S2. Hits from primary screens. Indicated are gene symbols, Z-scores and p-values.

Table S3.

	gene ID	Accession number	Function	validation
USP4 *	22258	NM_011678	DUB	2 out of 4
USP7 *	252870	NM_001003918	DUB	3 out of 4
USP8	84092	NM_019729	DUB	4 out of 4
DXIMX46E	54644	NM_138604	DUB	2 out of 4
E430004F17	327799	NM_183199	DUB	2 out of 4
USP5 *	22225	NM_013700	DUB	3 out of 4
RUFY1	216724	NM_172557	no known UB-function	2 out of 4
RCHY1 *	68098	NM_026557	E3	2 out of 4
Rfwd3 *	234736	NM_146218	E3	4 out of 4
4930470D19RIK	67610	NM_026274	no known UB-function	4 out of 4
ARIH1	23806	NM_019927	E3	4 out of 4
UBE1X	22201	NM_009457	E1	4 out of 4
SYTL4	94121	NM_013757	no known UB-function	3 out of 4
CHD4	107932	NM_145979	no known UB-function	3 out of 4
FBXW7	50754	NM_080428	E3	2 out of 4
LOC381621		XM_355579	no known UB-function	2 out of 4
UBE2D3	66105	NM_025356	E2	4 out of 4
DTX2	74198	NM_023742	E3	2 out of 4
ZNRF2	387524	NM_199143	E3	2 out of 4
RBX1	9978	NM_019712	E3	4 out of 4
TCE1	79043	NM_027141	no known UB-function	2 out of 4
TOPORS *	106021	NM_134097	E3	2 out of 4
C730024G19RIK	232566	XM_132975	no known UB-function	3 out of 4
BRCA1	NM_009764	NM_009764	E3	3 out of 4
TRIM21	20821	NM_009277	E3	4 out of 4
SHPRH	268281	NM_172937	E3	2 out of 4
AL033326*	24105	NM_019705	E3	3 out of 4
Fbxo7	69754	NM_153195	E3	3 out of 4

Table S3. Hits from secondary deconvolution screens. Indicated are gene symbols, Entrez IDs, Accession numbers, ubiquitination function and validation status. Asterisks indicate hits known to affect p53. Sensitising siRNAs in blue; protecting siRNAs in red.

5

REFERENCES

1. Ciccia, A. and S.J. Elledge, The DNA damage response: making it safe to play with knives. Mol Cell, 2010. 40(2): p. 179-204.

2. Jackson, S.P. and J. Bartek, The DNA-damage response in human biology and disease. Nature, 2009. 461(7267): p. 1071-8.

3. Matsuoka, S., et al., ATM and ATR substrate analysis reveals extensive protein networks responsive to DNA damage. Science, 2007. 316(5828): p. 1160-6.

4. Reinhardt, H.C. and M.B. Yaffe, Kinases that control the cell cycle in response to DNA damage: Chk1, Chk2, and MK2. Curr Opin Cell Biol, 2009. 21(2): p. 245-55.

5. Bergink, S. and S. Jentsch, Principles of ubiquitin and SUMO modifications in DNA repair. Nature, 2009. 458(7237): p. 461-7.

6. Komander, D., The emerging complexity of protein ubiquitination. Biochem Soc Trans, 2009. 37(Pt 5): p. 937-53.

7. Morris, J.R., More modifiers move on DNA damage. Cancer Research, 2010. 70(10): p. 3861-3.

8. Skaug, B. and Z.J. Chen, Emerging role of ISG15 in antiviral immunity. Cell, 2010. 143(2): p. 187-90.

9. Staub, O., Ubiquitylation and isgylation: overlapping enzymatic cascades do the job. Sci STKE, 2004. 2004(245): p. pe43.

10. Brooks, C.L. and W. Gu, p53 ubiquitination: Mdm2 and beyond. Mol Cell, 2006. 21(3): p. 307-15.

11. Crosetto, N., M. Bienko, and I. Dikic, Ubiquitin hubs in oncogenic networks. Mol Cancer Res, 2006. 4(12): p. 899-904.

12. Wood, L.M., et al., A novel role for ATM in regulating proteasome-mediated protein degradation through suppression of the ISG15 conjugation pathway. PLoS One, 2011. 6(1): p. e16422.

13. Kerscher, O., R. Felberbaum, and M. Hochstrasser, Modification of proteins by ubiquitin and ubiquitin-like proteins. Annu Rev Cell Dev Biol, 2006. 22: p. 159-80.

14. Nagy, V. and I. Dikic, Ubiquitin ligase complexes: from substrate selectivity to conjugational specificity. Biol Chem, 2010. 391(2-3): p. 163-9.

15. Wenzel, D.M., et al., UBCH7 reactivity profile reveals parkin and HHARI to be RING/HECT hybrids. Nature, 2011. 474(7349): p. 105-8.

16. Reinhardt, H.C., et al., Is post-transcriptional stabilization, splicing and translation of selective mRNAs a key to the DNA damage response? Cell Cycle, 2011. 10(1):

5

p. 23-7.

17.   Braunstein, S., et al., Regulation of protein synthesis by ionizing radiation. Molecular and Cellular Biology, 2009. 29(21): p. 5645-56.

18.   Connolly, E., et al., Hypoxia inhibits protein synthesis through a 4E-BP1 and elongation factor 2 kinase pathway controlled by mTOR and uncoupled in breast cancer cells. Molecular and Cellular Biology, 2006. 26(10): p. 3955-65.

19.   Silvera, D., S.C. Formenti, and R.J. Schneider, Translational control in cancer. Nat Rev Cancer, 2010. 10(4): p. 254-66.

20.   Kong, J. and P. Lasko, Translational control in cellular and developmental processes. Nat Rev Genet, 2012. 13(6): p. 383-94.

21.   Gross, J.D., et al., Ribosome loading onto the mRNA cap is driven by conformational coupling between eIF4G and eIF4E. Cell, 2003. 115(6): p. 739-50.

22.   Gingras, A.C., B. Raught, and N. Sonenberg, eIF4 initiation factors: effectors of mRNA recruitment to ribosomes and regulators of translation. Annu Rev Biochem, 1999. 68: p. 913-63.

23.   Moudry, P., et al., Ubiquitin-activating enzyme UBA1 is required for cellular response to DNA damage. Cell Cycle, 2012. 11(8): p. 1573-82.

24.   Puigvert, J.C., et al., Systems Biology Approach Identifies the Kinase Csnk1a1 as a Regulator of the DNA Damage Response in Embryonic Stem Cells. Sci Signal, 2013. 6(259).

25.   Dayal, S., et al., Suppression of the deubiquitinating enzyme USP5 causes the accumulation of unanchored polyubiquitin and the activation of p53. J Biol Chem, 2009. 284(8): p. 5030-41.

26.   Meulmeester, E., et al., Loss of HAUSP-mediated deubiquitination contributes to DNA damage-induced destabilization of Hdmx and Hdm2. Mol Cell, 2005. 18(5): p. 565-76.

27.   Zhang, X., et al., USP4 inhibits p53 through deubiquitinating and stabilizing ARF-BP1. EMBO J, 2011. 30(11): p. 2177-89.

28.   Fu, X., et al., RFWD3-Mdm2 ubiquitin ligase complex positively regulates p53 stability in response to DNA damage. Proc Natl Acad Sci U S A, 2010. 107(10): p. 4579-84.

29.   Yang, X., et al., Plk1-mediated phosphorylation of Topors regulates p53 stability. J Biol Chem, 2009. 284(28): p. 18588-92.

30.   Lin, J.R., et al., SHPRH and HLTF act in a damage-specific manner to coordinate different forms of postreplication repair and prevent mutagenesis. Mol Cell, 2011. 42(2): p. 237-49.

31.   Jung, Y.S., et al., Pirh2 E3 ubiquitin ligase monoubiquitinates DNA polymerase eta to suppress translesion DNA synthesis. Molecular and Cellular Biology, 2011.

5

31(19): p. 3997-4006.

32.   Roy, R., J. Chun, and S.N. Powell, BRCA1 and BRCA2: different roles in a common pathway of genome protection. Nat Rev Cancer, 2012. 12(1): p. 68-78.

33.   Liu, S., et al., RING finger and WD repeat domain 3 (RFWD3) associates with replication protein A (RPA) and facilitates RPA-mediated DNA damage response. J Biol Chem, 2011. 286(25): p. 22314-22.

34.   Tan, N.G.S., et al., Characterisation of the human and mouse orthologues of the Drosophila ariadne gene. Cytogenetics and Cell Genetics, 2000. 90(3-4): p. 242-245.

35.   Li, Z., P.R. Musich, and Y. Zou, Differential DNA damage responses in p53 proficient and deficient cells: cisplatin-induced nuclear import of XPA is independent of ATR checkpoint in p53-deficient lung cancer cells. Int J Biochem Mol Biol, 2011. 2(2): p. 138-145.

36.   Medema, R.H. and L. Macurek, Checkpoint control and cancer. Oncogene, 2012. 31(21): p. 2601-13.

37.   Kumar, V., et al., Regulation of the rapamycin and FKBP-target 1/mammalian target of rapamycin and cap-dependent initiation of translation by the c-Abl protein-tyrosine kinase. J Biol Chem, 2000. 275(15): p. 10779-87.

38.   Tan, N.G., et al., Human homologue of ariadne promotes the ubiquitylation of translation initiation factor 4E homologous protein, 4EHP. FEBS Lett, 2003. 554(3): p. 501-4.

39.   Okumura, F., W. Zou, and D.E. Zhang, ISG15 modification of the eIF4E cognate 4EHP enhances cap structure-binding activity of 4EHP. Genes Dev, 2007. 21(3): p. 255-60.

40.   Ardley, H.C., et al., Features of the parkin/ariadne-like ubiquitin ligase, HHARI, that regulate its interaction with the ubiquitin-conjugating enzyme, Ubch7. J Biol Chem, 2001. 276(22): p. 19640-7.

41.   Matsumoto, A., et al., Fbxw7-dependent degradation of Notch is required for control of „stemness" and neuronal-glial differentiation in neural stem cells. J Biol Chem, 2011. 286(15): p. 13754-64.

42.   Welcker, M. and B.E. Clurman, FBW7 ubiquitin ligase: a tumour suppressor at the crossroads of cell division, growth and differentiation. Nat Rev Cancer, 2008. 8(2): p. 83-93.

43.   Yi, Z., T. Yi, and Z. Wu, cDNA cloning, characterization and expression analysis of DTX2, a human WWE and RING-finger gene, in human embryos. DNA Seq, 2006. 17(3): p. 175-80.

44.   Balut, C.M., C.M. Loch, and D.C. Devor, Role of ubiquitylation and USP8-dependent deubiquitylation in the endocytosis and lysosomal targeting of plasma membrane KCa3.1. Faseb Journal, 2011. 25(11): p. 3938-48.

5

45.   Kuroda, T.S., et al., The Slp homology domain of synaptotagmin-like proteins 1-4 and Slac2 functions as a novel Rab27A binding domain. J Biol Chem, 2002. 277(11): p. 9212-8.

46.   Yamamoto, H., et al., Functional cross-talk between Rab14 and Rab4 through a dual effector, RUFY1/Rabip4. Molecular Biology of the Cell, 2010. 21(15): p. 2746-55.

47.   Larsen, D.H., et al., The chromatin-remodeling factor CHD4 coordinates signaling and repair after DNA damage. Journal of Cell Biology, 2010. 190(5): p. 731-40.

48.   Nakayama, E.E. and T. Shioda, Anti-retroviral activity of TRIM5 alpha. Rev Med Virol, 2010. 20(2): p. 77-92.

49.   Okumura, F., et al., The Role of Elongin BC-Containing Ubiquitin Ligases. Front Oncol, 2012. 2: p. 10.

50.   Cencic, R., et al., Reversing chemoresistance by small molecule inhibition of the translation initiation complex eIF4F. Proc Natl Acad Sci U S A, 2011. 108(3): p. 1046-51.

51.   Shamji, A.F., P. Nghiem, and S.L. Schreiber, Integration of growth factor and nutrient signaling: implications for cancer biology. Mol Cell, 2003. 12(2): p. 271-80.

52.   Clarke, R., et al., Endoplasmic reticulum stress, the unfolded protein response, autophagy, and the integrated regulation of breast cancer cell fate. Cancer Research, 2012. 72(6): p. 1321-31.

53.   Morita, M., et al., A novel 4EHP-GIGYF2 translational repressor complex is essential for mammalian development. Molecular and Cellular Biology, 2012. 32(17): p. 3585-93.

54.   Sonenberg, N. and A.C. Gingras, The mRNA 5' cap-binding protein eIF4E and control of cell growth. Curr Opin Cell Biol, 1998. 10(2): p. 268-75.

55.   Cho, P.F., et al., A new paradigm for translational control: inhibition via 5'-3' mRNA tethering by Bicoid and the eIF4E cognate 4EHP. Cell, 2005. 121(3): p. 411-23.

56.   Lasko, P., Posttranscriptional regulation in Drosophila oocytes and early embryos. Wiley Interdiscip Rev RNA, 2011. 2(3): p. 408-16.

57.   Bensimon, A., et al., ATM-dependent and -independent dynamics of the nuclear phosphoproteome after DNA damage. Sci Signal, 2010. 3(151): p. rs3.

58.   Bennetzen, M.V., et al., Site-specific phosphorylation dynamics of the nuclear proteome during the DNA damage response. Mol Cell Proteomics, 2010. 9(6): p. 1314-23.

59.   Joshi, B., A. Cameron, and R. Jagus, Characterization of mammalian eIF4E-family members. Eur J Biochem, 2004. 271(11): p. 2189-203.

60.   Wiseman, R.L. and W.E. Balch, A new pharmacology--drugging stressed folding pathways. Trends Mol Med, 2005. 11(8): p. 347-50.

5

61.   Campeau, E., et al., A versatile viral system for expression and depletion of proteins in mammalian cells. PLoS One, 2009. 4(8): p. e6529.

62.   Birmingham, A., et al., Statistical methods for analysis of high-throughput RNA interference screens. Nat Methods, 2009. 6(8): p. 569-75.

63.   Puigvert, J.C., et al., High-throughput live cell imaging of apoptosis. Curr Protoc Cell Biol, 2010. Chapter 18: p. Unit 18 10 1-13.

64.   Moody, C.A., et al., Modulation of the cell growth regulator mTOR by Epstein-Barr virus-encoded LMP2A. Journal of Virology, 2005. 79(9): p. 5499-506.

5

6

The E3 ubiquitin ligase ARIH1 regulates DSB repair

Dimitris Typas, Wouter W. Wiegant, Alex Pines, Martijn S. Luijsterburg, Louise von Stechow, Erik H.J. Danen, Leon H. Mullenders and Haico van Attikum

ABSTRACT

Genome stability is gravely endangered by exogenously or endogenously induced DNA Double Strand Breaks (DSBs). In order to counteract their detrimental effects, mammalian cells have evolved sophisticated mechanisms that allow for their efficient and timely removal. Those mechanisms are collectively known as the DSB response and are centered around the concerted mode of action of the kinases ATM/ATR and the E3 ubiqutiin ligases RNF8/RNF168. Although, these proteins constitute the master regulators of the DSB response, ongoing research has hinted that there are more ubiquitin-family enzymes promoting efficient DSB repair. We recently identified the E3 ubiquitin ligase ARIH1 in a cisPt lethality screen as a cytoprotective protein facilitating a significant, transient arrest of translation upon DSB induction. Intriguingly, ARIH1 also appears to be recruited to sites of DNA damage, while its depletion hinders DSB repair by homologous recombination. Interaction studies additionally indicate that ARIH1 directly interacts with the KU-heterodimeric complex which initiaties DSB repair by non-homologous end-joining. Cumulatively, our results favour a direct role of ARIH1 in regulating DSB repair.

6

INTRODUCTION

DNA Double Strand Breaks (DSBs) present cellular DNA repair mechanisms with a formidable challenge, as genetic information is simultaneously assaulted on both strands [1]. In order to counteract DSBs and their deleterious effects, mammalian cells trigger an elaborate response orchestrated by the ATM/ATR kinases [2] and the RNF8/RNF168 E3 ubiquitin ligases [3]. The DSB response is a multifaceted process entailing chromatin remodelling, cell-cycle checkpoint activation and DNA repair [4], primarily by either of the main DSB repair pathways, Non-Homologous End-Joining (NHEJ) [5] or Homologous Recombination (HR) [6].

Recent work has made it increasingly clear that protein post-translational modifications by ubiquitin or ubiquitin-like proteins exert key roles in orchestrating spatiotemporally the efficient execution of DSB repair [7-13]. Protein ubiquitylation constitutes an elaborate molecular switch that controls many aspects of DSB proteins, including their stability [8], recruitment and/or residence time at sites of damage [14, 15] and segregation from chromatin [16, 17]. Besides the mainstream known E3 ubiquitin ligases RNF8 and RNF168, which are known to regulate the DSB response at multiple levels [8, 15, 18-22], several alternative E3 ligases have been associated with DSB repair [10, 12, 23-25], indicating that ubiquitylation plays a much more extensive role than initially believed and that, most likely, more ubiquitin-related enzymes will be eventually implicated in DSB repair.

After performing a siRNA-screen for enzymes of the ubiquitin and SUMO family upon cisplatin-induced DNA damage, we identified the E3 ubiquitin ligase ARIadne Homolog 1 (ARIH1) (Chapter 5) as a primary, sensitising hit. We then illustrated that ARIH1 regulates a transient translation arrest that facilitates cell survival. Whilst investigating its role in inducing this translation arrest, we noticed that upon DNA damage induction by either cisplatin or Ionising Radiation (IR), ARIH1 increasingly translocated both to ribosomes and the nucleus (Chapter 5).

6

The DNA damage mediated nuclear localisation of ARIH1 prompted us to examine whether ARIH1 holds a nuclear function, and more specifically if it plays a direct role in regulating DSB repair. To our surprise, we witnessed that ARIH1 accumulated at laser-induced damage. Furthermore, ARIH1 depletion impaired not only general DSB repair but also specifically HR, evident by decreased end-resection and RAD51-recombinase loading on ssDNA. Intriguingly, when trying to identify potential partners of ARIH1 by Mass Spectrometry (MS) or co-immunoprecipiation coupled to western blotting, we stumbled upon the KU-complex, the known initiator of NHEJ. In conclusion, our initial results support the notion that ARIH1 directly impinges on DSB repair by HR and NHEJ, by affecting RAD51 loading and probably by interacting with the KU70-KU80 heterodimer, respectively.

RESULTS

ARIH1 protects cells against IR-induced damage

6

We recently demonstrated that the E3 ubiquitin ligase ARIH1 promotes cellular survival after treatment with cisplatin (Chapter 5), an agent known to induce intra/interstrand crosslinks as well as mono-adducts. Loss of ARIH1 renders cells incapable of launching a temporary halt of translation, thereby sensitising them to cisplatin. Knowing that ARIH1 is important for this translational arrest, we wondered if ARIH1 depletion would be detrimental to human cells exposed to forms of DNA damage other than the ones tested in our original study. We therefore exposed ARIH1-depleted cells (for knock-down efficiency please look at Fig. 2E of Chapter 5) to either IR or UVC light. Interestingly, cells lacking this E3 ligase were more sensitive to IR (Fig. 1A), but not to UV (Fig. 1B), indicating that ARIH1 may specifically confer a defect to DNA double-strand break inducing agents rather than to DNA intrastrand crosslinks per se. In agreement with this rationale, in our original study we had observed that ARIH1 depletion was detrimental to mouse ES cells upon treatment with agents, such as cisplatin, mitomycin C and doxorubicin, that induce DSBs either directly or upon replication (Chapter 5).

Given its role in establishing a translational arrest after cisplatin, we wondered whether ARIH1 exerts its cytoprotective role in a direct or indirect manner. Our previous results had hinted that, in parallel to facilitating a transient pause of protein synthesis, ARIH1 translocated to the nucleus upon DNA damage (Chapter 5). In order to validate the potential significance of this increased nuclear localisation, we examined the behaviour of ARIH1 upon laser micro-irradiation. To our surprise, GFP-tagged ARIH1 rapidly accumulated at laser-induced DNA damage (Fig. 1C). Similarly, an ARIH1-mutant (C208A) that is unable to interact with its major E2 partner (UBE2D3), and is therefore less proficient in ubiquitylating downstream substrates, could also assemble at sites of damage, albeit less readily than its wild-type counterpart (Fig. 1C)

We then sought to expand our findings by assaying if ARIH1 can form IR-Induced Foci (IRIF), as several factors involved in DSB signalling or DSB repair by HR do. We could not detect any ARIH1 IRIF, either at early time-points (1hr; Fig. 1D, left panel), indicative of DSB-signalling related complexes, or at later time-points (6hr; Fig. 1D, right panel), indicative of HR-related complexes. Along the same lines, wild-type or ubiquitylation-deficient GFP-tagged ARIH1 did not assemble at FokI-induced DSBs (Fig. 1E), implying that detection of ARIH1 at isolated DSBs may require specific extraction protocols, like several NHEJ factors do [26]. As expected from the lack of any phenotype upon UV exposure, ARIH1 did not accumulate at sites of UV-induced damage (Fig. 1F). Finally, we tried to exclude the possibility that ARIH1 exert its role in DSB repair by solely regulating the expression of specific repair proteins. Though much more comprehensive testing is needed to rule out a predominantly indirect role, all probed repair-proteins appeared to be expressed at similar levels upon ARIH1 depletion and control conditions (Supplemental Fig. 1). Taken together, these results suggest that ARIH1 might play a direct role in DSB repair.
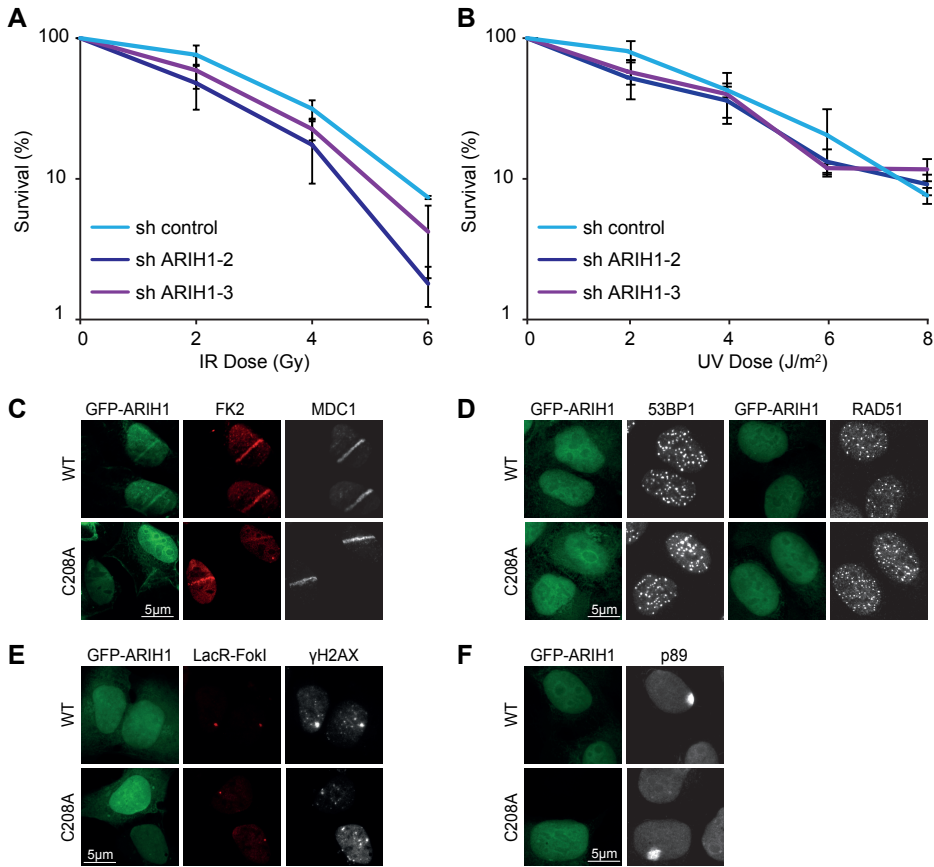
6

Figure 1. ARIH1 is involved in the DSB response. (A) Clonogenic survival of U2OS cells transfected with the indicated siRNAs and subsequently exposed to IR. (B) As in A only exposed to UVC irradiation. (C) Recruitment of GFP-tagged ARIH1 (wild-type or C208A mutant) (green) to FK2- (red) and MDC1- (white) marked DNA damage sites after laser micro-irradiation. (D) Lack of recruitment of the indicated GFP fusion proteins (green) at early IRIF, marked by 53BP1 (white; left), or late IRIF, marked by RAD51 (white; right). (E) Lack of recruitment of the indicated GFP fusion proteins (green) to FokI-mCherry-LacR-induced DSBs marked by γH2AX (white) in cells containing a LacO array. (F) Lack of accumulation of the indicated GFP-fusion proteins (green) to sites of UV-induced damage, marked by p89 (white).

ARIH1 depletion delays DNA repair by Homologous Recombination

Having shown that ARIH1 is necessary for the response to DNA damage inflicted by either cisplatin or IR, we investigated whether this E3 ligase directly affects DSB repair by assessing the rate of removal of γH2AX and 53BP1 foci. Stable, shRNA-mediated depletion of ARIH1 (Chapter 5 Fig. 2E) resulted in impaired repair kinetics at early time-points, assessed by γH2AX

(Fig.2A) and 53BP1 (Fig. 2B) IRIF removal, but relatively undisturbed repair kinetics at later time-points, indicating that ARIH1 is important for efficient DSB repair. Subsequently, we inquired upon which specific DSB repair pathway ARIH1 primarily regulates. In order to confirm a potential role in HR, we assayed if RPA and RAD51 IRIF formation is altered upon ARIH1 loss. We restricted our analysis to replicating cells by either utilising a U2OS cell-line stably expressing geminin, a known S/G2 marker, or immuno-staining for cyclin A, a protein expressed during late S/G2 phase. siRNA-mediated ARIH1 depletion (Supplemental Fig. 1) had a severe impact on DNA end-resection, as RPA IRIF formation was more than halved in ARIH1-less cells when compared to their control counterparts (Fig. 2C). In further agreement with ARIH1 holding a regulatory role in HR, loss of ARIH1 additionally abrogated RAD51 IRIF formation (Fig. 2D) in S/G2 cells. To consolidate our findings, we employed a well-described and widely-employed GFP-reporter assay that allows monitoring the efficiency of DSB repair by HR [27]. In line with our IRIF observations, ARIH1 loss led to a substantial decrease in the efficiency of HR execution (Fig. 2E), an effect not caused by gross alteration in cell-cycle progression (Fig. 2F), as both control and ARIH1-depleted cells contained comparable S/G2-phase populations.

6
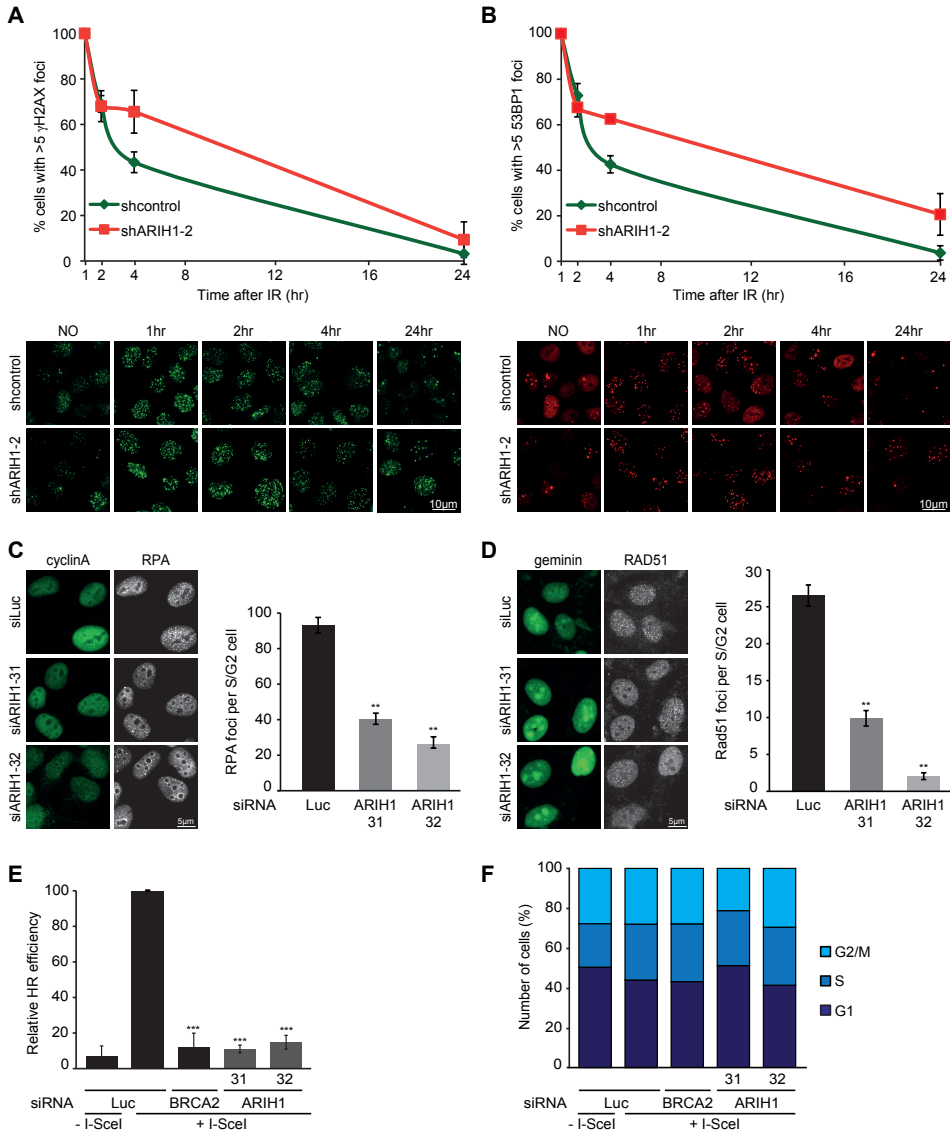
Figure 2. ARIH1 depletion hinders efficient DSB repair. (A) Effect of ARIH1 depletion on DSB repair, assayed by clearance of γH2AX foci multiple time-points after 2 Gy of IR. (B) As in A but for 53BP1 IRIF. (C) Effect of ARIH1 depletion on RPA (white) IRIF formation in cyclin A-expressing S/G2 cells (green) 4hr after 10 Gy of IR. (D) As in D but for RAD51 (white) IRIF in mAG-geminin-expressing S/G2 cells (green) 6hr after 10 Gy of IR. (E) Impact of the indicated siRNAs on HR efficiency measured using the DR-GFP reporter. (F) Cell cycle profiles of cells treated with the indicated siRNAs. Quantified data are represented as mean ± S.D. (n=3). *, P<0.05, **, P<0.01, ***, P<0.001 (student's t test).

ARIH1 interaction studies reveal an unexpected partnership with NHEJ factors

Having demonstrated that ARIH1 depletion attenuates HR execution, we tried to identify novel ARIH1 interacting proteins, hoping to retrieve repair-related proteins as potential partners. To this end, we generated cell lines stably expressing either FLAG- or GFP-tagged ARIH1, labelled them using SILAC, performed native immuno-precipitations and analysed samples by Mass Spectrometry. As expected, we were able to detect known ARIH1 interactors such as the E2 enzyme UBE2L (UBCH7) and the E1 enzyme (UBA1), verifying that we indeed isolated physiologically relevant ARIH1 complexes (Fig. 3A), primarily linked to ARIH1-related ubiquitylation. However, to our surprise, amongst the proteins we identified in our initial FLAG-ARIH1 IPs were Ku70 (XRCC6), Ku80 (XRCC5) and DNA-PKcs, all known regulators of NHEJ (Fig. 3A). Very similar results were obtained with FLAG-ARIH1-IP employing SILAC-label-swapped cells (Fig. 3B). To exclude the possibility of identifying false positive interactions due to non-specific binding to the M2-FLAG beads, we repeated our IP, this time utilising GFP-ARIH1 and including quantitative analysis of the basal complex, where samples from cells stably over-expressing GFP-ARIH1 are compared to samples from cells stably over-expressing GFP-NLS (control). Once more, Ku70 was specifically enriched upon ARIH1 purification (Fig. 3C), although this interaction appeared to be independent of IR-induced DNA damage (Fig. 3D). Finally, we tried to verify the observed ARIH1-Ku70 interaction by western blotting. In agreement with our MS data, endogenous Ku70 clearly co-immuno-precipitated with GFP-ARIH1 (Fig. 3E), albeit IR did not appear to affect this interaction. On the contrary, DNA-PKcs or HR-associated proteins RAD51 and RPA did not associate with ARIH1 (Fig. 3E). Put together, our interaction studies establish an interaction between the E3 ubiquitin ligase ARIH1 and the DSB-sensing heterodimeric KU complex.

6

A

Protein	Sequence Coverage (%)	cisplatin/untreated	SILAC ratio (H/L)
ARIH1	47,6	2,1	0,47
UBE2L3	10,4	1,56	0,64
UBA1	4,3	1,07	0,93
KU70 (XRCC6)	42	1,75	0,57
KU80 (XRCC5)	21,6	1,7	0,59
DNA-PK cs	9,8	1,15	0,87

B

Protein	Sequence Coverage (%)	cisplatin/untreated SILAC ratio (H/L)
ARIH1	46	1,19
UBE2L3	10,4	1,56
UBA1	2,2	1,07
KU70 (XRCC6)	33,8	0,99
KU80 (XRCC5)	16	1,01
DNA-PK cs	6	1,02

C

Protein	Sequence Coverage (%)	GFP-ARIH1/GFP-NLS (control) SILAC ratio (H/L)
ARIH1	17,1	7,01
KU70 (XRCC6)	15,9	2,24
KU80 (XRCC5)	6,4	1,35
DNA-PK cs	5,6	1,84

D

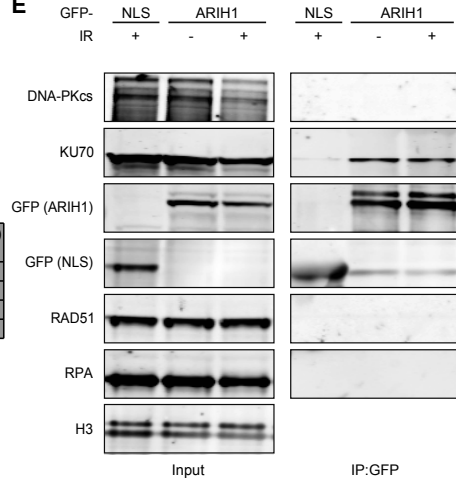| Protein	Sequence Coverage (%)	cisplatin/untreated SILAC ratio (H/L)
ARIH1	22,4	1,01
UBE2L3	18	1,03
KU70 (XRCC6)	12,3	0,96
KU80 (XRCC5)	3,6	0,92
DNA-PK cs	4,4	0,92

E

Figure 3. Exogenous ARIH1 interacts with the KU-complex. (A) Proteins identified by MS after FLAG-ARIH1-Immunoprecipitation. Sequence coverage represents the percentage of the indicated protein that was retrieved in individual peptides, while the SILAC ratio indicates the amount of Heavy:Light labelled protein copurified. Cells labelled with Heavy SILAC were left untreated, while cells labelled with Light SILAC were treated with 5µM cisplatin for 4hr. (B) As in A, but SILAC labels were swapped, namely untreated cells were pre-labelled in Light SILAC, while cisplatin-treated cells were pre-labelled in Heavy SILAC. (C) Proteins identified by MS after GFP-ARIH1- or GFP-NLS-Immunoprecipitation. GFP-ARIH1-IP took place in cells labelled with Heavy SILAC, while GFP-NLS was performed in cells labelled with Light SILAC. (D) Proteins identified by MS after GFP-ARIH1-Immunoprecipitation. Untreated cells were pre-labelled in Light SILAC, while IR-treated cells (10Gy/1hr) were pre-labelled in Heavy SILAC. (E) GFP-Immunoprecipitation of the indicated GFP-fusion proteins. Blots were probed for DNA-PKcs, KU70, GFP, RAD51, RPA, Histone H3 (loading control).

DISCUSSION

We previously demonstrated that the E3 ubiquitin ligase ARIH1 is responsible for inducing a transient translation arrest upon the induction of DNA damage by cisplatin, and concluded that the ARIH1-dependent temporary halting of protein synthesis benefits cellular survival (Chapter 5). However, our observation that ARIH1 increasingly translocates to the nucleus upon DNA

damage, by either cisplatin or IR, prompted us to investigate if ARIH1 has a secondary role in physically promoting DNA metabolism. The additional finding that ARIH1 depletion specifically sensitises to DSB-inducing agents, but not UV or non-genotoxic stressors, raised the possibility that ARIH1 is indeed directly involved in repair of DSB repair either generated directly or by DNA damage interference during replication (Chapter 5 and Fig. 1A, B). The swift accumulation of ARIH1 at laser-induced damage further promoted this rationale (Fig. 1C). Though the lack of recruitment at IRIF or FokI-induced DSB may seem perplexing, it is worth mentioning that specific conditions may be necessary in order to visualise ARIH1 accrual at sites of damage, as is the case for the KU70-KU80 heterodimer [26]. Follow-up immunofluorescence experiments under these conditions and ARIH1-ChIP experiments will be necessary to validate that the laser-induced-damage accumulation of ARIH1 is indeed physiologically relevant.

In agreement with this scenario, silencing ARIH1 inhibits DSB repair of a sub-fraction of DSBs, indicated by the approximately 2 fold reduced loss of γH2AX (Fig. 2A) and 53BP1 foci (Fig. 2B) during the first 4 hours after IR. More precisely, ARIH1 depletion seems to induce severe problems in HR execution, evident by a drop in resection rates (Fig. 2C) and loading of the RAD51 recombinase (Fig. 2D). These results are further solidified by the substantially diminished HR efficiency in the DR-GFP reporter assay (Fig. 2E). As ARIH1 knock-down does not compromise normal cell-cycle progression, (Fig. 2F) and barring unaccounted for, gross, siRNA off-target side-effects, our data support the hypothesis that ARIH1 plays a role in error-free repair of DSBs by HR.

Whatever the eventual mechanism will be, it has to account for the finding that the level of impairment of HR by ARIH1 depletion is comparable to that of BRCA2 a key player in HR (Fig.2E). However, the way that ARIH1 contributes to DSB repair is currently rather sketchy. Our initial search for ARIH1-interacting partners that are involved in DSB repair yielded unexpected results. Instead of identifying factors orchestrating HR in a complex with ARIH1, we stumbled upon a potential interaction between ARIH1 and the KU70-KU80 complex. Our MS data (Fig.3A-D) were confirmed by mainstream IP followed

6

by western blotting (Fig. 3E) and, therefore this novel interaction is in all probability true. Though we cannot exclude the possibility that we missed potential interactions between ARIH1 and one or more HR-related proteins, it seems reasonable to currently shift our attention towards the investigation of the KU-connection.

Numerous hypotheses can explain our thus far acquired data and certainly further experiments are going to be needed in order for a clear molecular mechanism to emerge, but one possible scenario is that ARIH1 promotes the timely removal of the KU complex, which has been shown to be subject to ubiquitylation-dependent removal from sites of damage [8, 28]. That would fit with the significantly decreased HR efficiency we observed upon ARIH1 depletion (Fig. 2E). According to this model, loss of ARIH1 would abnormally prolong KU70-KU80 residency at DSBs, therefore reinforcing the latter's antagonising effect on DNA end-resection [5].

Since ARIH1 appears to directly interact with KU70-KU80, it might ubiquitylate either of these proteins, thereby facilitating VCP- (or VCP-like)-dependent removal [16] of KU70-KU80 once its role is completed. Alternatively, ARIH1 might directly target KU70 (or KU80) for proteasomal degradation, in a fashion similar to RNF8 [8], which would also lift KU-imposed restraints on HR. Though it is not clear if ARIH1 can catalyse the formation of polyubiquitin chains and if so of what linkage, the major ARIH1-interacting E2 enzyme, UBE2L3, has been shown to promote the formation of degradative-poylubiquitin chains on certain substrates [29], but not of K63-chains [30]. Examining if and how ARIH1 affects the ubiquitylation status of KU70 (or KU80) by denaturing IPs followed by western blotting or MS would confirm whether ARIH1 can indeed ubiquitylate them. Along the same lines, it would be worthwhile to estimate KU70 protein stability in ARIH1-depleted cells by cycloheximide chase experiments. Furthermore, it would be interesting to assess the effect of ARIH1 depletion both on the accumulation of KU70 at laser-induced damage and in the EJ5-reporter cell line (to measure NHEJ efficiency), but also to investigate if loss of ARIH1 exacerbates IR sensitivity or DSB repair efficiency in KU70-/- cells. Finally, if ARIH1 does not primarily target either of the KU proteins, it is conceivable that it may control the steady-

6

state levels of another protein at the vicinity of the DSB, which is recruited at the same time frame as KU70. An exciting candidate fitting these criteria is 53BP1. Rather intriguingly, supporting this hypothesis, it was demonstrated that ARIH1's primary E2 partner, UBE2L3, regulates the stability of 53BP1 [29].

MATERIALS AND METHODS

Cell culture

Wild-type or lentivirally transduced U2OS were grown in DMEM (Gibco) containing 10% FCS (Bodinco BV). All lentivirally transduced cell-lines were kept under blasticidin selection. The ViraPower system (Life Science) was used to produce lentivirus for GFP-ARIH1 wild-type or C208A expression vectors.

Transfections and RNAi interference

siRNA and plasmid transfections were performed using Lipofectamine RNAiMAX (Invitrogen) and JetPEI (Polyplus Transfection) according to the manufacturer's instructions. Cells were transfected twice with siRNAs (40 nM) within 24 h and examined further 48 h after the second transfection, unless stated otherwise.

Generation of DSBs and UV-induced damage

IR was delivered by a YXlon X-ray generator (YXlon International, 200 KV, 10 mA, dose rate 2 Gy/min). UV-damage was generated by exposure to UVC light for 60sec at a rate of ~0.5J/m^2/sec

Cell survival assay

U2OS cells were transfected with siRNAs, trypsinised, seeded at low density and exposed to IR or UV. 7 days later cells were washed with 0.9% NaCl and stained with methylene blue. Colonies of more than 10 cells were scored.

FokI assay

6

U2OS 2-6-3 cells expressing inducible FokI-mCherry-LacR [31] were treated with 300 nM 4-OHT and 1 µM Shield-I for 5 hrs. Subsequently, cells were fixed with formaldehyde and immunostained with the indicated antibodies.

UV-A laser micro-irradiation

U2OS cells were grown on 18 mm coverslips and sensitised with 10 µM 5′-bromo-2-deoxyuridine (BrdU) for 24 hours as described [16, 32]. For micro-irradiation, the cells were placed in a Chamlide TC-A live-cell imaging chamber that was mounted on the stage of a Leica DM IRBE wide-field microscope stand (Leica, Wetzlar, Germany) integrated with a pulsed nitrogen laser (Micropoint Ablation Laser System; Photonic Instruments, Inc., Belfast, Ireland). The growth medium was replaced by CO_2-independent Leibovitz's L15 medium supplemented with 10% FCS and penicillin-streptomycin and cells were kept at 37°C. The laser output power was set to 78 to generate strictly localised sub-nuclear DNA damage. Following micro-irradiation, cells were incubated for the indicated time-points at 37°C in Leibovitz's L15 and subsequently fixed with formaldehyde before immunostaining.

Microscopy analysis

6

Images of fixed cells were acquired on a Zeiss AxioImager D2 widefield fluorescence microscope equipped with 40x, 63x and 100x PLAN APO (1.4 NA) oil-immersion objectives (Zeiss) and an HXP 120 metal-halide lamp used for excitation. Fluorescent probes were detected using previously described filters [33]. Images were recorded using ZEN 2012 software and analysed using ImageJ. The average reflects the quantification of 50-150 cells from 3 independent experiments.

IRIF analysis

RAD51 and RPA IRIF were analyzed in U2OS cells 6hr after 10Gy. IRIF were evaluated in ImageJ, using a custom-built macro that enabled automatic and objective analysis of the foci.

Immunofluorescent labelling

Immunofluorescent labelling was carried out as described previously [32, 34]. Briefly, cells were grown on glass coverslips and treated as indicated in the figure legends. Subsequently, cells were washed with PBS, then fixed

with 2% formaldehyde for 20 minutes and permeabilised with 0.25% Triton X-100 in PBS for 5 minutes. Cells were rinsed with phosphate-buffered saline (PBS) and then blocked with PBS containing 5% BSA. Finally, cells were equilibrated in PBS containing 0.5% BSA and 0.05% Tween 20, and incubated with primary antibodies. Detection was done using goat anti-mouse or goat anti-rabbit IgG coupled to Alexa 488, 555 or 647 (Invitrogen Molecular Probes). Samples were incubated with 0.1 µg/ml DAPI and mounted in Polymount.

Western blotting

Cell extracts were generated by boiling cell pellets in Laemmli buffer, separated by SDS-PAGE and transferred to PVDF membranes (Millipore). Membranes were probed with the indicated antibodies. Fluorescent signals were then detected using the Odyssey infrared imaging scanning system (LI-COR Biosciences).

HR assay

HEK293 cells containing a stably integrated copy of the DR-GFP reporter were used to measure the repair of I-SceI-induced DSBs by HR as described [27]. Briefly, 48 h after siRNA transfection, cells were transfected with the I-SceI expression vector pCBASce and an mCherry expression vector. 48 or 72 h later the fraction of GFP-positive cells among the mCherry-positive cells was determined by FACS on a LSRII flow cytometer (BD Bioscience) using FACSDiva software version 5.0.3. Quantifications were performed using Flowing Software (www.flowingsoftware.com).

Cell cycle profiling

For cell cycle analysis cells were fixed in 70% ethanol, followed by DNA staining with 50 µg/ml propidium iodide in the presence of RNase A (0.1 mg/ml). Cell sorting was performed on a LSRII flow cytometer (BD Bioscience) using FACSDiva software (version 5.0.3; BD). Quantifications were performed using Flowing Software.

FLAG/GFP-Immunoprecipitation

Cells were lysed in lysis buffer (for FLAG-IP: 50mM Tris-HCl pH 7.4, 150mM NaCl, 1mM $MgCl_2$, 0.5% NP-40, 0.5% Triton-X, 1mM PMSF, supplemented with complete protease inhibitor cocktail (Roche)/ For GFP-IP: 50mM HEPES-KOH pH 7.5, 150mM NaCl, 0.5% Triton-X, 1mM $MgCl_2$, supplemented with complete protease inhibitor cocktail (Roche)). After 30 min incubation on ice, lysates were cleared by centrifugation and then diluted 5 times with dilution buffer (For FLAG-IP: 50mM Tris-HCl pH 7.4, 150mM NaCl, 1mM EDTA, 1mM PMSF, supplemented with complete protease inhibitor cocktail/ For GFP-IP instead of 50mM Tris-HCl pH 7.4, 50mM HEPES-KOH pH 7.5 was used) and incubated with prewashed M2-FLAG magnetic beads (Sigma) for 3h or GFP-Trap® beads for 1hr. Subsequently, beads were washed 3 times for 5min with dilution buffer and FLAG-bound proteins were eluted by competition with the 3xFLAG peptide, whereas GFP-bound beads were directly trypsinised to obtain bound proteins. Following elution, samples were trypsinised over-night, desalted, freeze-dried and finally analysed by MS.
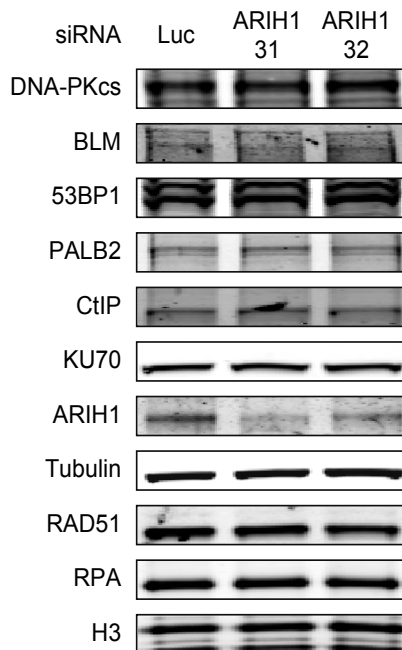
Supplemental Figure 1. ARIH1 loss does not affect the steady-state levels of key DSB repair proteins. Effect of ARIH1 depletion on the steady-state levels of various repair proteins. Blots were probed with the indicated antibodies for repair proteins and tubulin, histone H3 (loading controls).

REFERENCES

1.   Jackson, S.P. and J. Bartek, The DNA-damage response in human biology and disease. Nature, 2009. 461(7267): p. 1071-8.

2.   Marechal, A. and L. Zou, DNA damage sensing by the ATM and ATR kinases. Cold Spring Harb Perspect Biol, 2013. 5(9).

3.   Al-Hakim, A., et al., The ubiquitous role of ubiquitin in the DNA damage response. DNA Repair (Amst), 2010. 9(12): p. 1229-40.

4.   Luijsterburg, M.S. and H. van Attikum, Close encounters of the RNF8th kind: when chromatin meets DNA repair. Curr Opin Cell Biol, 2012. 24(3): p. 439-47.

5.   Deriano, L. and D.B. Roth, Modernizing the nonhomologous end-joining repertoire: alternative and classical NHEJ share the stage. Annu Rev Genet, 2013. 47: p. 433-55.

6.   Moynahan, M.E. and M. Jasin, Mitotic homologous recombination maintains genomic stability and suppresses tumorigenesis. Nat Rev Mol Cell Biol, 2010. 11(3): p. 196-207.

7.   Jackson, S.P. and D. Durocher, Regulation of DNA damage responses by ubiquitin and SUMO. Mol Cell, 2013. 49(5): p. 795-807.

8.   Feng, L. and J. Chen, The E3 ligase RNF8 regulates KU80 removal and NHEJ repair. Nat Struct Mol Biol, 2012. 19(2): p. 201-6.

9.   Zhao, G.Y., et al., A critical role for the ubiquitin-conjugating enzyme Ubc13 in initiating homologous recombination. Mol Cell, 2007. 25(5): p. 663-75.

10.   Gudjonsson, T., et al., TRIP12 and UBR5 suppress spreading of chromatin ubiquitylation at damaged chromosomes. Cell, 2012. 150(4): p. 697-709.

11.   Bergink, S., et al., Role of Cdc48/p97 as a SUMO-targeted segregase curbing Rad51-Rad52 interaction. Nat Cell Biol, 2013. 15(5): p. 526-32.

12.   Galanty, Y., et al., RNF4, a SUMO-targeted ubiquitin E3 ligase, promotes DNA double-strand break repair. Genes Dev, 2012. 26(11): p. 1179-95.

13.   Morris, J.R., et al., The SUMO modification pathway is involved in the BRCA1 response to genotoxic stress. Nature, 2009. 462(7275): p. 886-90.

14.   Lu, C.S., et al., The RING finger protein RNF8 ubiquitinates Nbs1 to promote DNA double-strand break repair by homologous recombination. J Biol Chem, 2012. 287(52): p. 43984-94.

15.   Tikoo, S., et al., Ubiquitin-dependent recruitment of the Bloom syndrome helicase upon replication stress is required to suppress homologous recombination. EMBO J, 2013. 32(12): p. 1778-92.

16.   Acs, K., et al., The AAA-ATPase VCP/p97 promotes 53BP1 recruitment by removing L3MBTL1 from DNA double-strand breaks. Nat Struct Mol Biol, 2011. 18(12): p.

6

1345-50.

17.   Meerang, M., et al., The ubiquitin-selective segregase VCP/p97 orchestrates the response to DNA double-strand breaks. Nat Cell Biol, 2011. 13(11): p. 1376-82.

18.   Bohgaki, M., et al., RNF168 ubiquitylates 53BP1 and controls its response to DNA double-strand breaks. Proc Natl Acad Sci U S A, 2013. 110(52): p. 20982-7.

19.   Doil, C., et al., RNF168 binds and amplifies ubiquitin conjugates on damaged chromosomes to allow accumulation of repair proteins. Cell, 2009. 136(3): p. 435-46.

20.   Mattiroli, F., et al., RNF168 ubiquitinates K13-15 on H2A/H2AX to drive DNA damage signaling. Cell, 2012. 150(6): p. 1182-95.

21.   Mailand, N., et al., RNF8 ubiquitylates histones at DNA double-strand breaks and promotes assembly of repair proteins. Cell, 2007. 131(5): p. 887-900.

22.   Zhang, F., et al., MDC1 and RNF8 function in a pathway that directs BRCA1-dependent localization of PALB2 required for homologous recombination. J Cell Sci, 2012. 125(Pt 24): p. 6049-57.

23.   Huang, J., et al., RAD18 transmits DNA damage signalling to elicit homologous recombination repair. Nat Cell Biol, 2009. 11(5): p. 592-603.

24.   Morris, J.R. and E. Solomon, BRCA1 : BARD1 induces the formation of conjugated ubiquitin structures, dependent on K6 of ubiquitin, in cells during DNA replication and repair. Hum Mol Genet, 2004. 13(8): p. 807-17.

25.   Wu, J., et al., Skp2 E3 ligase integrates ATM activation and homologous recombination repair by ubiquitinating NBS1. Mol Cell, 2012. 46(3): p. 351-61.

26.   Britton, S., J. Coates, and S.P. Jackson, A new method for high-resolution imaging of Ku foci to decipher mechanisms of DNA double-strand break repair. J Cell Biol, 2013. 202(3): p. 579-95.

27.   Pierce, A.J., et al., XRCC3 promotes homology-directed repair of DNA damage in mammalian cells. Genes Dev, 1999. 13(20): p. 2633-8.

28.   Postow, L., et al., Ku80 removal from DNA through double strand break-induced ubiquitylation. J Cell Biol, 2008. 182(3): p. 467-79.

29.   Han, X., et al., UbcH7 regulates 53BP1 stability and DSB repair. Proc Natl Acad Sci U S A, 2014. 111(49): p. 17456-61.

30.   Geisler, S., et al., The ubiquitin-conjugating enzymes UBE2N, UBE2L3 and UBE2D2/3 are essential for Parkin-dependent mitophagy. J Cell Sci, 2014. 127(Pt 15): p. 3280-93.

31.   Tang, J., et al., Acetylation limits 53BP1 association with damaged chromatin to promote homologous recombination. Nat Struct Mol Biol, 2013. 20(3): p. 317-25.

32.   Luijsterburg, M.S., et al., A new non-catalytic role for ubiquitin ligase RNF8 in unfolding higher-order chromatin structure. EMBO J, 2012. 31(11): p. 2511-27.

6

33.   Helfricht, A., et al., Remodeling and spacing factor 1 (RSF1) deposits centromere proteins at DNA double-strand breaks to promote non-homologous end-joining. Cell Cycle, 2013. 12(18): p. 3070-82.

34.   Smeenk, G., et al., Poly(ADP-ribosyl)ation links the chromatin remodeler SMARCA5/ SNF2H to RNF168-dependent DNA damage signaling. J Cell Sci, 2013. 126(Pt 4): p. 889-903.

6

7

General discussion
and perspectives

Though as scientists we strive to decipher the cellular conundrum, quite often our studies give rise to more questions instead of providing straightforward answers. This thesis is not different in that sense. Notwithstanding our identification of novel regulators of DSB-induced ubiquitylation (Chapter 3), novel interactions between important players in the DSB response (Chapter 4), an alternative mechanism of DNA-damage-induced translation arrest (Chapter 5) and a potential new modulator of DSB repair (Chapter 6), several points await to be addressed.

In the case of the newly-identified DUBs, structural studies may provide a detailed mode of action, while MS analysis may reveal additional proteins targeted for deubiquitylation by USP26 and USP37. On the subject of comprehending better the ubiquitylation-dependent part of the DSB response, recognition of RNF168-substrates has long eluded us. We therefore ought to take advantage of current MS approaches to pinpoint novel targets of DSB-induced ubiquitylation. With regards to the PALB2 dependency on RNF168-mediated ubiquitylation, in vitro interaction experiments examining the potential interaction between PALB2 and RNF168, in concert with immunoprecipitations (IPs) followed by MS, may elucidate the sequence of events that promote RNF168-modulated loading of PALB2/RAD51 on ssDNA. Finally, our discovery that ARIH1 holds a dual role in the DDR, temporarily halting protein synthesis, but also directly promoting DSB repair, dictates further work to understand how these rather different functions are accomplished and regulated. Monitoring the cellular compartmentalisation of ARIH1 upon genotoxic stress by live-cell imaging and identifying ARIH1-ubiquitylated proteins by MS would be steps towards the right direction. All the aforementioned scientific suggestions are placed into perspective and are elaborated in the following sections.

7

Deciphering the role of USP26/USP37 and developing inhibitors for clinical applications

The current mainstream approaches for cancer therapy are founded upon the premise of inducing excessive, irreparable DNA damage in tumour cells. An obvious caveat in this approach is the intrinsic lack of specificity as healthy cells will be targeted and killed as well. In order to circumvent this perilous side-effect, unique aspects of cancer cells acquired during transformation have to be exploited. Most typically, tumours lose one or more of the main DNA-repair pathways, therefore being disproportionately dependent on the remaining one(s). Inactivation of these residual repair pathways, in concert with chemotherapeutica, confers lethality predominantly to transformed rather than normal cells. This embodies the concept of synthetic lethality which has become the focal point of the development of novel anti-cancer drugs [1].

Given the demonstrated importance of PTMs in the regulation of the DDR, increasing emphasis is currently being placed in the development of small-molecule inhibitors of either the phosphorylation or ubiquitylation machinery [2]. As we showed in Chapter 3, USP26 and USP37 are important players in the DDR, because they regulate both major aspects of the DSB response, namely the RNF8/RNF168-signalling cascade and DSB repair. The significance of these two DUBs is further underscored by their deregulated expression patterns in cancer cells, where USP26 and USP37 are often either lost or amplified (for precise numbers please look at the Discussion of Chapter 3).

7

Since their depletion renders cells sensitive to IR and PARP-inhibition, by impairment of NHEJ and HR respectively, developing specific inhibitors against USP26 and/or USP37 function can be considered as an attractive strategy. However, before undertaking laborious screens to that end, further experiments identifying their substrates, other than histone H2A, will be crucial. USP26 or USP37 chromatin IP followed by MS, or alternatively KGG-antibody-IP followed by MS in DUB-depleted cells, would help in the search for novel substrates. Our preliminary experiments, entailing native IP and

then MS, indicate that USP37 may interact with key proteins orchestrating DNA-end resection, whereas results for USP26 were inconclusive.

On the other hand, it will also be necessary to obtain more insight in the mode of action of our DUBs, especially USP26. This can be achieved by a combination of structural studies and in vitro deubiquitylation assays. For USP37 it was recently shown that its 3 Ubiquitin-Interacting Motifs (UIMs) enable binding to stereochemically-diverse polyubiquitin chains, but convey limited specificity for chain linkage [3]. This is in line with our findings that over-expressed USP37 can deubiquitylate various HR-related proteins. These findings indicate that USP37 may be a promiscuous DUB whose activity is mainly regulated by direct interactions with its partners. The likelihood that USP26 behaves similarly is unlikely, yet still possible, as USP26 has evolutionarily retained a single UIM. Additionally, our results show that USP26 is more enzymatically active, at least towards H2A-type histones and RNF168-induced ubiquitylation. In agreement with a potential high-processivity, USP26 protein levels are significantly lower than USP37 [4, 5]. How does then USP26 remove ubiquitin from its substrates? Does it display chain-linkage specificity? The latter question could be answered by in vitro debiquitylation assays. If an array of targets for our DUBs exists, as we suspect, and this is identified, whilst their function becomes better understood, the task of developing small-molecule inhibitors would be worthwhile.

Finding new RNF8/RNF168 substrates

In recent years we have witnessed an unprecedented progress in the study of proteins PTMs, largely due to ever-improving MS facilities and innovative IP techniques, allowing the extensive analysis of modifications such as phosphorylation or ubiquitylation at the peptide level [6]. Current research indicates that the study of other protein PTMs, such as SUMOylation [7, 8], acetylation [9, 10] and poly-(ADP-ribose)ylation [11, 12], is following swiftly. Interestingly, though global profiles of protein phosphorylation or ubiquitylation, under basal conditions [13] or genotoxic stress [14-16], have been published, a report has yet to emerge, describing the ubiquitylome

upon depletion of key ubiquitin E3 ligases.

The case of DDR-orchestrating E3 ligases RNF8 and RNF168 is especially intriguing. Limited targets have been identified for RNF8 [17-20], and even less for RNF168 [21, 22], making it hard to resolve conflicting reports on their role in regulating DSB repair [17, 23-25]. Coupling either Crispr/Cas9- or inducible shRNA-depletion with KGG-antibody-IP and MS-analysis would provide a detailed picture of RNF8/RNF168-ubiquitylated substrates. Elucidating their common, but most importantly their divergent, targets would give crucial insight on several unresolved questions that have lingered in the DSB field. How do RNF8 and RNF168 modulate DSB-repair pathway choice? Do they have a singular or divergent role in promoting or antagonising error-free repair by HR? How do they integrate DSB signalling and repair with other simultaneous processes such as chromatin remodelling, checkpoint activation, replication and transcription restart?

Mechanistically explaining the RNF168-dependency of PALB2 recruitment at DSBs

Our unexpected discovery that RNF168-induced ubiquitylation promotes PALB2 recruitment at DSBs demonstrates that key DDR enzymes fulfill multiple roles with often varying macroscopic effects. On one hand, RNF168 ubiquitylates H2A-type histones [22], thereby promoting BRCA1 sequestration in the form of the RAP80-mediated BRCA1A complex [26, 27] and 53BP1 recruitment at the vicinity of DSBs [28, 29], which in turn inhibits extensive processing of DNA-ends [30]. In that sense RNF168 exerts an anti-recombinogenic role. On the other hand, RNF168 recruits PALB2 at sites of damage, thereby enabling RAD51 loading on resected DNA (Chapter 4). In that sense RNF168 bolsters HR. The emerging question lies in the chromatin parameters regulating the balance of these contradictory roles and possibly the nature of the inflicted DSB.

As mentioned in the previous section, establishing detailed RNF168-ubiquitylation profiles would be a key step towards answering this puzzle. The results we obtained from the LacR/LacO targeting system indicate that the RNF168-induced ubiquitylation signal promoting PALB2 recruitment at DSBs

7

is not the canonical one, i.e. H2A/H2AX ubiquitylation [22]. In line with this hypothesis, we have also observed that RNF168-induced ubiquitylation does not promote the association of PALB2 with histone H2A. Hence, RNF168 probably mediates PALB2-accumulation at DSBs in another manner.

Based on our thus far results, we favour a scenario of a direct interaction between RNF168 and PALB2, via the latter's WD40 domain. In vitro interaction experiments between recombinant RNF168 and PALB2 would help confirming our IP data. The way that the ubiquitylation activity of RNF168 facilitates PALB2 assembly is less clear. A simplistic explanation would be that the known increase of RNF168 at DSBs, upon RNF168-ubiquitylation of histones H2A/H2AX [28, 29], is sufficient to promote further PALB2 buildup. Simply put: more RNF168 begs more PALB2. Unfortunately, it is not easy to test this proposition, because utilising the ΔMIU-RNF168 mutant, which cannot mediate auto-amplification, would also abrogate RNF168 recruitment [29]. The alternative option of complementing RIDDLE cells with a catalytically inactive version of RNF168 would not give a definite answer either, as such cells would miss all RNF168-ubiquitylation-dependent PALB2 accrual. Another, not mutually exclusive, hypothesis is that RNF168 decorates PALB2 with K63-ubiquitin chains which somehow assist with either its recruitment or retention at the ssDNA compartment. This can be verified by a denaturing PALB2-IP in RNF168 over-expressing cells followed by MS analysis. Finally, it is also possible that RNF168 ubiquitylates another protein which bridges the interaction between the E3 ligase and PALB2. Common interactors identified in independent IPs for PALB2 and RNF168 would be prime candidates to fulfill this bridging role.

No matter which scenario proves to be correct, an inescapable issue that arises, if RNF168 and PALB2 indeed interact, is that those two proteins do not completely overlap in their positions with respect to the DSB. While PALB2 remains strictly associated within the ssDNA compartment, RNF168 is known to spread away from the DSB [31], with its associated ubiquitin-chains also being repositioned away from the DSB at latter stages [32]. This difference is also evident by the distinct size of IR-induced foci that these proteins form [33]. Therefore, a mechanism inhibiting the PALB2-RNF168

interaction distally from the DSB is rather likely to exist. The potential PALB2 K63-ubiquitylation or a constraint in the number of interactions mediated by the WD40 domain of PALB2, due to spatial limitations, are just two of possible mechanisms restricting the PALB2-RNF168 interaction at the ssDNA compartment.

Exploiting ARIH1-dependent translation inhibition

Cancer cells universally display deregulated growth patterns, favouring accelerated expansion and survival under challenging conditions. One of the main ways they obtain this growth advantage is by lifting constraints in protein synthesis. Expectedly, transformed cells boast increased translation rates, evident by the increase in their ribosomal content [34]. On the contrary, untransformed cells are subject to numerous ways of inhibiting translation, especially at the rate-limiting step of translation initiation [35]. This notable difference has driven intensive research into the development of translation initiation inhibitors as potential drugs, augmenting the action of mainstream cancer treatments [34, 36, 37].

Our finding that the E3 ubiquitin ligase ARIH1 facilitates 4EHP-dependent translation stalling upon DSB induction may provide in the future a new weapon in the increasing arsenal of translation inhibitors. Importantly, we demonstrate that the ARIH1-induced response is unique, in that it is retained in cancer cells, unlike the more prevalent 4E-BP1-dependent path which is often silenced [38]. Subsequent efforts should initially focus on identifying the part of the proteome that is affected by the ARIH1-induced translational arrest. Establishing ARIH1- and 4EHP-dependent proteome-profiles can be accomplished by isolating and analysing by MS newly-synthesised proteins. A complementary approach could also be undertaken, in which mRNAs bound to polysomes are purified and sequenced. The emergence of a more detailed picture of the affected proteins would provide important insight on the mechanism of the observed ARIH1-dependent sensitisation. Eventually, the development or discovery of substances that can potentiate ARIH1-dependent translation inhibition, by enhancing its stability or facilitating 4EHP modification, might even prove valuable for clinical applications.

7

With regards to the apparent, direct involvement of ARIH1 in DSB repair, though a lot of work remains to elucidate its precise role, an obvious riddle arises: how can a protein directly regulating a cytoplasmic function, such as translation, be simultaneously involved in the nuclear process of DNA repair? A straightforward answer has yet to emerge, but several observations indicate unique behavioural aspects for ARIH1. Firstly, upon DSB induction ARIH1 increasingly translocates to ribosomes and the nucleus, placing it at the correct micro-environment. Secondly, ARIH1 is part of a special family of E3 ubiquitin ligases, the RING-In-Between-RING (RBR) enzymes, which have retained characteristics from both traditional E3 families, namely the RINGs and HECTs [39]. As such, ARIH1 may contain unique structural aspects that enable it to target distinct substrates, but also exhibit unusual auto-inhibitory effects [40]. Finally, as with most E3 ubiquitin ligases, their role is largely dictated by their binding partners and their associated E2s. ARIH1 is known to directly interact with 4EHP [41, 42] which resides in the cytosol, while its primary E2 partner, UBCH7 (UBE2L3) [43], also resides both in the cytoplasm and in the nucleus, where it has been shown to regulate the half-life of 53BP1 [44].

7

REFERENCES

1. Curtin, N.J., DNA repair dysregulation from cancer driver to therapeutic target. Nat Rev Cancer, 2012. 12(12): p. 801-17.

2. Cohen, P. and M. Tcherpakov, Will the ubiquitin system furnish as many drug targets as protein kinases? Cell, 2010. 143(5): p. 686-93.

3. Tanno, H., et al., Ubiquitin-interacting motifs confer full catalytic activity, but not ubiquitin chain substrate specificity, to deubiquitinating enzyme USP37. J Biol Chem, 2014. 289(4): p. 2415-23.

4. Kim, M.S., et al., A draft map of the human proteome. Nature, 2014. 509(7502): p. 575-81.

5. Wilhelm, M., et al., Mass-spectrometry-based draft of the human proteome. Nature, 2014. 509(7502): p. 582-7.

6. Choudhary, C. and M. Mann, Decoding signalling networks by mass spectrometry-based proteomics. Nat Rev Mol Cell Biol, 2010. 11(6): p. 427-39.

7. Hendriks, I.A., et al., Uncovering global SUMOylation signaling networks in a site-specific manner. Nat Struct Mol Biol, 2014. 21(10): p. 927-36.

8. Matic, I., et al., Site-specific identification of SUMO-2 targets in cells reveals an inverted SUMOylation motif and a hydrophobic cluster SUMOylation motif. Mol Cell, 2010. 39(4): p. 641-52.

9. Lundby, A., et al., Proteomic analysis of lysine acetylation sites in rat tissues reveals organ specificity and subcellular patterns. Cell Rep, 2012. 2(2): p. 419-31.

10. Guan, K.L., et al., Generation of acetyllysine antibodies and affinity enrichment of acetylated peptides. Nat Protoc, 2010. 5(9): p. 1583-95.

11. Gagne, J.P., et al., Quantitative proteomics profiling of the poly(ADP-ribose)-related response to genotoxic stress. Nucleic Acids Res, 2012. 40(16): p. 7788-805.

12. Jungmichel, S., et al., Proteome-wide identification of poly(ADP-Ribosyl)ation targets in different genotoxic stress responses. Mol Cell, 2013. 52(2): p. 272-85.

13. Olsen, J.V., et al., Quantitative phosphoproteomics reveals widespread full phosphorylation site occupancy during mitosis. Sci Signal, 2010. 3(104): p. ra3.

14. Pines, A., et al., Global phosphoproteome profiling reveals unanticipated networks responsive to cisplatin treatment of embryonic stem cells. Mol Cell Biol, 2011. 31(24): p. 4964-77.

15. Povlsen, L.K., et al., Systems-wide analysis of ubiquitylation dynamics reveals a key role for PAF15 ubiquitylation in DNA-damage bypass. Nat Cell Biol, 2012. 14(10): p. 1089-98.

7

16.   Matsuoka, S., et al., ATM and ATR substrate analysis reveals extensive protein networks responsive to DNA damage. Science, 2007. 316(5828): p. 1160-6.

17.   Tikoo, S., et al., Ubiquitin-dependent recruitment of the Bloom syndrome helicase upon replication stress is required to suppress homologous recombination. EMBO J, 2013. 32(12): p. 1778-92.

18.   Lu, C.S., et al., The RING finger protein RNF8 ubiquitinates Nbs1 to promote DNA double-strand break repair by homologous recombination. J Biol Chem, 2012. 287(52): p. 43984-94.

19.   Feng, L. and J. Chen, The E3 ligase RNF8 regulates KU80 removal and NHEJ repair. Nat Struct Mol Biol, 2012. 19(2): p. 201-6.

20.   Mailand, N., et al., RNF8 ubiquitylates histones at DNA double-strand breaks and promotes assembly of repair proteins. Cell, 2007. 131(5): p. 887-900.

21.   Bohgaki, M., et al., RNF168 ubiquitylates 53BP1 and controls its response to DNA double-strand breaks. Proc Natl Acad Sci U S A, 2013. 110(52): p. 20982-7.

22.   Mattiroli, F., et al., RNF168 ubiquitinates K13-15 on H2A/H2AX to drive DNA damage signaling. Cell, 2012. 150(6): p. 1182-95.

23.   Munoz, M.C., D.A. Yanez, and J.M. Stark, An RNF168 fragment defective for focal accumulation at DNA damage is proficient for inhibition of homologous recombination in BRCA1 deficient cells. Nucleic Acids Res, 2014. 42(12): p. 7720-33.

24.   Peuscher, M.H. and J.J. Jacobs, DNA-damage response and repair activities at uncapped telomeres depend on RNF8. Nat Cell Biol, 2011. 13(9): p. 1139-45.

25.   Sy, S.M., et al., Critical roles of ring finger protein RNF8 in replication stress responses. J Biol Chem, 2011. 286(25): p. 22355-61.

26.   Coleman, K.A. and R.A. Greenberg, The BRCA1-RAP80 complex regulates DNA repair mechanism utilization by restricting end resection. J Biol Chem, 2011. 286(15): p. 13669-80.

27.   Hu, Y., et al., RAP80-directed tuning of BRCA1 homologous recombination function at ionizing radiation-induced nuclear foci. Genes Dev, 2011. 25(7): p. 685-700.

28.   Doil, C., et al., RNF168 binds and amplifies ubiquitin conjugates on damaged chromosomes to allow accumulation of repair proteins. Cell, 2009. 136(3): p. 435-46.

29.   Stewart, G.S., et al., The RIDDLE syndrome protein mediates a ubiquitin-dependent signaling cascade at sites of DNA damage. Cell, 2009. 136(3): p. 420-34.

30.   Panier, S. and S.J. Boulton, Double-strand break repair: 53BP1 comes into focus. Nat Rev Mol Cell Biol, 2014. 15(1): p. 7-18.

31.   Gudjonsson, T., et al., TRIP12 and UBR5 suppress spreading of chromatin ubiquitylation at damaged chromosomes. Cell, 2012. 150(4): p. 697-709.

32.   Kakarougkas, A., et al., Co-operation of BRCA1 and POH1 relieves the barriers

7

posed by 53BP1 and RAP80 to resection. Nucleic Acids Res, 2013. 41(22): p. 10298-311.

33.   Bekker-Jensen, S., et al., Spatial organization of the mammalian genome surveillance machinery in response to DNA strand breaks. J Cell Biol, 2006. 173(2): p. 195-206.

34.   Silvera, D., S.C. Formenti, and R.J. Schneider, Translational control in cancer. Nat Rev Cancer, 2010. 10(4): p. 254-66.

35.   Sonenberg, N. and A.G. Hinnebusch, Regulation of translation initiation in eukaryotes: mechanisms and biological targets. Cell, 2009. 136(4): p. 731-45.

36.   Graff, J.R., et al., Targeting the eukaryotic translation initiation factor 4E for cancer therapy. Cancer Res, 2008. 68(3): p. 631-4.

37.   Chu, J. and J. Pelletier, Targeting the eIF4A RNA helicase as an anti-neoplastic approach. Biochim Biophys Acta, 2014.

38.   Kong, J. and P. Lasko, Translational control in cellular and developmental processes. Nat Rev Genet, 2012. 13(6): p. 383-94.

39.   Wenzel, D.M., et al., UBCH7 reactivity profile reveals parkin and HHARI to be RING/HECT hybrids. Nature, 2011. 474(7349): p. 105-8.

40.   Duda, D.M., et al., Structure of HHARI, a RING-IBR-RING ubiquitin ligase: autoinhibition of an Ariadne-family E3 and insights into ligation mechanism. Structure, 2013. 21(6): p. 1030-41.

41.   Okumura, F., W. Zou, and D.E. Zhang, ISG15 modification of the eIF4E cognate 4EHP enhances cap structure-binding activity of 4EHP. Genes Dev, 2007. 21(3): p. 255-60.

42.   Tan, N.G., et al., Human homologue of ariadne promotes the ubiquitylation of translation initiation factor 4E homologous protein, 4EHP. FEBS Lett, 2003. 554(3): p. 501-4.

43.   Moynihan, T.P., et al., The ubiquitin-conjugating enzymes UbcH7 and UbcH8 interact with RING finger/IBR motif-containing domains of HHARI and H7-AP1. J Biol Chem, 1999. 274(43): p. 30963-8.

44.   Han, X., et al., UbcH7 regulates 53BP1 stability and DSB repair. Proc Natl Acad Sci U S A, 2014. 111(49): p. 17456-61.

7

A

Addendum

Summary

The genome contains, in the form of DNA building blocks, the necessary information for orchestrating all cellular functions and ensuring species continuity. However, though being chemically stable, DNA is under constant assault by various endogenous or exogenous sources. To counteract the perils arising due to DNA damage and to ensure genome integrity, life has evolutionarily acquired an arsenal of protective mechanisms, amongst which prominent is DNA repair. Depending on the nature of the inflicted DNA damage, specialised DNA repair pathways are activated in order to restore the original genetic information.

During this work I focused on the elucidation of DNA repair- or other cytoprotective-mechanisms ensuing upon the induction of primarily DNA Double Strand Breaks (DSBs) or secondarily helix-distorting lesions. DSBs are mainly repaired by two pathways: error-prone Non-Homologous End-Joining (NHEJ) and error-free Homologous Recombination (HR). On the other hand, helix-distorting lesions, such as those arising due to UV-irradiation or cisplatin-induced mono-adducts, are rectified by Nucleotide Excision Repair (NER).   More specifically, I put emphasis on the role of protein-ubiquitylation, a widespread protein Post-Translational Modification (PTM), in the spatiotemporal regulation of an efficient DSB response.

In Chapter 2, I summarise recent developments, integrate novel findings and present our speculative views on the possible ways that ubiquitylation and other PTMs coordinate diverse processes, such as chromatin remodelling and repair-protein retention at the sites of damage, in order to regulate NER.

In Chapter 3, I present our findings establishing a role for the De-Ubiquitylating (DUB) enzymes USP26 and USP37 in the regulation of the DSB response. Upon performing over-expression screens, we identified the aforementioned DUBs as factors regulating both the DSB signalling cascade and DSB repair. More specifically, we show that USP26 and USP37 readily accumulate at sites of damage where they keep RNF8- and RNF168-dependent ubiquitylation in check. Thereby, these DUBs limit the repressive effect of RAP80 on both DNA end-resection and BRCA1 accumulation on resected DNA, effectively

A

promoting homologous recombination.

In Chapter 4, I describe a novel, unexpected mechanism of PALB2-dependent control of homologous recombination. I demonstrate that RNF168 facilitates error-free repair, due to PALB2 accumulation at RNF168-modified chromatin. PALB2 accrual at RNF168-ubiquitylated chromatin requires the former's WD40 domain and is probably mediated by direct protein-protein interaction between PALB2 and RNF168.

In Chapter 5, I put forward our results from a functional genomics screen for potential regulation of the cisplatin response by enzymes of the ubiquitin family. I show that ARIH1, one of the top hits, promotes cellular survival upon cisplatin-induced damage in a manner independent of p53-status. I further on manifest that ARIH1 orchestrates a transient translation arrest upon DNA damage, which is both required and retained in untransformed and cancer cells.

In Chapter 6, I describe our initial results indicating that ARIH1, in addition to inducing a temporary arrest of translation, translocates to the nucleus and accumulates at DSBs. Moreover, I show that ARIH1 appears to exert a direct role in the regulation of DSB repair by promoting efficient HR.

Finally, in Chapter 7, I provide an overview of our discoveries in a broader context, incorporating recent, relevant developments in the DDR field. Additionally, I try to put our findings in perspective, speculating about the entailed molecular mechanisms, with the ultimate goal of using this knowledge for clinical applications.

A

Nederlandse Samenvatting

Het genoom bevat, in de vorm van DNA-bouwstenen, de informatie noodzakelijk voor het orkestreren van alle cellulaire functies en het waarborgen van de continuïteit van een soort. Ook al is DNA chemisch redelijk stabiel, de integriteit van het DNA wordt constant bedreigd door verschillende endogene of exogene bronnen van DNA-schade. Om de integriteit van het genoom te waarborgen en DNA-schade te neutraliseren is er een arsenaal aan beschermende mechanismen geëvolueerd, met een prominente rol voor DNA-herstelmechanismen. Afhankelijk van de aard van de toegebrachte DNA-schade, zijn gespecialiseerde herstelmechanismen ontstaan die de oorspronkelijke genetische informatie herstellen.

Tijdens mijn werkzaamheden als promovendus heb ik mij gericht op het ontrafelenvandeDNAreparatieroutesencellulairebeschermingsmechanismen die volgen na de inductie van DNA dubbelstrengs breuken (DSBs) en/of DNA-helix verstorende lesies. DSBs worden voornamelijk gerepareerd door twee reparatieroutes: foutgevoelige Non-Homologe End-Joining (NHEJ) en accurate Homologe Recombinatie (HR). Helix-verstorende lesies, zoals die ontstaan door UV-bestraling of cisplatina behandeling, worden gerepareerd door Nucleotide Excision Repair (NER). In het bijzonder heb ik de nadruk gelegd op de rol van eiwit-ubiquitinering, een wijdverspreide post-translationele modificatie (PTM) van eiwitten, in de spatiotemporele regulering van een efficiënte DSB respons.

In hoofdstuk 2 vat ik de recente wetenschappelijke ontwikkelingen, onze nieuwe bevindingen en onze speculatieve opvattingen samen betreffende de mogelijke manieren waarop ubiquitinering en andere PTMs diverse aspecten van NER kunnen reguleren, waaronder het herstructureren van chromatine of het behouden van reparatie-eiwitten op de plaats van DNA-schade.

In hoofdstuk 3 presenteer ik onze bevindingen omtrent de De-ubiquitinering (DUB) enzymen USP26 en USP37 en hun rol in de DSB-respons. Door het uitvoeren van overexpressie screens, hebben we de eerder genoemde DUBs geïdentificeerd als factoren in zowel de signaleringscascade als de reparatie route van DSBs. We tonen aan dat USP26 en USP37 ophopen

A

op plaatsen van DNA-schade, waar ze RNF8- en RNF168-afhankelijke ubiquitinering onder controle houden. Bovendien bevorderen deze DUBs homologe recombinatie, door het repressieve effect van RAP80 te beperken op zowel DNA eind-resectie als BRCA1-accumulatie op DNA breuken.

In hoofdstuk 4 beschrijf ik een nieuw, onverwacht mechanisme van PALB2-afhankelijke regulering van homologe recombinatie. Ik toon aan dat RNF168 foutloze DNA-reparatie faciliteert via PALB2 accumulatie op RNF168 gemodificeerd chromatine. De rekrutering van PALB2 naar RNF168-geubiquitineerd chromatine vereist het WD40 domein van PALB2 en wordt waarschijnlijk gemedieerd door een directe eiwit-eiwit interactie tussen PALB2 en RNF168.

In hoofdstuk 5, presenteer ik onze resultaten van een functional genomics screen gericht op de regulering van de respons op cisplatina door enzymen van de familie van ubiquitines. Ik laat zien dat ARIH1, een van de tophits, de cellulaire overleving bevordert na cisplatina-geïnduceerde schade, op een manier die onafhankelijk is van de p53-status. Ik toon verder aan dat ARIH1 een tijdelijke translatie-stop implementeert na DNA-schade, welke behouden en essentieel is in getransformeerde- en kankercellen.

In hoofdstuk 6 beschrijf ik onze initiële resultaten die aangeven dat ARIH1, naast het induceren van een tijdelijke translatie-stop, ook accumuleert op DSBs in de celkern. Bovendien laat ik zien dat ARIH1 een directe rol lijkt te hebben in de regulatie van DSB reparatie door het bevorderen van efficiënte HR.

Tenslotte wordt in hoofdstuk 7 een overzicht gegeven van onze ontdekkingen in een bredere context, in het licht van recente, relevante ontwikkelingen op het gebied van DNA-schade. Daarnaast probeer ik onze bevindingen in een klinisch perspectief te plaatsen en speculeer ik over het uiteindelijke doel om de besproken kennis over de moleculaire mechanismen in te zetten voor medische toepassingen.

A

Abbreviations

4E-BPs: eiF4E-Binding Proteins

BER: Base Excision Repair

ChAM: Chromatin Association Motif

CHX: Cycloheximide

CP: Cisplatin

DAPI: 4, 6-diamidino-2-phenylindole

DDR: DNA Damage Response

DEM: Diethylmaleate

DOX: Doxorubicin

DSBs: Double Strand Breaks

DUBs: De-Ubiquitylating Enzymes

ETO: Etoposide

GG-NER: Global Genome Nucleotide Excision Repair

HJs: Holliday Junctions

HR: Homologous Recombination

IR: Ionising Radiation

IRIF: Ionising Radiation Induced Foci

MMC: Mitomycin C

MMEJ: Microhomology-Mediated End-Joining

MMR: Mismatch Repair

NER: Nucleotide Excision Repair

NHEJ: Non-Homologous End-Joining

PIC: Pre-Initiation Complex

PTMs: Post-Translational Modifications

A

ROS: Reactive Oxygen Species

SAL: Salubrinal

SDSA: Synthesis Dependent Strand Annealing

SSA: Single Strand Annealing

SSBs: Single Strand Breaks

ssDNA: single-stranded DNA

TC-NER: Transcription Coupled Nucleotide Excision Repair

THAPS: Thapsigargin

TLS: Translesion Synthesis

TMEJ: Theta-Mediated End-Joining

UBD: Ubiquitin Binding Domain

UIM: Ubiquitin Interacting Motif

VINC: Vincristine

A

Curriculum Vitae

Dimitris Typas was born on the 5th of May 1983 in Athens, Greece and grew up in Chalkida, the capital of the island of Euboea. He was admitted with distinction in the Department of Chemistry of the National and Kapodistrian University of Athens in 2001. He undertook his diploma thesis, with eventual distinction, at the Department of Chemical carcinogenesis and Genetic toxicology of the National Hellenic Research Foundation. Upon the conclusion of his undergraduate studies in 2007, he carried out a year-long internship at the nucleotide excision group of the Department of Toxicogenetics in the LUMC. Subsequently, he commenced his PhD as part of the Netherlands Toxicogenomics Center initiative in the same department under the supervision of Prof. Dr. Mullenders. During his tenure as a PhD student he also participated in the organising committees of several successful events such as the 2011 MGC PhD student workshop in Maastricht and the monthly meeting of PhD students at the LUMC (2010-2013).

A

List of publications

Madelon Dijk, Dimitris Typas, Leon Mullenders and Alex Pines. Insight in the multilevel regulation of NER. *Experimental Cell Research 2014, 2014 Nov 15;329(1):116-23.*

Louise von Stechow[*], Dimitris Typas[*], Jordi Carreras Puigvert, Laurens Oort, Ramakrishnaiah Siddappa, Alex Pines, Harry Vrieling, Bob van de Water, Leon Mullenders and Erik Danen. The E3 ubiquitin ligase ARIH1 protects against genotoxic stress by initiating a 4EHP-mediated mRNA translation arrest. *Molecular and Cellular Biology 2015. 2015 Apr 1;35(7):1254-68.* [*]equal contribution

Dimitris Typas[*], Martijn Luijsterburg[*], Wouter Wiegant, Michaela Diakatou, Angela Helfricht, Peter Thijssen, Bram van de Broek, Leon Mullenders and Haico van Attikum. The De-ubiquitylating Enzymes USP26 and USP37 Regulate Homologous Recombination By Counteracting RAP80. *Under second revision in Nucleic Acids Research.* [*]equal contribution

Dimitris Typas[*], Martijn Luijsterburg[*], Wouter Wiegant, Marie-Christine Caron, Jean-Yves Masson, Leon Mullenders and Haico van Attikum. The RNF168 Ubiquitin Ligase Orchestrates PALB2-Mediated Homologous Recombination. *Submitted to Nature Communications.* [*]equal contribution

Alex Pines, Christian Kelstrup, Mischa Vrouwe, Jordi Puigvert, Dimitris Typas, Branislav Misovic, Anton de Groot, Louise von Stechow, Bob van de Water, Erik Danen, Harry Vrieling, Leon Mullenders and Jesper Olsen. Global Phosphoproteome Profiling Reveals Unanticipated Networks Responsive to Cisplatin Treatment of Embryonic Stem Cells. *Molecular and Cellular Biology, 2011 Dec;31(24):4964-77.*

Alex Pines[*], Mischa Vrouwe[*], Jurgen Marteijn, Dimitris Typas, Martijn Luijsterburg, Medine Cansoy, Paul Hensbergen, Andre Deelder, Anton de Groot, Syota Matsumoto, Kaoru Sugasawa, Nicolas Thoma, Wim Vermeulen, Harry Vrieling and Leon Mullenders. PARP1 promotes nucleotide excision repair DDB2 through stabilization and recruitment of ALC1. *Journal of Cell Biology, 2012 Oct 15;199(2):235-49.* [*]equal contribution

A

Acknowledgements

Though I cannot think of many things I would rather do, science is always challenging, often overwhelming and occasionally demoralising, especially at the PhD level where we hold very little leverage. I would not be in the fortunate position I stand right now without the help of all the following people.

Firstly, my gratitude goes to Leon for allowing me to work in a great lab. Leon, you always provided insightful supervision but also allowed creative freedom.

I would like to thank Haico for our fruitful collaboration and the many things I learned from him, particularly how to properly prepare my work for publication.

We had an excellent collaboration with Erik and his team, particularly his former, bright PhD student, Louise; for this I am very grateful to both.

I am also thankful to the other group-leaders of the Department of Toxicogenetics, Harry, Marcel and Niels, as they helped me progress as a scientist via their constructive criticism.

We shared a lab with the people of the NER-group for more than seven years, so it is next to impossible not to be grateful to all of them for their help, advice and compassion. First and foremost, I want to thank il mio amico Friulano Alex, because he taught me a lot and he put up with me for a long time. Alex, nonostante a volte volessimo ucciderci, it was actually great for me as a person and a scientist to work with you. I would like to thank Hanneke and Anton, our hard-working technicians that deserve much more recognition than we often give them; they always helped me out and gracefully passed on their experimental knowledge. Without the guidance and suggestions of Mischa, Saskia, René and Madelon, my fellow PhD students, I would not have been able to either become at ease at the lab or learn so much.

From Haico's group, I am immensely indebted to my good friend Wouter for all his experimental help and his companionship. Along with Godelieve, Wouter was literally ubiquitous at the lab and for that I am glad. Many thanks are also due to Martijn for our common scientific endeavours and for all his tutoring.

No man is an island; without friends I would not have made it either scientifically or as a person all these years. To my chronologically first friends in the Netherlands: Erik and Agata, thanks for all your support

A

and the great times. To my fellow PhD students, some post-docs and other friends: Robin, Bennie, Mila, Godelieve, Angie, Thomas, Wouter W, Eleni, Iris, Mark, Suming, Maartje, Jordi, Joost M, Pierre, Ivo, Wouter K, Sophie, Branco, Joost S, Evelina, Bharath, Nick, Peter, Petra and Maikel: our (scientific) discussions were often challenged due to mitigating circumstances (see various intoxicants), but they were always rewarding to the mind and cathartic to the soul. To my good old friends: Παναγιώτη, Ηλία, Γιάννη, ας αρχίσουν οι καραβολίδες, το διδακτορικό τελείωσε! To the Mediterranean Association of Rotterdam: Chiara, Maria, Theodoris, Sara, Hegias, Luca, Jessica, Thomas, Marti and Andrea, being around you guys is so much fun and it helps tons with keeping me in check.

I have been blessed to know two exceedingly intelligent individuals and soon-to-be leading scientists, but most importantly to have two good friends in my paranymphs: Robin and Bennie. They have been on my side through thick and thin, they are brilliant, truthful and supportive, and for that I am thankful.

Nobody gets to choose their family but almost all of us do cherish them. However, how many are fortunate enough to also like them? I can safely say that I am. Without my mother's example of persistence to meeting your goals, sticking to your morals and dealing with adversity, I am not sure if I would have been able to overcome the lack of results early in my PhD. Without my father's inherent curiosity and desire to understand how life operates via genetics, I may not have even started. But most importantly, without the never-ending support, wit, encouragement and love of my brother and my sister-in-law, I would not have been able to finish my PhD. I guess they may not fully see it, but they are bright beacon in my (scientific) life.

Infine, alla mia bella, intelligente e gentile morosa: Ile mia, grazie per il tuo sostegno, comprensione e amore. Sono sicuro che faremo l'un l'altro felice per un lungo, lungo tempo.

A